NAVAL POSTGRADUATE SCHOOL
Monterey, California

THESIS

STABILITY OF THE VORTEX MOTION
IN OSCILLATING FLOW

by

William T. McCoy

December 1986

Thesis Advisor T. Sarpkaya

UNCLASSIFIED

SECURITY CLASSIFICATION OF THIS PAGE

REPORT DOCUMENTATION PAGE

1a REPORT SECURITY CLASSIFICATION UNCLASSIFIED	1b RESTRICTIVE MARKINGS
2a SECURITY CLASSIFICATION AUTHORITY	3 DISTRIBUTION/AVAILABILITY OF REPORT Approved for public release; distribution is unlimited.
2b DECLASSIFICATION/DOWNGRADING SCHEDULE	
4 PERFORMING ORGANIZATION REPORT NUMBER(S)	5 MONITORING ORGANIZATION REPORT NUMBER(S)
6a NAME OF PERFORMING ORGANIZATION Naval Postgraduate School 6b OFFICE SYMBOL (If applicable) 69	7a NAME OF MONITORING ORGANIZATION Naval Postgraduate School
6c ADDRESS (City, State, and ZIP Code) Monterey, California 93943-5000	7b ADDRESS (City, State, and ZIP Code) Monterey, California 93943-5000
8a NAME OF FUNDING/SPONSORING ORGANIZATION 8b OFFICE SYMBOL (If applicable)	9 PROCUREMENT INSTRUMENT IDENTIFICATION NUMBER
8c ADDRESS (City, State, and ZIP Code)	10 SOURCE OF FUNDING NUMBERS PROGRAM ELEMENT NO / PROJECT NO / TASK NO / WORK UNIT ACCESSION NO

11 TITLE (Include Security Classification)
STABILITY OF THE VORTEX MOTION IN OSCILLATING FLOW

12 PERSONAL AUTHOR(S)
McCoy, William T.

13a TYPE OF REPORT	13b TIME COVERED	14 DATE OF REPORT (Year Month Day)	15 PAGE COUNT
Master's Thesis	FROM ___ TO ___	1986 December	111

16 SUPPLEMENTARY NOTATION

17 COSATI CODES			18 SUBJECT TERMS (Continue on reverse if necessary and identify by block number)
FIELD	GROUP	SUB-GROUP	Vortex Advection, Chaos, Vortices, Vortex Motion, Coherence Length, Aspect Ratio

19 ABSTRACT (Continue on reverse if necessary and identify by block number)

Previous experimental investigations have shown that the characteristics of flow about a circular cylinder immersed in a time-dependent flow exhibit cycle-to-cycle variations. These variations have been attributed to the variations in the spanwise coherence, aspect ratio, nonuniformity of the flow, and random disturbances in the ambient flow. A theoretical investigation was undertaken to examine the stability of the flow characteristics in terms of the initial state of the vortices. An idealized model has been devised and the position of the vortex was

20 DISTRIBUTION/AVAILABILITY OF ABSTRACT	21 ABSTRACT SECURITY CLASSIFICATION
☒ UNCLASSIFIED/UNLIMITED ☐ SAME AS RPT ☐ DTIC USERS	UNCLASSIFIED
22a NAME OF RESPONSIBLE INDIVIDUAL T. Sarpkaya	22b TELEPHONE (Include Area Code) (408) 646-3425 22c OFFICE SYMBOL 69SL

DD FORM 1473, 84 MAR 83 APR edition may be used until exhausted
All other editions are obsolete

SECURITY CLASSIFICATION OF THIS PAGE
UNCLASSIFIED

19. Abstract contd.

varied systematically. The results have shown that finite-precision information about the characteristics of the flow does not lead to finite-precision information at a later stage. In fact the advection of the vortices can give rise to chaotic behavior in the calculated lift and drag forces and in the velocity field. It is concluded that the cycle-to-cycle variations are not entirely due to lack of spanwise coherence and that they are mostly a consequence of the chaotic motion which can result from the advection of the vortices in a time-dependent flow.

Approved for public release; distribution is unlimited.

Stability of the Vortex Motion in Oscillating Flow

by

William T. McCoy
Lieutenant, United States Navy
B.S.M.E, Tulane University, 1979

Submitted in partial fulfillment of the
requirements for the degrees of

MASTER OF SCIENCE IN MECHANICAL ENGINEERING
and
MECHANICAL ENGINEER

from the

NAVAL POSTGRADUATE SCHOOL
December 1986

ABSTRACT

Previous experimental investigations have shown that the characteristics of flow about a circular cylinder immersed in a time-dependent flow exhibit cycle-to-cycle variations. These variations have been attributed to the variations in the spanwise coherence, aspect ratio, nonuniformity of the flow, and random disturbances in the ambient flow. A theoretical investigation was undertaken to examine the stability of the flow characteristics in terms of the initial state of the vortices. An idealized model has been devised and the position of the vortex was varied systematically. The results have shown that finite-precision information about the characteristics of the flow does not lead to finite-precision information at a later stage. In fact the advection of the vortices can give rise to chaotic behavior in the calculated lift and drag forces and in the velocity field. It is concluded that the cycle-to-cycle variations are not entirely due to lack of spanwise coherence and that they are mostly a consequence of the chaotic motion which can result from the advection of the vortices in a time-dependent flow.

TABLE OF CONTENTS

LIST OF FIGURES

TABLE OF SYMBOLS AND ABBREVIATIONS

c	Radius of the Circular Cylinder
D	Drag Coefficient
K_c	Keulegan-Carpenter Number
L	Lift Coefficient
q	Velocity Vector
r	Radial Distance
r_v	Radial DistanceBetween Real and Image Vortices
Re	Reynolds Number
t	Time
T	Period of the Flow
Ti	Initial Starting Time
U_{max}	Maximum Flow Velocity
u	x-Component of Velocity
v	y-Component of Velocity
Z(1)	Initial Location of the Vortex
ε_r	Incremental Radial Scaling Factor
ε_K	Incremental Stregth Scaling Factor
Γ	Circulation of the Vortex
Γ_o	Initial Circulation of the Vortex
K	Strength of the Vortex
K_A	Strength of Vortex A (clockwise rotation)
K_B	Strength of Vortex B (counterclockwise rotation)
ν	Kinematic Viscosity of Water
ζ	Nondimensional Location in Complex Space
ζ_o	Location of the Vortex
ζ_A	Location of Vortex A
ζ_B	Location of Vortex B

ACKNOWLEDGEMENTS

The author wishes to express his sincere thanks to Distinguished Professor T. Sarpkaya for his invaluable assistance, guidance and, most of all, patience throughout the investigation and writing for this thesis. It has been a privilege and an honor to work with a man with such powerful insight, knowledge and dedication. He is a true teacher of men.

I. INTRODUCTION

In the past ten years there has been much effort to analyze the separated time dependent flow about bluff bodies in general and circular cylinders in particular. Shortfalls in the Morison Equation to adequately predict in-line forces as well as the advent of sophisticated computational and experimental techniques have stimulated a great deal of research in this area. The accumulation of this numerical, experimental and visual data has generated the need for a deeper understanding of the motion of vortices in time dependent flow. Specifically in oscillating flow the stability of the vortices generated is of particular importance. The significance of the stability of the vortices is a result of its possible exposition of documented cycle-to-cycle variations in measured forces on the cylinder.

In this application, stability is not a characteristic of the vortex life or demise but of the vortex motion or path. A system is referred to as stable in any particular state of equilibrium if, after being given a finite perturbation, it tends to return to the state of equilibrium existing before it was disturbed. On the contrary an unstable system subjected to a finite perturbation catastrophically fails to return to its initial state of equilibrium. Many real systems in nature do not fall into either of these two categories though. In these systems there are certain times when finite disturbances do not lead to finite results nor catastrophic or runaway reactions. These complicated systems are described as neither stable nor unstable but as systems susceptible to chaos.

Whether or not the stability of the vortex motion in oscillating flows can be categorized as chaotic requires not only an analysis of the vortex motion but also a clear definition and understanding of chaos. Unfortunately the pursuit of this understanding remains the subject of ongoing research and a concise definition is yet elusive. Strides have been made however in identifying chaotic behavior. Systems studied that demonstrate chaotic behavior could best be described as bifurcating systems that operate along a razor's edge or precipice. The slightest disturbance will push the system one way or the other and will lead to decidedly different (but not unstable) results. Additionally, the systems studied reveal that the state of chaotic behavior is not all encompassing but exists more in regions of susceptibility to chaotic behavior preceded and followed by regions of stable behavior.

The application of this analysis of chaotic behavior to vortex motion in oscillating flow is particularly useful due to the complexity of the factors driving the vortex trajectory. The coupling of relative position to other vortices (real or image) in a time dependent flow is both intricate and inseparable. Additionally, the flow field about a bluff body near the surface, combined with the problems of multiple vortices, viscous dissipation, wall reflection and boundary layer and limited coherence length, is extremely intricate. Consequently, the motion of the vortex at times becomes subject to finite perturbations without finite results. The specific coupling that makes the system susceptible to chaotic behavior gives rise to the regions of chaos preceded and followed by regions of stability.

In order to understand these complicated causes and effects first an understanding of the motion of a single potential vortex in oscillating flow about a bluff body is required. Therein lies the impetus of this study. In an ideal two dimensional potential flow, wall reflection, wall boundary layers and coherence length are eliminated. Additional vortices can be added to study mutual induction effects. Further, advanced models of the vortex (i.e. Rankine and Gaussian time dependent models) can clarify the broad effects of viscous dissipation.

The scope of this study includes the potential flow of one and two vortices placed in the vicinity of a circular cylinder in oscillating flow. Emphasis is placed on identifying the onset of chaotic behavior and its effects on the flow characteristics.

II. BACKGROUND

The concept of chaos in dynamic systems is by no means new. However, the detailed investigation as to the onset and mechanisms of chaos is still comparatively young. The primary difficulty in the investigation of chaos is the fact that by definition chaotic behavior is non-integrable. Because of this the first attempts to define the concept of chaos were undertaken by mathematicians. In 1984 Holmes [Ref. 1] investigated chaotic motion in forced oscillations. Here the onset of chaos was linked to periodicity or aperiodic behavior of the function through scrutiny of the harmonics. Although this is a credible definition its application appears limited to the idealized mathematical system from which it was developed. In 1980 Aref [Ref. 2] expanded on this definition and the use of Poincare' maps by illustrating chaotic behavior in paths of finite, ideal, and controllable vortices. His motivation for the investigation was the onset and mechanisms of chaos. Therefore, while the idealized system that he designed was useful for demonstrating chaotic behavior, its application to real world dynamics was severly limited.

Other efforts were made to try to link the study of chaos to systems more closely resembling those found in nature. In 1984 Hardin & Mason [Ref. 3] investigated the two dimensional system of axial vortices in a pipe. This was the first attempt to examine a system that resembled real phenomena and that also underwent chaotic behavior. All previous studies examined chaotic behavior by generating systems susceptible to chaos and then extrapolating the results to possible real world problems.

Finally, in 1986 Dowell & Pezeshki [Ref. 4] investigated the one dimensional Duffings Equation and the onset of chaos. In its relation to real systems Duffings Equations could be used to describe the snap buckling of a beam and other phenomena. In the beam the onset of chaos is easily observed but the integration of the equation to predict or study the mechanisms of chaos is somewhat abstract. Of particular interest in this study was the examination of the onset of chaos by Phase Plane Plots (displacement - velocity plots).

By reasons of their treatment of fluid dynamics in general and vortex motion in particular, Aref's chaotic advection and Hardin & Mason's vortices in a pipe have direct application to this investigation and will be discussed in greater detail.

A. CHAOTIC ADVECTION

Aref [Ref. 2] devised a numerical model to represent the motion of an incompressible inviscid fluid within a circular bounding contour. A stirring agitator was modelled as a potential point vortex. The agitator(s) provided the potential flow within the boundary. A global Eulerian view of an array of markers was traced to examine and verify the poor efficiency of the laminar mixing.

In a follow-up study, he examined the case of two fixed agitators (point vortices) in the fluid that generated "piecewise-constant stirrer motion." The vorticity of the agitators was controllable (on or off) and switched back and forth at prescribed times to generate unsteady flow. Again a marker array of particles was traced. The mixing was clearly superior and Aref classified the motion as chaotic. The parameters that dictate the switching of the vortices and therefore the chaotic regions were cited as mechanisms for chaos.

Extrapolations to real phenomena include enhanced mixing chambers with controllable agitators and similarities to gravitational systems.

B. VORTICES IN A PIPE

The motion of axial vortices was investigated by Hardin and Mason [Ref. 3] because of its widespread appearance in physical situations. These vortices occur in virtually every flow that changes axial directions (i.e. rivers, pipes, lung bronchial tubes, etc.). In these physical systems pairs of counterrotating vortices are produced. This study investigated the effects of one and two pairs of equal strength counterrotating two dimensional potential vortices enclosed in a circular boundary. Vortex advection by induced velocities (real or image) was determined and displayed by means of Eulerian paths of the vortices.

Controlling factors on this investigation were initial locations of the vortices within the boundary. For the case of single pair of vortices the paths were found to be periodic or stable. In the case of two-vortex pairs (four vortices within the boundary), the periodicity of the vortex path and flow was a function of where the vortices were placed initially. This supports the concept of chaotic motions occurring within regions of susceptibility. It was found that within these regions of susceptibility that small perturbations (0.001 radii of the enclosing boundary) were sufficient to drive the vortex path aperiodic and demonstrate chaotic behavior. Hardin & Mason [Ref. 3] do note that experimental evidence indicates that bifurcating or branching flows are

quantitatively more stable in real viscous flows than these numerical results suggest. This is attributed to the complexity of this secondary flow as well as viscous dissipation, vortex decay and coring influences. It does not, however, diminish the validity of the study or the qualitative results of the susceptibility of fluid flows to the onset of chaos.

III. ANALYSIS

A. INTRODUCTION

In 1976 Sarpkaya [Ref. 5] presented extensive data on oscillating flow about circular cylinders. In addition to modifying the long standing Morison Equation, this data also provided extreme insight into transverse forces on the cylinder. Performed at Reynolds numbers of prototype magnitude and across a wide spectrum of Keulegan-Carpenter [Ref. 6] numbers, these experiments provided a data base to which all subsequent publications and literature on the subject has been based. Of particular significance and not predicted by the Morison Equation was the documentation of cycle-to-cycle variations in pressures and forces across the cylinder in pure harmonic flow (see Figure E.1). These variations, particularly significant in the transverse direction, were attributed primarily to limited coherence lengths and to a lesser extent wall reflections and boundary layers.

The distorting effects of coherence length on the wake of a circular cylinder in uniform flow was clearly discussed by Gerlach [Ref. 7] and Graham [Ref. 8.] In oscillating flows, however, the von Karman street forms perpendicular or transverse to the flow direction in the range $8 < K_c < 13$. This makes experimentation to identify the coherence length extremely difficult. In an effort to specifically examine the effects of spanwise coherence, O'Keefe [Ref. 9] in 1986 undertook similar experiments to Sarpkaya [Ref. 5] but with the minimum aspect ratio (L/D = 2.0) that could be accurately instrumented. These nearly two dimensional experiments provided extremely accurate data that was not blurred by the influence of a limited coherence length. Cycle-to-cycle variations in in-line and transverse forces remained though; particularly in the Keulegan-Carpenter number range $8 < K_c < 13$.

Knowing that at any given point in time the forces acting on the cylinder is governed primarily by one dominant vortex, a detailed investigation of one potential vortex in the vicinity of a circular cylinder in harmonically oscillating flow was dictated. After an investigation of the single vortex case the follow-up was to investigate two potential vortices in the vicinity of a circular cylinder.

B. POTENTIAL FLOW MODELING

1. One Vortex Model

In the complex plane the potential flow field for a vortex in the vicinity of a circular cylinder in harmonically oscillating flow is given by the following expression:

$$f(z) = U_{max}\sin(\omega t)(z+\frac{c^2}{z}) + i\frac{\Gamma}{2\pi}\ln(z-z_o) - i\frac{\Gamma}{2\pi}\ln(z-\frac{c^2}{\overline{z}_o}) \qquad (3.1)$$

where: c - radius of the cylinder
Γ - strength of the vortex
ω - frequency of the oscillating flow
U_{max} - maximum amplitude of the flow velocity
z_o - location of the vortex

In nondimensional form this expression becomes:

$$f(\zeta) = \sin(2\pi\tau)(\zeta+\frac{1}{\zeta}) + iK\ln(\zeta-\zeta_o) - iK\ln(\zeta-\frac{1}{\overline{\zeta}_o}) \qquad (3.2)$$

where: $K = \Gamma/(2\pi c U_{max})$
$\tau = t/T$ (T - period of the flow)
$\zeta = z/c$

This expression can be differentiated with respect to ζ to determine the flow field velocities. At $\zeta = \zeta_o$ the expression for the velocity of the vortex becomes:

$$\frac{\partial f}{\partial \zeta}\Big|_{\zeta=\zeta_o} = u - iv = \sin(2\pi\tau)(1-\frac{1}{\zeta^2}) - \frac{iK}{r_v} \qquad (3.3)$$

where r_v is the radius between the real and image vortex and is given by:

$$r_v = \zeta_o - \frac{1}{\overline{\zeta}_o} \qquad (3.4)$$

(Note that the second term of eqn 3.2 is dropped since a vortex does not impart velocity to itself.)

Calculations for the forces acting on the cylinder were made by integrating the Blasius Force Equation:

$$D - iL = \frac{1}{2} i\rho \oint \left(\frac{\partial f}{\partial z}\right)^2 dz + i\rho \frac{\partial}{\partial t} \oint \bar{f}\, d\bar{z} \tag{3.5}$$

Nondimensionalized and evaluated at $\zeta = \zeta_o$, this equation reduces to the following form:

$$D' - iL' = \frac{2\pi^2}{K_c} \cos(2\pi\tau) + \frac{\pi K}{K_c} \frac{\partial}{\partial \tau} \left(\zeta_o - \frac{1}{\bar{\zeta}_o}\right) \tag{3.6}$$

where: $K_c = (U_{max} T)/(2c)$

2. Two Vortex Model

Invoking the same procedure as the one vortex model it can be shown that the velocity of two vortices A and B in the vicinity of a the circular cylinder is given by:

$$\left.\frac{\partial f}{\partial \zeta}\right|_{\zeta = \zeta_A} = u - iv = \sin(2\pi\tau)\left(1 - \frac{1}{\zeta_A^2}\right) - \left(\frac{iK}{\zeta_A - 1/\bar{\zeta}_A}\right) - \left(\frac{iK}{\zeta_A - \zeta_B}\right) + \left(\frac{iK}{\zeta_A - 1/\bar{\zeta}_B}\right) \tag{3.7}$$

$$\left.\frac{\partial f}{\partial \zeta}\right|_{\zeta = \zeta_B} = u - iv = \sin(2\pi\tau)\left(1 - \frac{1}{\zeta_B^2}\right) - \left(\frac{iK}{\zeta_B - 1/\bar{\zeta}_A}\right) - \left(\frac{iK}{\zeta_B - \zeta_A}\right) + \left(\frac{iK}{\zeta_B - 1/\bar{\zeta}_B}\right) \tag{3.8}$$

3. Rankine Vortex Model

A standard rankine vortex model was used with linear velocity distribution between 0 and r_{core}. The value of the core radius was chosed to be 0.10 times the radius of the cylinder generating the vortices.

4. **Gaussian Time Dependent Vortex Model**

A standard Gaussian time dependent vortex model was used where the generalized expression for the velocity distribution is:

$$V = \frac{\Gamma_o}{2\pi r}\{1 - \exp(-\frac{r^2}{\nu t_v})\} \tag{3.9}$$

Here t_v is not the clock time of the flow but the life time of the vortex. It has been shown that differentiating this with respect to the radius yields $r^* = 2.24\sqrt{(\nu t_v)}$ as the expression for the core radius of the vortex. Nondimensionalizing eqn 3.8 in terms of the oscillating flow parameters, and examing the velocity of a vortex from eqn 3.3, the velocity of a Gaussian time dependent vortex is given by:

$$\frac{\partial f}{\partial \zeta}\Big|_{\zeta=\zeta_o} = u - iv = \sin(2\pi\tau)(1-\frac{1}{\zeta^2}) - \frac{iK}{r_v}\{1 - \exp(-\frac{r_v^2\sqrt{(K_c/Re)}}{16(t_v/T)})\} \tag{3.10}$$

For the modeling the Reynolds Number was chosen to be Re = 10,000 and t_v was set such that the core of the vortex was $r^* = 0.10$ at inception.

5. **Numerical Integration and Accuracy**

In this analysis a finite differencing technique was employed. The study of potentially chaotic systems requires a high degree of accuracy. Due to its guaranteed stability and overall efficiency, the Adams-Moulton predictor corrector method was selected to convect the vortices:

$$z_{np} = z_{n-1} + (55\, q_{n-1} - 59\, q_{n-2} + 37\, q_{n-3} - 9\, q_{n-4})\frac{\Delta t}{24} \tag{3.11}$$

$$z_n = z_{n-1} + (9\, q_{np} + 19\, q_{n-1} - 5\, q_{n-2} + q_{n-3})\frac{\Delta t}{24} \tag{3.12}$$

In addition to ensured stability, this method provided fourth order accuracy with local error $O(h^5)$. With 1440 time steps per cycle, the local error remained at the limits of double precission machine accuracy. Initial startup was made using the fourth order Runge-Kutta scheme. All continuations were based on the last four calculated locations of the vortices, thereby ensuring accuracy and duplication at any cycle.

While discussing accuracy it must be noted, as mentioned earlier, that by definition chaotic behavior is non-integrable. Whatever scheme used can only illustrate qualitatively the onset of chaos. If used for comparison universally, all methods yield equally valid qualitative results. The effort devoted here to accuracy is therefore to ensure the validity of the results and add to overall integrity of this report.

IV. RESULTS

A. GENERAL

From Sarpkaya [Ref. 5] and other studies, it is concluded that the region of special interest in the field of oscillating flows is confined to $8 < K_c < 13$, an interval in which a half transverse vortex street is generated. It is because of this reason that in the present numerical experimentation K_c was chosen equal to 10.0.

The vortex path is a function of both the imposed ambient flow field and the velocities induced by the vortices (real or image). This coupling was first investigated through the use of a single vortex in uniform flow in the vicinity of a circular cylinder. Figure E.2 illustrates the path of the vortex for various vortex strengths ($\mathbf{K} = 0.5, 0.625, 0.75$). It is seen that the *capture* by the image vortex (partial looping) lasts only until the flow field around the cylinder *pushes* the vortex away from the image. It is also seen that this capture is a function of the initial location of the vortex. When the vortex is captured, sharp cusps appear where the direction of motion of the vortex is quickly reversed. These characteristics played even more decisive roles in the unsteady case. With the exception of the foregoing, the vortex strengths used in the numerical experimentation were all set at $\mathbf{K} = 0.50$.

B. ONE VORTEX MODEL

Initial experimentation included varying the starting locations and times of the single point vortex in order to observe the vortex path and force coefficients. Figures E.3 through E.6 show the force coefficients for various starting locations and times and varying numbers of cycles. These figures clearly show cycle-to-cycle variations in both the inline and transverse force coefficients. In comparison to experimental force traces shown in Figure E.1, of comparable K_c, the variations are of similar magnitude and shape.

Understanding the origin of these cycle-to-cycle variations required a scrutiny of the vortex paths themselves. Figures E.7 and E.8 show two starting positions of the vortex of (0, 1.5083) and (0, 1.5084). The oscillating flow velocity was set at $U_o = 0^+$ (superscript indicates the initial x-direction). Figures E.7(a) and E.8(a) show that for at least the first five cycles of the flow the vortex paths are virtually identical. Also noted in this figure are sharp cusps where the overall direction of the vortices is abruptly changed.

Although the difference in the begining locations of the sixth cycle is virtually inperceptible {$\zeta = (0.995, 0.723)$ vice $\zeta = (0.970, 0.753)$}, the vortex in Figure E.7(b) forms a sharp cusp at the top of the cylinder (geographical location of the maximum velocity at any time in the flow) but the vortex in Figure E.8(b) is captured by its image and orbits the cylinder. The ending points for cycle six are grossly different {see Figures E.7(c) and E.8(c)} and the vortex paths never again become similar. The finite perturbation in starting location has yielded explicitly different results. Nevertheless, the vortex paths in Figures E.7(c) and E.8(c) remain bounded. Extending the calculations to 100 cycles of the flow, Figure E.9 shows that while neither vortex paths are identical, both remain bounded. They clearly seem to slide in and out of chaotic behavior, preceded and followed by periods of stability.

Figure E.10 is a plot of the magnitude of the velocity of the vortices. It is again evident that these two vortices have virtually identical velocity magnitudes until the sixth cycle of flow. The capture and looping depicted in Figures E.7(b) and E.8(b) is also evident in Figure E.10. Breaking down this velocity magnitude into its u and v components, Figures E.11 through E.13 show that overall periods of stability are intermixed with these vortex captures.

Figures E.14 through E.19 and E.20 through E.25 are similar investigations that document two starting points of the vortices where both initial x-locations were set at $x = 0.0$ and the oscillating flow velocity was set at $U_o = U^{+}_{max}$ and $U_o = U^{-}_{max}$, respectively. Figures E.26 through E.31 are similar investigations that document two starting points of the vortex in the vicinity of $x = 1.0$, $y = 1.0$, and the oscillating flow velocity was set at $U_o = 0^{+}$. These investigations support the conclusions of the first investigation and demonstrate once again a finite precission input does not yield a finite precission output. They also demonstrate the periods of stability that precede and follow chaotic behavior, (i.e., chaos in order and order in chaos).

As seen in the proceeding set of experiments, the looping or continued looping of the vortex tightly around the cylinder, was a function not only of the location of the vortex but also of the current state of the oscillating flow. This suggests that at a given initial location, a variance of initial velocity or phase shift of the oscillating flow could drive the system from stable to chaotic behavior at a given point in time. Figure E.32 is a series of vortex paths that supports this concept. Four vortex paths were generated with the initial location of $x = y = 1.0$ and a variance of initial velocity by a phase shift from 0.75 ($U_o = U^{-}_{max}$) to 1.0 ($U_o = 0^{+}$). It is clear that while the Figure

E.32(a) documents stability even after ten cycles, the cusps and asymmetric tracks in Figure E.32(d) demonstrate the mixture of stable and chaotic regions.

Figure E.33 depicts the results of a similar investigation where the initial location of the vortices is at (0, 2.2192) and (0, 2.2193). These results also show that the chaotic behavior depends not only on the vortex location but also on the flow environment. In fact, the two are coupled inseparably.

The stability and symmetry of Figures E.32(a) and E.33(a) also suggest, however, that chaotic motion may not be inevitable. They infer that the location of the vortex and field flow may be *tuned* in such a way as to permanently avoid chaos. This would be paramount to permanently balancing on a razor's edge. However, such a balance is unstable. As seen in the first investigation, the slightest disturbance is sufficient to push the system into chaotic behavior.

The final phase of the one vortex experiment was to examine the effects of higher order models of a potential vortex in an effort to better understand vortices in nature. Figure E.34 is a comparison of the results obtained with ideal, Rankine, and Gaussian time dependent vortex models. It is clear from these figures that while the onset of chaos may be different, the chaotic behavior and susceptibility to chaos remains virtually the same.

C. TWO VORTEX MODEL

Separated flow past a bluff body generates pairs of counterrotating vortices. In both steady and oscillating flow about a circular cylinder, the first vortex pair is formed symmetrically and is significantly stronger than subsequent asymmetric vortices. Additionally, it has been documented that in oscillating flow in the region $8 < K_c < 13$, a half von-Karman vortex street forms perpendicular or transverse to the flow direction. In this section of the experimentation, two vortices were placed in the vicinity of a circular cylinder immersed in a harmonically oscillating flow. The vortices were tracked through various numbers of cycles of flow. The locations and strengths of the vortices were varied in order to examine the mechanism for the formation of a half von-Karman street. Additionally, the stability of the vortices as discussed in the one vortex model was examined. For all of the investigations, the characteristic of the flow was set at $K_c = 10.0$. The strength of the vortices was set at $\mathbf{K} = 0.50 \pm \delta$ (although contrary in direction), and their locations at $\zeta_A = (a,a)$ and $\zeta_B = (a \pm \delta, -a \pm \delta)$, where $0.80 < a < 1.414$, and $\delta << 1$. Based on flow visualization, the initial velocity was set at $U_o = \bar{U}_{max}$.

The first part of the investigation required the analysis of vortices, symmetric in strength and location. Figure E.35 demonstrates that within the regions examined, the mutual induction velocities between the real vortices dominate the advection of the vortices. It is also clear that the vortices are quickly convected away in parallel paths. The initial radial location determines the separation distance of the two parallel paths. This separation distance combined with the strength of the vortices determines the rate at which the vortices are swept away.

Figures E.36 through E.38 are of a series of investigations where the vortices have equal strengths ($K_A = K_B$) but the locations are asymmetric ($|\zeta_B| = \varepsilon_r \times |\zeta_A|$). The overall result is a general curving of the vortex path toward the vortex that had the larger initial radial distance from the cylinder. This is a result of the image vortices having a greater effect on the vortex that was closer to the cylinder. It is seen from Figure E.37 that a 10% difference ($\varepsilon_r = 0.90$) in the two starting locations is sufficient to significantly curve the vortex paths. The vortex paths do not gravitate to each other though and the vortices do not become coincident.

Figures E.39 through E.42 are of a series of investigations where the vortices have symmetric initial locations ($\zeta_A = \zeta_B$) and asymmetric strengths ($K_B = \varepsilon_K \times K_A$). The result here is a curvature similar to that of the previous investigation. From Figure E.41 it is seen that only a 5% difference ($\varepsilon_K = 0.95$) in the vortex strengths is sufficient to significantly alter the vortex paths. Clearly the results indicate that the system is much more sensitive to asymmetry in vortex strengths than to asymmetry in vortex location. Again the vortices do not become coincident.

Figure E.43 is a combination of the previous investigations where there is asymmetry in both the vortex strengths ($K_B = \varepsilon_K \times K_A$) and in initial location ($|\zeta_B| = \varepsilon_r \times |\zeta_A|$). Again both vortex tracks bend toward the dominant vortex but as expected, with a more severe curvature. Although in real flow two vortices are generated every time the oscillating flow direction changes, this study of two vortices moving together to either the top or bottom of the cylinder is particularly significant. It suggests the evolution of a half von-Karman vortex street transverse to the flow based on the asymmetry of the vortices in the street.

Finally, an investigation was made where the asymmetry of the vortices was so extensive that the vortex paths curved back to the vicinity of the cylinder. Although in viscous flow the life of a vortex is finite, combinations of additional vortices coupled with the flow field make this situation plausible and warrants its investigation. Figure

E.44 documents the sharp cusps, capture, and chaotic behavior of the vortices as discussed in the previous section. With the additional vortex (and image) the coupling is much more complicated between the geographical location of the vortex and the flow field. The identification of chaotic behavior is none the less possible.

V. CONCLUSIONS

The results presented herein warranted the following conclusions:

1. Finite precision information about the initial characteristics of a vortex (or of larger number of vortices) provides no finite-precision information about the characteristics of flow at later times and that the lack of spanwise coherence of the vortices is not the sole cause of cycle-to-cycle variations in the measured quantities.
2. An idealized vortex model suggests that the sensitivity of the characteristics of the flow to random disturbances superimposed on the motion of vortices at an earlier time is the main flow feature responsible for the observed cycle-to-cycle variations.
3. The chaotic behavior of the vortex in oscillating flow occurs in regions of susceptibility similar to those found by Dowell and Pezeshki [Ref. 4] with similar sensitivity.
4. The susceptible regions for chaos in oscillating flow are coupled inseperably with the location of the vortices and the state of the environmental flow field. In other worlds, for a given flow phase there is a vortex location that will lead to chaos. Likewise, for every vortex position near the cylinder, there is a particular flow phase that will eventually lead to chaos.
5. The formation of a half von-Karman vortex street in the range of $8 < K_c < 13$ may be attributed to the asymmetry in the formation of the vortices.
6. The extent to which the sensitivity of the flow to the conditions prevailing in the previous cycles is damped by finite core effects and viscosity has been investigated and it has been shown that they change only the time of onset of the chaos, not its invevitable occurrence.

APPENDIX A
ONE VORTEX COMPUTER MODEL

```
C ***********************************************************************
C *                                                                     *
C *                          V O R T E X                                *
C *                                                                     *
C *                        BY LT. W.T. MCCOY                            *
C *                                                                     *
C ***********************************************************************
C
C                          DESCRIPTION
C
C THIS PROGRAM TRACKS A VORTEX IN COMPLEX SPACE AROUND A UNIT CYLINDER
C IN OSCILLATING FLOW.  INITIAL LOCATION, STARTING TIME, AND THE NUMBER
C OF CYCLES OF THE OSCILLATING FLOW ARE REQUIRED INPUT.
C
C THE PROGRAM IS DESIGNED TO RUN ON DISSPLA BY USING THE FOLLOWING
C DISSPLA EXEC COMMAND:'DISSPLA VORTEX'. IT IS CURRENTLY
C DIMENSIONED TO RUN A MAX OF 10 CYCLES AT 1440 STEPS PER CYCLE.
C 2.0M OF VIRTUAL MEMORY IS REQUIRED TO RUN THE PROGRAM AT MAXIMUM
C CAPACITY.  THE PROGRAM IS INTERACTIVE FOR INPUT OPTIONS.
C
C ALL CONSTANTS ARE SET IN THE MAIN PROGRAM.  PREVIOUS INPUT OPTIONS
C ARE READ FROM FILE 'FILE FT25F001'.  FAILURE TO GENERATE THIS FILE
C PRIOR TO INITIAL RUNNING RESULTS IN A ERROR MESSAGE AND TERMINATION
C OF THE RUN.  PRIOR TO RUNNING, FILE 'FILE FT25F001' SHOULD BE
C INITIATED CONTAINING 4 COMPLEX NUMBERS, 1 REAL NUMBER, AND 1 INTEGER.
C WITH THIS INPUT THE PROGRAM DOES  NOT NEED TO BE TO BE RECOMPILED
C FOR EACH RUN.
C
C THIS PROGRAM IS WRITTEN IN DOUBLE PRECISION AND EMPLOYS THE MILNE
C PREDICTOR-CORRECTOR CONVECTION SCHEME, WITH INITIAL POINTS GENER-
C ATED BY A 4TH ORDER RUNGE-KUTTA SCHEME.
```

```
C
C OUTPUT OF THE PROGRAM INCLUDES THE LAST FOUR VALUES OF THE LOCATION
C OF THE VORTEX, FINISH TIME, AND THE NUMBER OF CYCLES.  THESE VALUES
C ARE WRITTEN IN FILE 'FILE FT25F001' AND ALLOW FOR OBSERVATIONS BEYOND
C THE MAX LIMIT OF 10 CYCLES BY CONTINUING WITH ADDITIONAL RUNS.
C
C OUTPUT FOR THE VORTEX PATH AS WELL AS FORCE COEFFICIENTS AND
C VELOCITY MUNIPULATIONS ARE MADE GRAPHICALLY.  SELECTIONS OF PLOTS
C FOR OUTPUT ARE MADE INTERACTIVELY.  PLOTS MAY BE MADE ON
C A TEK618 OR SENT TO A METAFILE (PRE-EDIT SUBROUTINE 'GRAPH').
C
C
C.....................................................................
C
C           ALPHABETICAL LISTING OF VARIABLES
C
C     VARIABLE     (SUBROUTINE USED) DESCRIPTION.
C
C.....................................................................
C
C     CD(N).........(GRAPH)NON-DIMENSIONAL ARRAY OF INLINE (DRAG)
C                   FORCE COEFFICIENTS FOR VORTEX POSITION Z(N).
C
C     CL(N).........(GRAPH)NON-DIMENSIONAL ARRAY OF PERPENDICTULAR
C                   (LIFT) FORCE COEFFICIENTS FOR VORTEX POSITION
C                   Z(N).
C
C     COEF..........(FORCE,GRAPH)COMPLEX VARIABLE CONTAINING AS ITS
C                   PARTS THE NON-DIMENSIONAL FORCE COEFFICIENTS.
C
C     DELTAT........(STEP,Q,OUTPUT,FORCE,GRAPH)INCREMENTAL STEP
C                   IN NON-DIMENSIONAL TIME (INVERSE OF STEPS PER
C                   CYCLE).
C
C     DELZ..........(STEP)COMPLEX INCREMENTAL STEP OF THE LOCATION
```

```
C                 OF THE VORTEX (FROM Z1 TO Z2).
C
C     DFDZ.....(Q)COMPLEX PARTIAL DERIVATIVE OF THE COMPLEX
C                 FUNCTION F WITH TO RESPECT Z.
C
C     DISP(N)......(STEP,GRAPH)ARRAY CONTAINING THE TOTAL DISPLACEMENT
C                 OF THE VORTEX FOR A CORRESPONDING LOCATION Z(N).
C
C     I............(Q,FORCE)CONSTANT COMPLEX NUMBER = (0.0,1.0)
C
C     ILHS.....(GRAPH)LEFT HAND VALUE OF THE TIME AXIS OF THE
C                 FORCE COEFFICIENT PLOT.
C
C     IRHS.....(GRAPH)RIGHT HAND VALUE OF THE TIME AXIS OF THE
C                 FORCE COEFFICIENT PLOT.
C
C     ISTEPS.......(ALL)NUMBER OF INCREMENTAL STEPS PER CYCLE TO BE
C                 TAKEN FOR ALL ITERATIONS.
C
C     K1-4.....(RUNGE) RUNGE-KUTTA CONSTANTS
C
C     KAPPA........(ALL)STRENGTH OF THE VORTEX (GAMMA/(2*PI*UMAX))
C
C     KC...........(ALL) KEULLEGAN-CARPENTER NUMBER FOR THE OSCILLATING
C                 FLOW.
C
C     L1...........(INPUT,GRAPH) LOGICAL OPERATOR.
C
C     NUMCYC.......(INPUT)TOTAL NUMBER OF CYCLES TO BE EVALUATED.
C
C     NUMPTS.......(ALL)TOTAL NUMBER OF POINTS TO BE DETERMINED.
C                 (NUMCYC * ISTEPS)
C
C     PHSHFT.......(GRPAH)INITIAL PHASE SHIFT OF THE FLOW (0<PHSHFT<1)
C
```

```
C     PI.....(ALL)CONSTANT = 3.141592654
C
C     Q.....(Q)FUNCTION SUBROUTINE WHERE Q IS THE COMPLEX
C                VELOCITY OF THE VORTEX.
C
C     QMAG(N).....(GRAPH)ARRAY CONTAINING THE MAGNITUDE OF THE
C                COMPLEX VELOCITY QVECT(N).
C
C     QVECT(N).....(STEP,GRAPH)COMPLEX ARRAY CONTAINING THE VELOCITY
C                OF THE VORTEX AT ANY POINT Z(N).
C
C     RV.....(Q) VECTOR BETWEEN THE VORTEX AND ITS IMAGE
C                WITHIN THE CYLINDER
C
C     T.....(GRAPH)NON-DIMENSIONAL TIME (0-1 FOR A CYCLE).
C
C     TE.....(RUNGE,Q)NON-DIMENSIONAL ENVIRONMENTAL FLOW TIME.
C
C     TT.....(STEP,Q,FORCE)NON-DIMENSIONAL TIME CHANGED TO
C                RADIANS FOR COS/SIN EVALUATIONS (0-2*PI FOR A CYCLE).
C
C     TTF.....(OUTPUT)NON-DIMENSIONAL FINISH TIME OF THE RUNS.
C
C     TTI.....(ALL)INITIAL NON-DIMENSIONAL STARTING TIME FOR THE
C                OSCILLATING FLOW.
C
C     TV.....(Q)NON-DIMENSIONAL TIME LIFE OF THE VORTEX.
C                (TE + CONSTANT FOR R-CORE AT INCEPTION)
C
C     U.....(GRAPH)X-DIRECTION VELOCITY MAGNITUDE.
C
C     V.....(GRAPH)Y-DIRECTION VELOCITY MAGNITUDE.
C
C     Z.....(ALL)INSTANTANEOUS COMPLEX LOCATION OF THE VORTEX.
C
```

```
C     ZI.....(GRAPH)IMAGINARY(Y) LOCATIONOF THE VORTEX.
C
C     ZP.....(Q)COMPLEX PREDICTED VALUE FOR Z(N)
C
C     ZR.....(GRAPH)REAL(X) LOCATION OF THE VORTEX.
C
C     ZZ.....(Q)DUMMY ARGUMENT FOR THE FUNCTION SUBROUTINE Q
C                 WHICH CONTAINS THE PASSED VALUE OF Z(N).
C                 (RUNGE) DUMMY ARGUMENT CALL FUNCTION SUBROUITNE Q
C
C ..............................................................
C
C
C ***************************************************************
C *                        MAIN PROGRAM                         *
C ***************************************************************
C
      IMPLICIT REAL*8 (A-H,O-Z)
      REAL*8 KC,KAPPA
      REAL*4 DISP(14409),CD(14409),CL(14409)
      COMPLEX*16 Z(14409),QVECT(14409)
      COMMON /FIRST/ TTI,ISTEPS /SECOND/ NUMPTS /THIRD/ KC,KAPPA
     1       /FOURTH/ PI
C
C  SET CONSTANTS
C
      KAPPA = 0.5D0
      KC = 10.D0
      PI = 3.141592654D0
      ISTEPS = 1440
C
   10 CALL INPUT (Z)
      CALL STEP (Z,QVECT,DISP)
      CALL OUTPUT(Z)
      CALL FORCE(Z,CD,CL)
```

```
      CALL GRAPH (Z,QVECT,DISP,CD,CL)
C
      WRITE (6,*)'DO YOU WISH TO RE-RUN THE PROGRAM?  1-YES, 0-NO'
      READ (5,*) L1
      IF (L1.NE.1) GOTO 20
      WRITE (6,*) 'EXECUTION CONTINUES ..... '
      GOTO 10
   20 CONTINUE
C
      CALL DONEPL
      STOP
      END
C
C
C ***********************************************************************
C *                    SUBROUTINE INPUT                                 *
C ***********************************************************************
C
C THIS SUBROUTINE INTERACTIVELY INPUTS THE VALUES FOR THE INITIAL
C LOCATION OF THE VORTEX, STARTING TIME, AND THE NUMBER OF CYCLES
C TO BE EXAMINED.
C
      SUBROUTINE INPUT (Z)
      IMPLICIT REAL*8 (A-H,O-Z)
      COMPLEX*16 Z(14409)
      COMMON /FIRST/ TTI,ISTEPS /SECOND/ NUMPTS
C
C  READ THE LAST 4 POINTS FOR CONTINUATION OPTION
C
      REWIND 25
      DO 10 N = 1,4
   10 READ(25,*) Z(N)
      READ(25,*) TTI
      READ(25,*) NUMCYC
C
```

```
C  CONTINUATION OPTION
C
       WRITE(6,*) 'DO YOU WISH TO CONTINUE THIS RUN FORM THE LAST?  1-YES
      #  0-NO'
       READ(5,*) L1
       IF (L1.NE.0) GOTO 20
       WRITE(6,*)'INPUT THE NEW STARTING POINT Z(1): (REAL,IMAG)'
       READ(5,*) Z(1)
       WRITE(6,*)'INPUT THE NEW VALUE OF TTI:'
       READ(5,*) TTI
C
C  CALL SUBROUTINE RUNGE TO GENERATE THE FIRST 4 POINTS
C
       CALL RUNGE (Z)
C
C  INPUT THE NUMBER OF CYCLES TO BE ANALYZED
C
   20 WRITE(6,*)'THE LAST VALUE FOR NUMCYC =',NUMCYC
       WRITE(6,*)'DO YOU WISH TO CHANGE IT?  1-YES 0-NO'
       READ(5,*) L1
       IF(L1.NE.1) GOTO 30
       WRITE(6,*) 'INPUT THE NEW VALUE OF NUMCYC:'
       READ(5,*) NUMCYC
   30 CONTINUE
C
       NUMPTS = NUMCYC * ISTEPS + 4
C
       RETURN
       END
C
C
C ***************************************************************************
C *                        SUBROUTINE RUNGE                                 *
C ***************************************************************************
C
```

```
C THIS SUBROUTINE USES A 4TH ORDER RUNGE-KUTTA METHOD TO GENERATE THE
C FIRST FOUR VALUES OF Z.
C
      SUBROUTINE RUNGE (Z)
      IMPLICIT REAL*8 (A-H,O-Z)
      COMPLEX*16 Z(14409),Q,K1,K2,K3,K4,ZP1,ZZ
      COMMON /FIRST/ TTI,ISTEPS
C
      DELTAT = 1.D0/DFLOAT(ISTEPS)
C
C  RUNGE-KUTTA EVALUATION FOR FIRST FOUR POINTS
C
      DO 5 N = 1,3
      ZZ = Z(N)
      TE1 = (DFLOAT(N-1) * DELTAT + TTI)
      K1 = DLETAT * Q(ZZ,TE1)
      ZZ = Z(N)+0.5D0*K1
      TE2 = TE1+ 0.5D0*DELTAT
      K2 = DELTAT * Q(ZZ,TE2)
      ZZ = Z(N)+0.5D0*K2
      K3 = DELTAT * Q(ZZ, TE2)
      ZZ = Z(N) + K3
      TE4 = TE1 + DELTAT
      K4 = DELTAT * Q(ZZ, TE4)
C
    5 Z(N+1) = Z(N) + (K1-2.D0*K2+2.D0*K3+K4)/6.D0
C
C
C
      RETURN
      END
C
C
C ***********************************************************************
C *                      SUBROUTINE STEP                                *
```

```
C ***************************************************************
C
C THIS SUBROUTINE PROGRESSIVELY CALCULATES THE VALUES OF Z(N), BASED ON
C A PREDICTOR-CORRECTOR CONVECTION SCHEME.
C IT ALSO DETERMINES THE VELOCITY VECTOR, MAGNITUDE AND PARTS FOR
C FUTURE MUNIPULATION AS WELL AS OVERALL DISPLACEMENT MAGNITUDES.
C
      SUBROUTINE STEP (Z,QVECT,DISP)
      IMPLICIT REAL*8 (A-H,O-Z)
      REAL*4 DISP(14409)
      REAL*8 KC,KAPPA
      COMPLEX*16 Z(14409),QVECT(14409),DELZ,ZP,Q,ZZ
      COMMON /FIRST/ TTI,ISTEPS /SECOND/ NUMPTS/THIRD/ KC,KAPPA
C
      DELTAT = 1.D0/DFLOAT(ISTEPS)
C
C  EVALUATE VELOCITIES AND DISPLACEMENTS FOR FIRST 4 POINTS
C
      DISP(1) = 0.0
C
      DO 7 N = 1,4
      TE = (DFLOAT(N-1) * DELTAT + TTI)
      ZZ = Z(N)
      QVECT(N) = Q(ZZ,TE)
    7 DISP(N+1) = Z(N+1) - Z(N)
C
      DO 10 N = 5, NUMPTS
      NM1 = N-1
      NM2 = N-2
      NM3 = N-3
      NM4 = N-4
      TE = (DFLOAT(N-1)*DELTAT+TTI)
C
C  CALCULATE PREDICTED VALUE OF Z(N)
C
```

```
       ZP = Z(NM1)+(55.D0*QVECT(NM1) -59.D0*QVECT(NM2) +37.D0*QVECT(NM3)
      1 -9.D0*QVECT(NM4))*DELTAT* 2.D0 * KC / 24.D0
C
C CALCULATE ACTUAL VALUE OF Z(N)
C
       DELZ = (9.D0*Q(ZP,TE) + 19.D0*QVECT(NM1) -5.D0*QVECT(NM2)
      1 +QVECT(NM3) )*DELTAT * 2.D0 * KC / 24.D0
       Z(N) = Z(NM1) + DELZ
C
C  EVALUATE VELOCITIES AT Z(N)
C
       QVECT(N) = Q(Z(N),TE)
    10 DISP(N) = DISP(NM1) + ABS(DELZ)
C
C
       RETURN
       END
C
C
C ---------------------------------------------------------------------
C |                FUNCTION SUBPROGRAM Q                              |
C ---------------------------------------------------------------------
C
C THIS FUNCTION SUBPORGRAM IS USED TO EVALUATE VALUES OF Q
C
       COMPLEX FUNCTION Q*16(ZZ,TE)
       IMPLICIT REAL*8 (A-H,O-Z)
       REAL*8 KC, KAPPA
       COMPLEX*16 ZZ, DFDZ, I,RV
       COMMON /FIRST/ TTI,ISTEPS /THIRD/ KC,KAPPA /FOURTH/ PI
C
       I = (0.D0,1.D0)
       DELTAT = 1.D0/DFLOAT(ISTEPS)
       TT = TE * 2.D0* PI
C
```

```
      RV = ZZ - 1.D0 / DCONJG(ZZ)
C
      DFDZ =DSIN(TT)*(1.D0-1.D0/(ZZ*ZZ))-I*KAPPA/RV
C
      Q = DCONJG(DFDZ)
C
      RETURN
      END
C
C
C ***************************************************************************
C *                     SUBROUTINE OUTPUT                                   *
C ***************************************************************************
C
C  THIS SUBROUTINE IS USED TO SAVE THE FINAL VALUES OF Z,TT, AND NUMCYC
C  FOR POSSIBLE CONTINUATION OF THE PLOTS.
C  THE VALUES ARE SAVED IN FILE 'FILE FT25F001'.
C
      SUBROUTINE OUTPUT(Z)
      IMPLICIT REAL*8 (A-H, O-Z)
      COMPLEX*16 Z(14409)
      COMMON /FIRST/ TTI,ISTEPS /SECOND/ NUMPTS
C
      DELTAT = 1.D0/FLOAT(ISTEPS)
      NN = NUMPTS - 4
      TTF = DFLOAT(NN)* DELTAT + TTI
      NUMCYC = NN / ISTEPS
C
      REWIND 25
      DO 10 N = 1,4
      NN = NN + 1
   10 WRITE(25,*) Z(NN)
      WRITE(25,*) TTF
      WRITE(25,*) NUMCYC
C
```

```
      RETURN
      END
C
C
C ***********************************************************************
C *                        SUBROUTINE FORCE                             *
C ***********************************************************************
C
C  THIS SUBROUTINE IS USED TO CALCULATE THE FORCE COEFFICIENTS CD, AND
C  CL FOR THE CYLINDER BASED ON THE LOCATIONS OF THE VORTEX AND A
C  FINITE DIFFERENCING SCHEME.
C
      SUBROUTINE FORCE(Z,CD,CL)
      IMPLICIT REAL*8 (A-H, O-Z)
      REAL*4 CD(14409),CL(14409)
      REAL*8 KC, KAPPA
      COMPLEX*8 COEF
      COMPLEX*16 Z(14409), I
      COMMON /FIRST/ TTI,ISTEPS /SECOND/ NUMPTS /THIRD/ KC,KAPPA
     1       /FOURTH/ PI
C
      I = (0.D0, 1.D0)
      DELTAT = 1.D0/DFLOAT(ISTEPS)
C
      DO 10 N = 2, NUMPTS
C
      TT = (DFLOAT(N-1) * DELTAT + TTI) * 2.D0 * PI
C
      COEF = (2.D0*PI*PI/KC)*DCOS(TT)
     1       + ((PI*KAPPA)/(KC*DELTAT))*I*
     2       ((Z(N)-1.D0/DCONJG(Z(N)))-
     3       (Z(N-1) - 1.D0/DCONJG(Z(N-1))))
      COEF = CONJG(COEF)
      CD(N) = REAL(COEF)
   10 CL(N) = IMAG(COEF)
```

```
C
      RETURN
      END
C
C
C ***************************************************************************
C *                      SUBROUTINE GRAPH                                   *
C ***************************************************************************
C
      SUBROUTINE GRAPH (Z,QVECT,DISP,CD,CL)
      IMPLICIT REAL*8 (A-H, O-Z)
      REAL*4 ZR(14409),ZI(14409),X(361),Y(361),QMAG(14409)
      REAL*4 DISP(14409),CD(14409),CL(14409),T(14409)
      REAL*4 U(14409),V(14409),GARRAY(1)
      COMPLEX*16 Z(14409),QVECT(14409)
      COMMON /FIRST/ TTI,ISTEPS /SECOND/ NUMPTS /FOURTH/ PI
C
C  DEFINE CYLINDER OF RADIUS 1.0
C
      DO 10 N = 1,361
      RAD = FLOAT(N-1) * PI /180.0
      X(N) = COS(RAD)
   10 Y(N) = SIN(RAD)
C
C  DEFINE REAL SINGLE PRECISION NUMBERS FOR PLOT ROUTINES
C
      DELTAT = 1.D0/DFLOAT(ISTEPS)
C
      DO 20 N =1, NUMPTS
      ZR(N) =DREAL(Z(N))
      ZI(N) =DIMAG(Z(N))
      QMAG(N) = ABS(QVECT(N))
      U(N) = DREAL(QVECT(N))
   20 V(N) = DIMAG(QVECT(N))
C
```

```
C GENERATE PLOTS
C
       CALL COMPRS
C     CALL TEK618
       CALL BLOWUP(.3365655)
C     CALL BLOWUP(.55)
C     CALL BLOWUP(2.0)
C     CALL NOBRDR
C
C    VORTEX TRACK PLOT
C
       CALL GRACE (0.0)
       CALL NOCHEK
       CALL PAGE (11.0,8.5)
       CALL AREA2D(10., 5.71425)
       CALL YNAME('Y$',100)
       CALL XNAME('X$',100)
       CALL YAXANG(0.0)
       CALL INTAXS
C
       CALL XTICKS(2)
       CALL YTICKS(2)
       CALL GRAF(-7,1,7,-4,1,4)
C
       CALL CURVE(X,Y,361,0)
       GARRAY(1) = 0.08
       CALL SHADE(X,Y,361,45,GARRAY,1,0,0)
C
       CALL CURVE(ZR,ZI,NUMPTS,20000)
C     CALL CURVE(ZR,ZI,NUMPTS,0)
       CALL ENDPL(0)
C
C MAKE CONTINUATION SELECTIONS
C
       WRITE(6,*) '           CONTINUATION MEMO'
```

```
      WRITE(6,*)
      WRITE(6,*)
      WRITE(6,*)'TERMINATION OF PROGRAM.....................0'
      WRITE(6,*)'RERUN PROGRAM..............................1'
      WRITE(6,*)'CONTINUE WITH NORMAL SEQUENCE OF PLOTS.....2'
      WRITE(6,*)
      WRITE(6,*)'PLEASE ENTER YOUR SELECTION: (0,1,2)'
      READ(5,*)L1
      IF(L1.LT.1)GOTO 100
      IF(L1.EQ.1)GOTO 100
      CONTINUE
C
      PHSHFT = TTI - DFLOAT(INT(TTI))
C
      DO 40 N = 1,NUMPTS
   40 T(N) = (DFLOAT(N-1) * DELTAT + TTI - PHSHFT)
C
      WRITE(6,*)'DO YOU WANT A FORCE PLOT?  1-YES, 0-NO'
      READ(5,*) L1
      IF (L1.NE.1)GOTO 50
C
C  FORCE VS TIME PLOTS
C
      WRITE(6,*) 'ENTER VALUE OF THE LEFT HAND SIDE OF THE TIME SCALE:'
      READ(5,*) ILHS
      WRITE(6,*) 'ENTER VALUE OF THE RIGHT HAND SIDE OF THE TIME SCALE:'
      READ(5,*) IRHS
C
      CALL AREA2D(10.0, 7.5)
      CALL YNAME('COEF$',100)
      CALL XNAME('T*$',100)
      CALL YAXANG(0.0)
      CALL INTAXS
C
      CALL GRAF(ILHS,.5,IRHS,-4,1.,4.0)
```

```
C
      CALL CURVE(T,CD,NUMPTS,0)
      CALL DASH
      CALL CURVE(T,CL,NUMPTS,0)
      CALL RESET ('DASH')
      CALL ENDPL(0)
C
   50 WRITE(6,*)'DO YOU WANT A Q-MAG VS DISP PLOT?  1-YES, 0-NO'
      READ(5,*) L1
      IF (L1.NE.1)GOTO 60
C
C  MAGNITUDE OF Q VS. DISPLACEMENT PLOT
C
      CALL AREA2D(10.0, 7.5)
      CALL YNAME('Q$',100)
      CALL XNAME('S$',100)
      CALL YAXANG(0.0)
      CALL INTAXS
C
      CALL GRACE(2.)
      CALL GRAF(0,10,160,0,1.,10.0)
C
      CALL CURVE(DISP,QMAG,NUMPTS,0)
      CALL ENDPL(0)
C
   60 WRITE(6,*)'DO YOU WANT A Q-MAG VS TIME PLOT?  1-YES, 0-NO'
      READ(5,*) L1
      IF (L1.NE.1)GOTO 70
C
C  MAGNITUDE OF Q VS. TIME PLOT
C
      CALL AREA2D(10.0, 7.5)
      CALL YNAME('Q$',100)
      CALL XNAME('T*$',100)
      CALL YAXANG(0.0)
```

```
      CALL INTAXS
C
      CALL GRAF(0,1,10,0,1.,10.0)
C
      CALL CURVE(T,QMAG,NUMPTS,0)
      CALL ENDPL(0)
C
   70 WRITE(6,*)'DO YOU WANT A U-VEL VS X-POS PLOT?  1-YES, 0-NO'
      READ(5,*) L1
      IF (L1.NE.1)GOTO 80
C
C  U-VELOCITY POSITION PLOTS
C
      CALL AREA2D(10.0, 7.5)
      CALL YNAME('U-VELOCITY$',100)
      CALL XNAME('X-POSITION$',100)
      CALL YAXANG(0.0)
      CALL INTAXS
C
      CALL GRAF(-7,1,7,-10,2.,10.0)
C
      CALL CURVE(ZR,U,NUMPTS,0)
      CALL ENDPL(0)
C
   80 WRITE(6,*)'DO YOU WANT A V-VEL VS Y-POS PLOT?  1-YES, 0-NO'
      READ(5,*) L1
      IF (L1.NE.1)GOTO 90
C
C  V-VELOCITY POSITION PLOTS
C
      CALL AREA2D(10.0, 7.5)
      CALL YNAME('V-VELOCITY$',100)
      CALL XNAME('Y-POSITION$',100)
      CALL YAXANG(0.0)
      CALL INTAXS
```

```
C
      CALL GRAF(-4,.5,4,-7,1.,7.0)
C
      CALL CURVE(ZI,V,NUMPTS,0)
      CALL ENDPL(0)
C
   90 WRITE(6,*)'DO YOU WANT A U-VEL VS V-VEL PLOT?  1-YES, 0-NO'
      READ(5,*) L1
      IF (L1.NE.1)GOTO 100
C
C  U VS V VELOCITY  PLOTS
C
      CALL AREA2D(7.5, 7.5)
      CALL YNAME('V-VELOCITY$',100)
      CALL XNAME('U-VELOCITY$',100)
      CALL YAXANG(0.0)
      CALL INTAXS
C
      CALL GRAF(-10,2,10,-10,2.,10.0)
C
      CALL CURVE(U,V,NUMPTS,0)
      CALL ENDPL(0)
C
  100 CONTINUE
C
      RETURN
      END
```

APPENDIX B
RANKINE VORTEX COMPUTER MODEL

```
C
C THIS FUNCTION SUBROUTINE IS WRITTEN FOR USE WITH PROGRAM 'VORTEX
C FORTRAN'.  IT CONTAINS VELOCITY CALCULATIONS FOR A RANKINE
C VORTEX MODEL.  IT MAY BE INSERTED IN PLACE OF THE IDEAL
C VORTEX MODEL (FUNCTION SUBROUITNE Q IN 'VORTEX FORTRAN')
C
C
C ---------------------------------------------------------------------
C |         FUNCTION SUBPROGRAM Q (RANKINE MODEL)                      |
C ---------------------------------------------------------------------
C
C THIS FUNCTION SUBPORGRAM IS USED TO EVALUATE VALUES OF Q
C
      COMPLEX FUNCTION Q*16(ZZ,TE)
      IMPLICIT REAL*8 (A-H,O-Z)
      REAL*8 KC, KAPPA
      COMPLEX*16 ZZ, DFDZ, I, RV, VINDUC
      COMMON /FIRST/ TTI,ISTEPS /THIRD/ KC,KAPPA /FOURTH/ PI
C
      RCORE = 0.1D0
      I = (0.D0,1.D0)
      DELTAT = 1.D0/DFLOAT(ISTEPS)
      TT = TE * 2.D0 * PI
C
      RV = ZZ - 1.D0 / DCONJG(ZZ)
      CHECK = ABS(RV)
C
      IF (RCORE.GT.CHECK) GOTO 10
C
          VINDUC = -1.D0 / RV
          GOTO 20
```

```
C
   10    VINDUC = -RV / RCORE**2
C
   20 DFDZ =DSIN(TT)*(1.D0-1.D0/(ZZ*ZZ))+KAPPA*I*VINDUC
C
      Q = DCONJG(DFDZ)
C
      RETURN
      END
```

APPENDIX C
GAUSSIAN VORTEX COMPUTER MODEL

```
C
C THIS FUNCTION SUBROUTINE IS WRITTEN FOR USE WITH PROGRAM 'VORTEX
C FORTRAN'.  IT CONTAINS VELOCITY CALCULATIONS FOR A GAUSSIAN TIME
C DEPENDENT VORTEX MODEL.  IT MAY BE INSERTED IN PLACE OF THE IDEAL
C VORTEX MODEL (FUNCTION SUBROUITNE Q IN 'VORTEX FORTRAN')
C
C
C ---------------------------------------------------------------------
C |          FUNCTION SUBPROGRAM Q (GAUSSIAN MODEL)                     |
C ---------------------------------------------------------------------
C
C THIS FUNCTION SUBPORGRAM IS USED TO EVALUATE VALUES OF Q
C
      COMPLEX FUNCTION Q*16(ZZ,TE)
      IMPLICIT REAL*8 (A-H,O-Z)
      REAL*8 KC, KAPPA
      COMPLEX*16 ZZ, DFDZ, I,RV
      COMMON /FIRST/ TTI,ISTEPS /THIRD/ KC, KAPPA /FOURTH/ PI
C
      I = (0.D0,1.D0)
      DELTAT = 1.D0/DFLOAT(ISTEPS)
      TT = TE * 2.D0* PI
      TVINV = 1.D0 /(TE + .497440685D0)
C
      RV = ZZ - 1.D0 / DCONJG(ZZ)
      RVMAG = ABS(RV)
      ARG =  -62.5D0*TVINV*RVMAG**2
      IF (ARG.LE.50.D0) GOTO 10
      ARG = 50.D0
C
   10 VMOD =  1.D0 -  DEXP(ARG)
```

```
C
      DFDZ =DSIN(TT)*(1.D0-1.D0/(ZZ*ZZ))-I*(KAPPA/RV)*VMOD
C
      Q = DCONJG(DFDZ)
C
      RETURN
      END
```

APPENDIX D
TWO VORTEX COMPUTER MODEL

```
C ***********************************************************************
C *                                                                     *
C *                          T W O V O R                                *
C *                                                                     *
C *                        BY LT. W.T. MCCOY                            *
C *                                                                     *
C ***********************************************************************
C
C                          DESCRIPTION
C
C THIS PROGRAM TRACKS TWO VORTICIES IN COMPLEX SPACE AROUND A UNIT
C CYLINDER IN OSCILLATING FLOW.  INITIAL LOCATION, STARTING TIME, AND
C THE NUMBER OF CYCLES OF THE OSCILLATING FLOW ARE REQUIRED INPUT.
C
C THE PROGRAM IS DESIGNED TO RUN ON DISSPLA BY USING THE FOLLOWING
C DISSPLA EXEC COMMAND:'DISSPLA TWOVOR'. IT IS CURRENTLY
C DIMENSIONED TO RUN A MAX OF 6 CYCLES AT 1440 STEPS PER CYCLE.
C 2.0M OF VIRTUAL MEMORY IS REQUIRED TO RUN THE PROGRAM AT MAXIMUM
C CAPACITY.  THE PROGRAM IS INTERACTIVE FOR INPUT OPTIONS.
C
C ALL CONSTANTS ARE SET IN THE MAIN PROGRAM.  PREVIOUS INPUT OPTIONS
C ARE READ FROM FILE 'FILE FT35F001'.  FAILURE TO GENERATE THIS FILE
C PRIOR TO INITIAL RUNNING RESULTS IN A ERROR MESSAGE AND TERMINATION
C OF THE RUN.  PRIOR TO RUNNING, FILE 'FILE FT35F001' SHOULD BE
C INITIATED CONTAINING 8 COMPLEX NUMBERS, 1 REAL NUMBER, AND 1 INTEGER.
C WITH THIS INPUT THE PROGRAM DOES  NOT NEED TO BE TO BE RECOMPILED
C FOR EACH RUN.
C
C THIS PROGRAM IS WRITTEN IN DOUBLE PRECISION AND EMPLOYS THE MILNE
C PREDICTOR-CORRECTOR CONVECTION SCHEME, WITH INITIAL POINTS GENER-
C ATED BY A 4TH ORDER RUNGE-KUTTA SCHEME.
```

```
C
C OUTPUT OF THE PROGRAM INCLUDES THE LAST FOUR VALUES OF THE LOCATION
C OF THE VORTICES, FINISH TIME, AND THE NUMBER OF CYCLES.  THESE VALUES
C ARE WRITTEN IN FILE 'FILE FT35F001' AND ALLOW FOR OBSERVATIONS BEYOND
C THE MAX LIMIT OF 6 CYCLES BY CONTINUING WITH ADDITIONAL RUNS.
C
C OUTPUT FOR THE VORTEX PATHS ARE MADE GRAPHICALLY.  PLOTS MAY BE MADE
C ON A TEK618 OR SENT TO A METAFILE (PRE-EDIT SUBROUTINE 'GRAPH').
C
C
C.....................................................................
C
C           ALPHABETICAL LISTING OF VARIABLES
C
C     VARIABLE     (SUBROUTINE USED) DESCRIPTION.
C
C.....................................................................
C
C     DELTAT.......(STEP,Q,OUTPUT,FORCE,GRAPH)INCREMENTAL STEP
C                  IN NON-DIMENSIONAL TIME (INVERSE OF STEPS PER
C                  CYCLE).
C
C     DFDZ.........(QA,QB)COMPLEX PARTIAL DERIVATIVE OF THE COMPLEX
C                  FUNCTION F WITH TO RESPECT Z.
C
C     I............(QA,QB,FORCE)CONSTANT COMPLEX NUMBER = (0.0,1.0)
C
C     ISTEPS.......(ALL)NUMBER OF INCREMENTAL STEPS PER CYCLE TO BE
C                  TAKEN FOR ALL ITERATIONS.
C
C     K1-4.........(RUNGE) RUNGE-KUTTA CONSTANTS
C
C     KAPPAA.......(ALL)STRENGTH OF THE VORTEX (GAMMA/(2*PI*UMAX))
C
C     KAPPAB.......(ALL)STRENGTH OF THE VORTEX (GAMMA/(2*PI*UMAX))
```

```
C
C     KC.....(ALL) KEULLEGAN-CARPENTER NUMBER FOR THE OSCILLATING
C                  FLOW.
C
C     L1.....(INPUT) LOGICAL OPERATOR.
C
C     NUMCYC.....(INPUT)TOTAL NUMBER OF CYCLES TO BE EVALUATED.
C
C     NUMPTS.....(ALL)TOTAL NUMBER OF POINTS TO BE DETERMINED.
C                  (NUMCYC * ISTEPS)
C
C     PI.....(ALL)CONSTANT = 3.141592654
C
C     QA.....(QA)FUNCTION SUBROUTINE WHERE Q IS THE COMPLEX
C                  VELOCITY OF THE VORTEX.
C
C     QB.....(QB)FUNCTION SUBROUTINE WHERE Q IS THE COMPLEX
C                  VELOCITY OF THE VORTEX.
C
C     QVECTA(N)....(STEP,GRAPH)COMPLEX ARRAY CONTAINING THE VELOCITY
C                  OF THE VORTEX AT ANY POINT Z(N).
C
C     QVECTA(N)....(STEP,GRAPH)COMPLEX ARRAY CONTAINING THE VELOCITY
C                  OF THE VORTEX AT ANY POINT Z(N).
C
C     TE.....(RUNGE,QA,QB)NON-DIMENSIONAL ENVIRONMENTAL FLOW TIME.
C
C     TT.....(STEP,QA,QB)NON-DIMENSIONAL TIME CHANGED TO
C                  RADIANS FOR COS/SIN EVALUATIONS (0-2*PI FOR A CYCLE).
C
C     TTF.....(OUTPUT)NON-DIMENSIONAL FINISH TIME OF THE RUNS.
C
C     TTI.....(ALL)INITIAL NON-DIMENSIONAL STARTING TIME FOR THE
C                  OSCILLATING FLOW.
C
```

```
C     ZA..........(ALL)INSTANTANEOUS COMPLEX LOCATION OF THE VORTEX.
C
C     ZB..........(ALL)INSTANTANEOUS COMPLEX LOCATION OF THE VORTEX.
C
C     ZAI.........(GRAPH)IMAGINARY(Y) LOCATIONOF THE VORTEX.
C
C     ZBI.........(GRAPH)IMAGINARY(Y) LOCATIONOF THE VORTEX.
C
C     ZP..........(QA,QB)COMPLEX PREDICTED VALUE FOR Z(N)
C
C     ZAR.........(GRAPH)REAL(X) LOCATION OF THE VORTEX.
C
C     ZBR.........(GRAPH)REAL(X) LOCATION OF THE VORTEX.
C
C     ZZ..........(QA,QB)DUMMY ARGUMENT FOR THE FUNCTION SUBROUTINE QA
C                  AND QB WHICH CONTAINS THE PASSED VALUE OF Z(N).
C                  (RUNGE) DUMMY ARGUMENT CALL FUNCTION SUBROUITNE QA
CAND QB
C ..............................................................
C
C
C
C**********************************************************************
C *                        MAIN PROGRAM                                *
C**********************************************************************
C
       IMPLICIT REAL*8 (A-H,O-Z)
       REAL*8 KC,KAPPAA,KAPPAB
       COMPLEX*16 ZA(8649),QVECTA(8649)
       COMPLEX*16 ZB(8649),QVECTB(8649)
       COMMON /FIRST/ TTI,ISTEPS /SECOND/ NUMPTS /THIRD/ KC,KAPPAA,
     1       KAPPAB/FOURTH/ PI
C
C  SET CONSTANTS
C
```

```
      KAPPAA = 0.5D0
      KC = 10.D0
      PI = 3.141592654D0
      ISTEPS = 1440
C
   10 CALL INPUT (ZA,ZB)
      CALL STEP (ZA,QVECTA, ZB,QVECTB)
      CALL OUTPUT(ZA,ZB)
      CALL GRAPH (ZA,QVECTA,ZB,QVECTB)
C
      WRITE (6,*)'DO YOU WISH TO RE-RUN THE PROGRAM?  1-YES, 0-NO'
      READ (5,*) L1
      IF (L1.NE.1) GOTO 20
      WRITE (6,*) 'EXECUTION CONTINUES ..... '
      GOTO 10
   20 CONTINUE
C
      CALL DONEPL
      STOP
      END
C
C
C ***********************************************************************
C *                    SUBROUTINE INPUT                                 *
C ***********************************************************************
C
C THIS SUBROUTINE INTERACTIVELY INPUTS THE VALUES FOR THE INITIAL
C LOCATION OF THE VORTEX, STARTING TIME, ITERATION STEP SIZE, AND
C THE NUMBER OF CYCLES TO BE EXAMINED.
C
      SUBROUTINE INPUT (ZA,ZB)
      IMPLICIT REAL*8 (A-H,O-Z)
      REAL*8 KC, KAPPAA, KAPPAB
      COMPLEX*16 ZA(8649),ZB(8649)
      COMMON /FIRST/ TTI,ISTEPS /SECOND/ NUMPTS/THIRD/KC,KAPPAA,KAPPAB
```

```
C
C  READ LAST 4 POINTS OF EACH ARRAY FOR CONTINUATION OPTIONS
C
      REWIND 35
      DO 10 N = 1,4
   10 READ(35,*) ZA(N),ZB(N)
      READ(35,*) TTI
      READ(35,*) NUMCYC
C
C  CONTINUATION OPTIONS
C
      WRITE(6,*) 'DO YOU WISH TO CONTINUE THIS RUN FORM THE LAST?  1-YES
     #  0-NO'
      READ(5,*) L1
      IF (L1.NE.0) GOTO 20
C
      WRITE(6,*)'INPUT THE VALUE OF X : ZA(1)=(X,X)'
      READ(5,*) X
      ZA(1) = DCMPLX(X,X)
C
      WRITE(6,*)'INPUT THE VALUE OF EPSILON RADIUS:'
      READ(5,*) ER
      X = ER * X
      ZB(1) = DCMPLX(X,-X)
C
      WRITE(6,*) 'INPUT THE VALUE OF EPSILON KAPPA:'
      READ(5,*) EK
      KAPPAB = KAPPAA * EK
C
      TTI = 0.5D0
C
C  CALL SUBROUTINE RUNGE TO GENERATE FIRST 4 POINTS FOR EACH ARRAY
C
      CALL RUNGE (ZA,ZB)
C
```

```
C  INPUT THE NUMBER OF CYCLES TO BE ANALYZED
C
   20 WRITE(6,*)'THE LAST VALUE FOR NUMCYC =',NUMCYC
      WRITE(6,*)'DO YOU WISH TO CHANGE IT?  1-YES 0-NO'
      READ(5,*) L1
      IF(L1.NE.1) GOTO 30
      WRITE(6,*) 'INPUT THE NEW VALUE OF NUMCYC:'
      READ(5,*) NUMCYC
   30 CONTINUE
C
      NUMPTS = NUMCYC * ISTEPS + 4
C
      RETURN
      END
C
C
C ***************************************************************************
C *                        SUBROUTINE RUNGE                                 *
C ***************************************************************************
C
C THIS SUBROUTINE USES A 4TH ORDER RUNGE-KUTTA METHOD TO GENERATE THE
C FIRST FOUR VALUES OF Z.
C
      SUBROUTINE RUNGE(ZA,ZB)
      IMPLICIT REAL*8 (A-H,O-Z)
      COMPLEX*16 ZA(8649),ZB(8649),QA,K1,K2,K3,K4,ZP1,ZZ
      COMMON /FIRST/ TTI,ISTEPS
C
      DELTAT = 1.D0/DFLOAT(ISTEPS)
C
C  RUNGE-KUTTA EVALUATION FOR FIRST FOUR POINTS
C
      DO 5 N = 1,3
      ZZ = ZA(N)
      TE1 = (DFLOAT(N-1) * DELTAT + TTI)
```

```
      K1 = DLETAT * QA(ZZ,ZB(N),TE1)
      ZZ = ZA(N)+0.5D0*K1
      TE2 = TE1+ 0.5D0*DELTAT
      K2 = DELTAT * QA(ZZ,ZB(N),TE2)
      ZZ = ZA(N)+0.5D0*K2
      K3 = DELTAT * QA(ZZ,ZB(N), TE2)
      ZZ = ZA(N) + K3
      TE4 = TE1 + DELTAT
      K4 = DELTAT * QA(ZZ,ZB(N), TE4)
C
      ZA(N+1) = ZA(N) + (K1-2.D0*K2+2.D0*K3+K4)/6.D0
C
      ZZ = ZB(N)
      K1 = DLETAT * QB(ZA(N),ZZ,TE1)
      ZZ = ZB(N)+0.5D0*K1
      K2 = DELTAT * QB(ZA(N),ZZ,TE2)
      ZZ = ZB(N)+0.5D0*K2
      K3 = DELTAT * QB(ZA(N),ZZ, TE2)
      ZZ = ZB(N) + K3
      TE4 = TE1 + DELTAT
      K4 = DELTAT * QB(ZA(N),ZZ,TE4)
C
    5 ZB(N+1) = ZB(N) + (K1-2.D0*K2+2.D0*K3+K4)/6.D0
C
C
      RETURN
      END
C
C
C ***************************************************************************
C *                        SUBROUTINE STEP                                  *
C ***************************************************************************
C
C THIS SUBROUTINE PROGRESSIVELY CALCULATES THE VALUES OF ZA(N) AND
C ZB(N) BASED ON PREDICTOR-CORRECTOR CONVECTION SCHEME.
```

```
C
      SUBROUTINE STEP (ZA,QVECTA,ZB,QVECTB)
      IMPLICIT REAL*8 (A-H,O-Z)
      REAL*8 KC,KAPPAA,KAPPAB
      COMPLEX*16 ZA(8649),QVECTA(8649),ZP,QA,QB
      COMPLEX*16 ZB(8649),QVECTB(8649)
      COMMON /FIRST/ TTI,ISTEPS /SECOND/ NUMPTS/THIRD/ KC,KAPPAA,KAPPAB
C
      DELTAT = 1.D0/DFLOAT(ISTEPS)
C
C  MAKE VELOCITY EVALUATIONS FOR POINTS 1 THROUGH 4
C
      DO 7 N = 1,4
      TE = (DFLOAT(N-1) * DELTAT + TTI)
      QVECTA(N) = QA(ZA(N),ZB(N),TE)
    7 QVECTB(N) = QB(ZA(N),ZB(N),TE)
C
      DO 10 N = 5, NUMPTS
      NM1 = N-1
      NM2 = N-2
      NM3 = N-3
      NM4 = N-4
      TE = (DFLOAT(N-1)*DELTAT+TTI)
C
C  CALCULATE PREDICTED VALUE OF ZA(N) BASED ON ZB(N-1)
C
      ZP = ZA(NM1)+(55.D0*QVECTA(NM1) -59.D0*QVECTA(NM2)
     1     +37.D0*QVECTA(NM3)-9.D0*QVECTA(NM4))
     2     *DELTAT* 2.D0 * KC / 24.D0
C
C  CALCULATE 1ST ESTIMATE OF ZA(N) BASED ON ZB(N-1)
C
      ZA(N) = ZA(NM1) + (9.D0*QA(ZP,ZB(NM1),TE) + 19.D0*QVECTA(NM1)
     1       -5.D0*QVECTA(NM2)+QVECTA(NM3) )*DELTAT * 2.D0 * KC / 24.D0
C
```

```
C  CALCULATE PREDICTED VALUE OF ZB(N) BASED ON ESTIMATED ZA(N)
C
       ZP = ZB(NM1)+(55.D0*QVECTB(NM1) -59.D0*QVECTB(NM2)
      1     +37.D0*QVECTB(NM3)-9.D0*QVECTB(NM4))
      2     *DELTAT* 2.D0 * KC / 24.D0
C
C  CALCULATE 1ST ESTIMATE OF ZB(N) BASED ON ESTIMATED ZA(N)
C
       ZB(N) = ZB(NM1) + (9.D0*QB(ZA(N),ZP,TE) + 19.D0*QVECTB(NM1)
      1       -5.D0*QVECTB(NM2)+QVECTB(NM3) )*DELTAT * 2.D0 * KC / 24.D0
C
C  CALCULATE PREDICTED VALUE OF ZA(N) BASED ON ESTIMATED ZB(N)
C
       ZP = ZA(NM1)+(55.D0*QVECTA(NM1) -59.D0*QVECTA(NM2)
      1     +37.D0*QVECTA(NM3)-9.D0*QVECTA(NM4))
      2     *DELTAT* 2.D0 * KC / 24.D0
C
C  CALCULATE ACTUAL ZA(N) BASED ON ESTIMATED ZB(N)
C
       ZA(N) = ZA(NM1) + (9.D0*QA(ZP,ZB(N),TE) + 19.D0*QVECTA(NM1)
      1       -5.D0*QVECTA(NM2)+QVECTA(NM3) )*DELTAT * 2.D0 * KC / 24.D0
C
C  CALCULATE PREDICTED VALUE OF ZB(N) BASED ON ACTUAL ZA(N)
C
       ZP = ZB(NM1)+(55.D0*QVECTB(NM1) -59.D0*QVECTB(NM2)
      1     +37.D0*QVECTB(NM3)-9.D0*QVECTB(NM4))
      2     *DELTAT* 2.D0 * KC / 24.D0
C
C  CALCULATE ACTUAL ZB(N) BASED ON ACTUAL ZA(N)
C
       ZB(N) = ZB(NM1) + (9.D0*QB(ZA(N),ZP,TE) + 19.D0*QVECTB(NM1)
      1       -5.D0*QVECTB(NM2)+QVECTB(NM3) )*DELTAT * 2.D0 * KC / 24.D0
C
C  EVALUATE VELOCITIES AT ZA(N) AND ZB(N)
C
```

```
      QVECTA(N) = QA(ZA(N),ZB(N),TE)
   10 QVECTB(N) = QB(ZA(N),ZB(N),TE)
C
      RETURN
      END
C
C
C ---------------------------------------------------------------------
C |                FUNCTION SUBPROGRAM QA                             |
C ---------------------------------------------------------------------
C
C THIS FUNCTION SUBPORGRAM IS USED TO EVALUATE VALUES OF QA
C
      COMPLEX FUNCTION QA*16(ZA,ZB,TE)
      IMPLICIT REAL*8 (A-H,O-Z)
      REAL*8 KC, KAPPAA,KAPPAB
      COMPLEX*16 ZA,ZB, DFDZ, I,AA,AB,AC
      COMMON /FIRST/ TTI,ISTEPS /THIRD/ KC,KAPPAA,KAPPAB /FOURTH/ PI
C
      I = (0.D0,1.D0)
      TT = TE * 2.D0* PI
C
      AA = 1.D0/(ZA-1.D0/(DCONJG(ZA)))
      AB = 1.D0/(ZA-ZB)
      AC = 1.D0/(ZA-1.D0/(DCONJG(ZB)))
C
      DFDZ =DSIN(TT)*(1.D0-1.D0/(ZA*ZA))-I*KAPPAA*AA-I*KAPPAB*(AB-AC)
C
      QA = DCONJG(DFDZ)
C
      RETURN
      END
C
C
```

```
C ------------------------------------------------------------------
C |                FUNCTION SUBPROGRAM QB                          |
C ------------------------------------------------------------------
C
C THIS FUNCTION SUBPORGRAM IS USED TO EVALUATE VALUES OF QB
C
      COMPLEX FUNCTION QB*16(ZA,ZB,TE)
      IMPLICIT REAL*8 (A-H,O-Z)
      REAL*8 KC, KAPPAA,KAPPAB
      COMPLEX*16 ZA,ZB, DFDZ, I,BA,BB,BC
      COMMON /FIRST/ TTI,ISTEPS /THIRD/ KC,KAPPAA,KAPPAB /FOURTH/ PI
C
      I = (0.D0,1.D0)
      TT = TE * 2.D0* PI
C
      BA = 1.D0/(ZB-ZA)
      BB = 1.D0/(ZB-1.D0/(DCONJG(ZA)))
      BC = 1.D0/(ZB-1.D0/(DCONJG(ZB)))
C
      DFDZ =DSIN(TT)*(1.D0-1.D0/(ZB*ZB))+I*KAPPAA*(BA-BB)+I*KAPPAB*BC
C
      QB = DCONJG(DFDZ)
C
      RETURN
      END
C
C
C ******************************************************************
C *                    SUBROUTINE OUTPUT                           *
C ******************************************************************
C
C  THIS SUBROUTINE IS USED TO SAVE THE FINAL VALUES OF Z,TT, AND NUMCYC
C  FOR POSSIBLE CONTINUATION OF THE PLOTS.
C  THE VALUES ARE SAVED IN FILE 'FILE FT35F001'.
C
```

```
      SUBROUTINE OUTPUT(ZA,ZB)
      IMPLICIT REAL*8 (A-H, O-Z)
      COMPLEX*16 ZA(8649),ZB(8649)
      COMMON /FIRST/ TTI,ISTEPS /SECOND/ NUMPTS
C
      DELTAT = 1.D0/FLOAT(ISTEPS)
      NN = NUMPTS - 4
      TTF = DFLOAT(NN)* DELTAT + TTI
      NUMCYC = NN / ISTEPS
C
      REWIND 35
      DO 10 N = 1,4
      NN = NN + 1
   10 WRITE(35,*) ZA(NN),ZB(NN)
      WRITE(35,*) TTF
      WRITE(35,*) NUMCYC
C
      RETURN
      END
C
C
C
C
C ***************************************************************************
C *                              SUBROUTINE GRAPH                           *
C ***************************************************************************
C
      SUBROUTINE GRAPH (ZA,QVECTA,ZB,QVECTB)
      IMPLICIT REAL*8 (A-H, O-Z)
      REAL*4 ZRA(8649),ZIA(8649),X(361),Y(361),GARRAY(1)
      REAL*4 ZRB(8649),ZIB(8649)
      COMPLEX*16 ZA(8649),QVECTA(8649)
      COMPLEX*16 ZB(8649),QVECTB(8649)
      COMMON /FIRST/ TTI,ISTEPS /SECOND/ NUMPTS /FOURTH/ PI
C
```

```
C  DEFINE CYLINDER OF RADIUS 1.0
C
       DO 10 N = 1,361
       RAD = FLOAT(N-1) * PI /180.0
       X(N) = COS(RAD)
   10 Y(N) = SIN(RAD)
C
C  DEFINE REAL SINGLE PRECISION NUMBERS FOR PLOT ROUTINES
C
       DELTAT = 1.D0/DFLOAT(ISTEPS)
       NPTSM4 = NUMPTS - 4
C
       DO 20 N =1, NPTSM4
       ZRA(N) =DREAL(ZA(N))
       ZIA(N) =DIMAG(ZA(N))
       ZRB(N) =DREAL(ZB(N))
   20 ZIB(N) =DIMAG(ZB(N))
C
C GENERATE PLOTS
C
C     CALL COMPRS
C     CALL BLOWUP(1.0)
       CALL TEK618
       CALL BLOWUP(2.0)
       CALL NOBRDR
       CALL GRACE (0.0)
C
C    VORTEX TRACK PLOT
C
       CALL NOCHEK
       CALL PAGE (11.0,8.5)
       CALL AREA2D(8.0,6.0)
       CALL YNAME('Y$',100)
       CALL XNAME('X$',100)
       CALL YAXANG(0.0)
```

```
      CALL INTAXS
C
      CALL XTICKS(2)
      CALL YTICKS(2)
      CALL GRAF(-26,1,2,-2,1,19)
C
      CALL CURVE(X,Y,361,0)
      GARRAY(1) = 0.08
      CALL SHADE(X,Y,361,45,GARRAY,1,0,0)
C
      CALL CURVE(ZRA,ZIA,NPTSM4,0)
C
      CALL DASH
      CALL CURVE(ZRB,ZIB,NPTSM4,0)
      CALL ENDPL(0)
C
      RETURN
      END
```

APPENDIX E

FIGURES

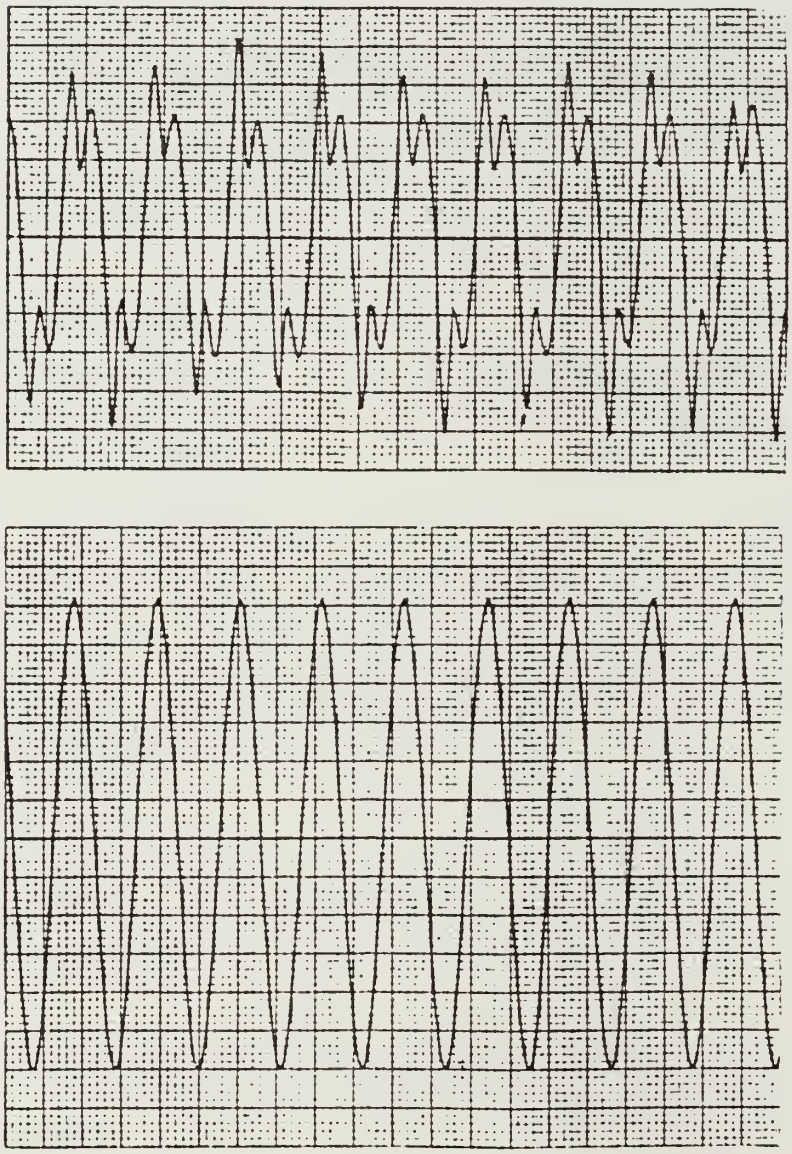

Figure E.1a Experimental In-line Force Trace
Top - Force Coefficient, Bottom - Flow Velocity
$K_c = 10.0$

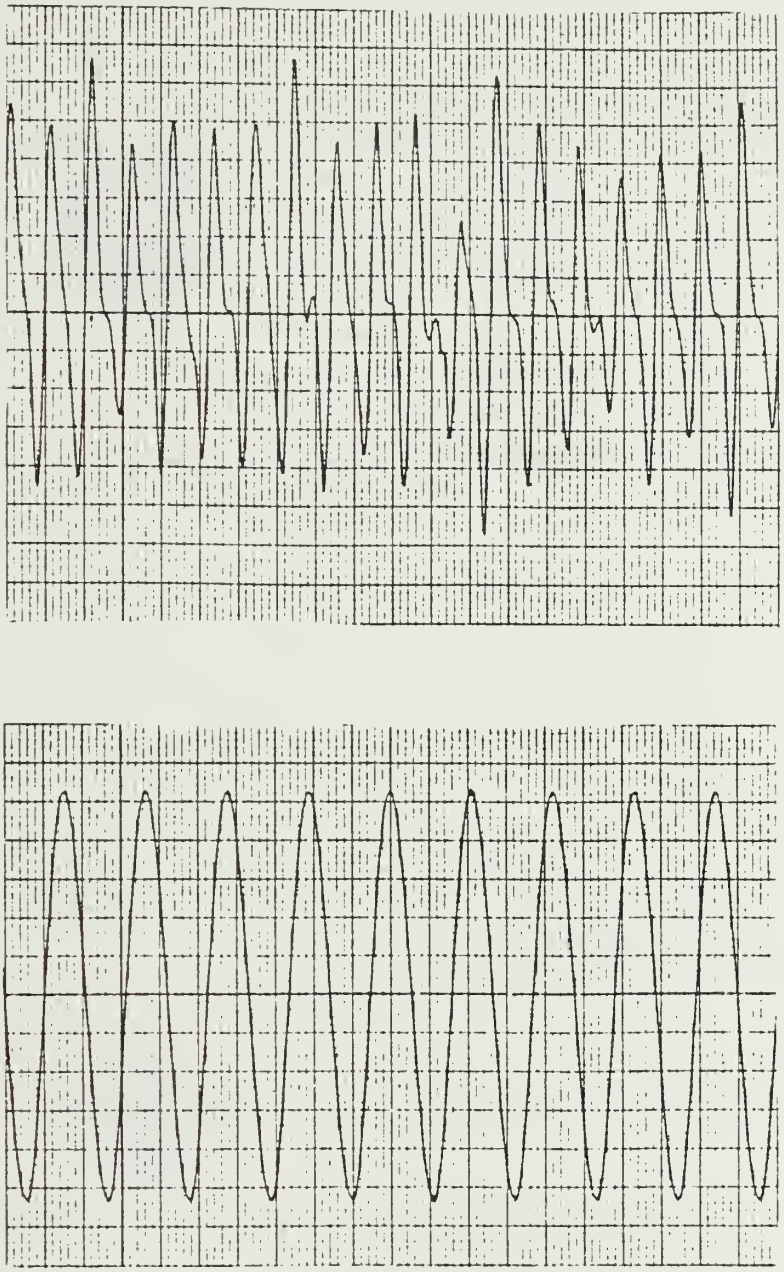

Figure E.1b Experimental Transverse Force Trace
Top - Force Coefficient, Bottom - Flow Velocity
$K_c = 10.0$

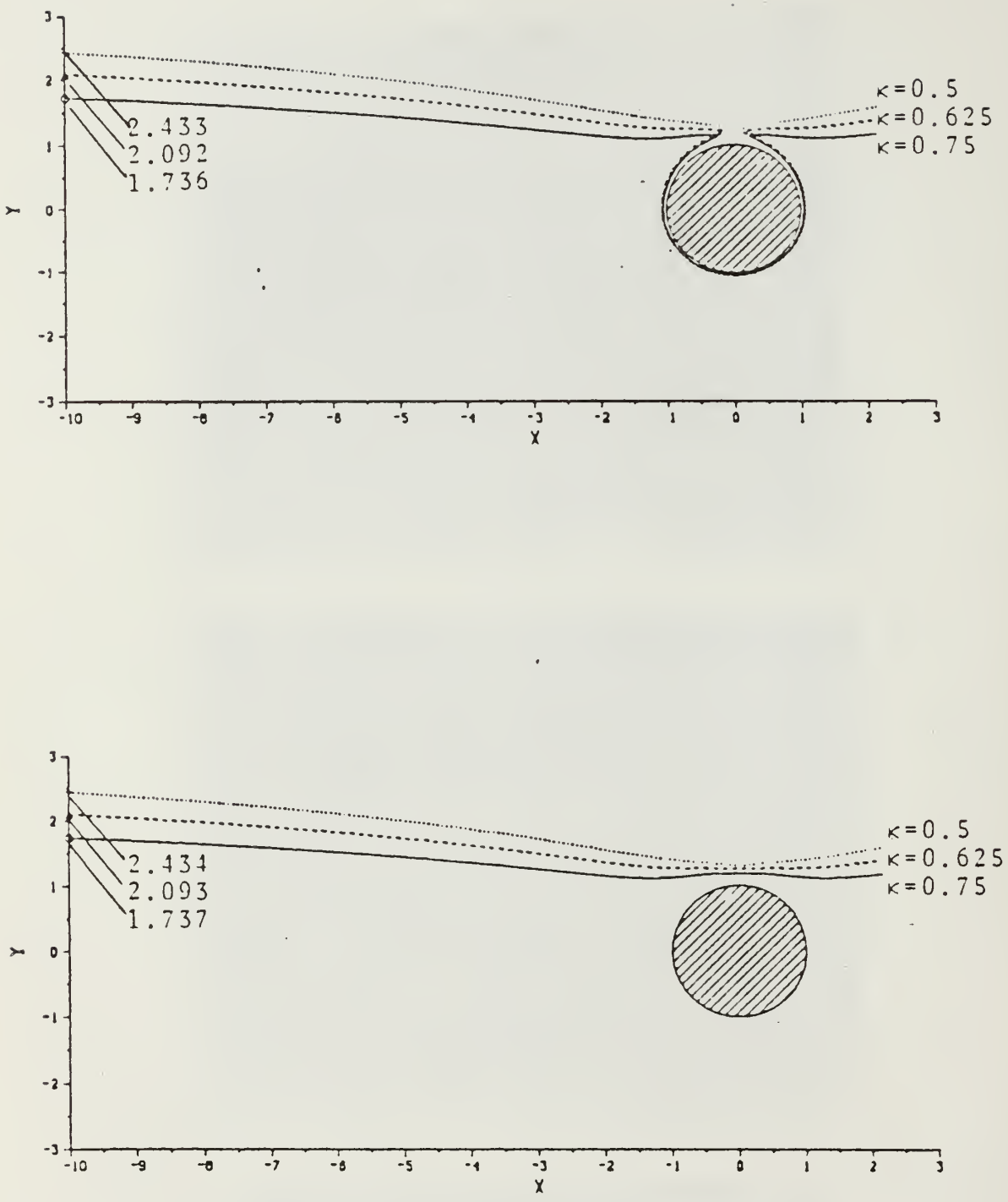

Figure E.2 Vortex Path in Uniform Flow

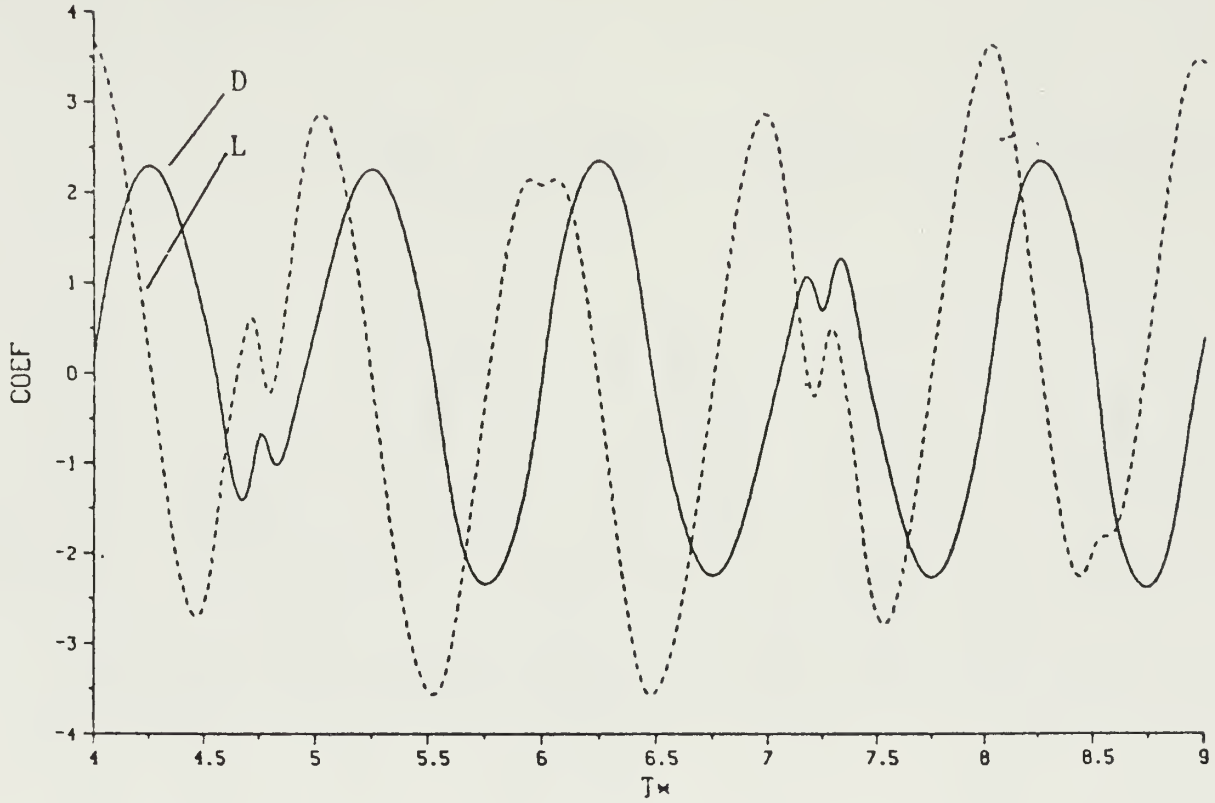

Figure E.3 Force Coefficients for Z(1) = (1.9, 1.9) and Ti = 0.75

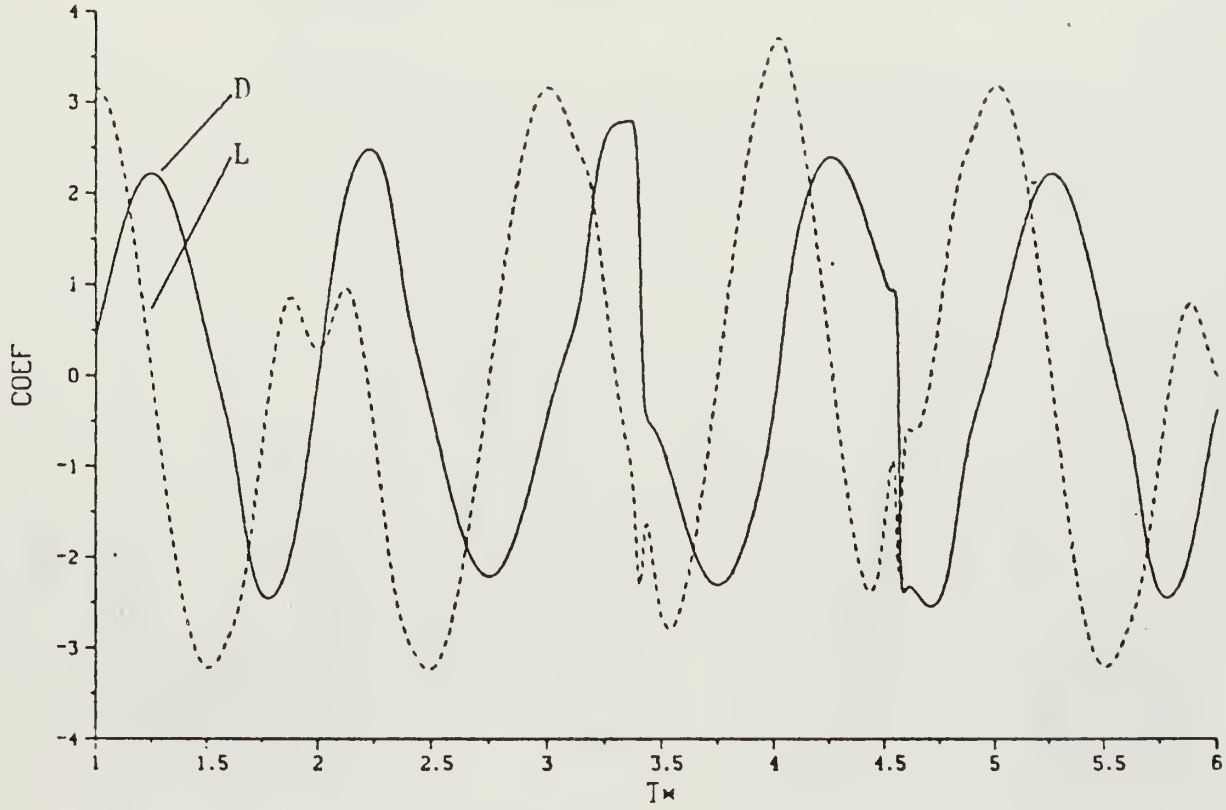

Figure E.4 Force Coefficients for Z(1)= (0, 2.2192) and Ti= 0.75

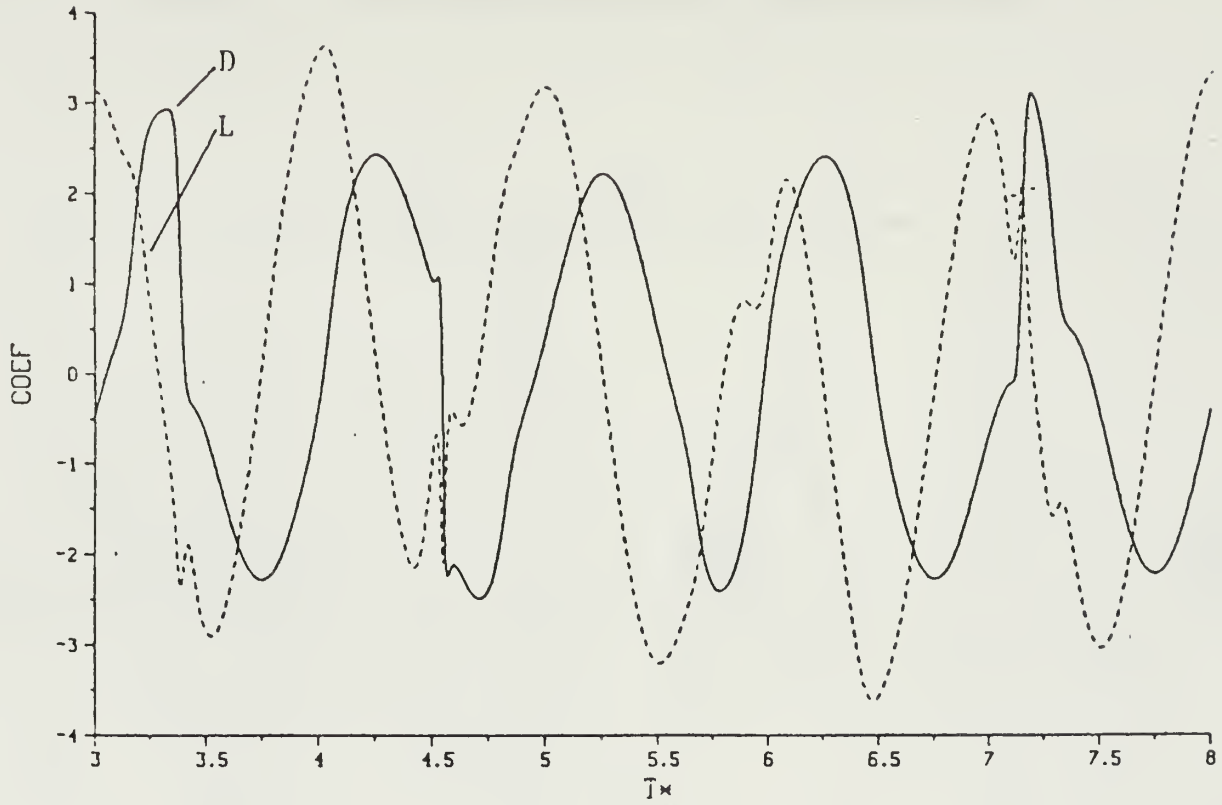

Figure E.5 Force Coefficients for Z(1)= (0, 2.2193) and Ti= 0.75

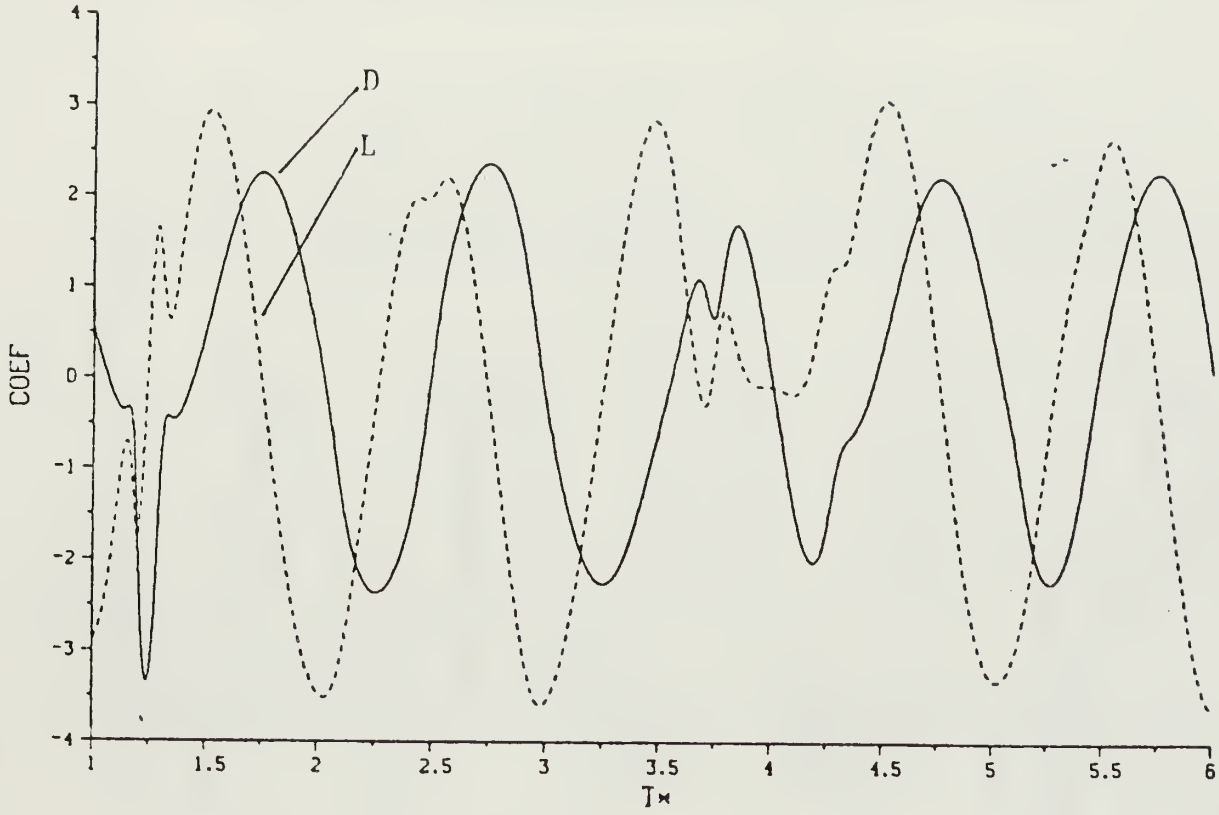

Figure E.6 Force Coefficients for Z(1) = (0, 1.6885) and Ti = 0.25

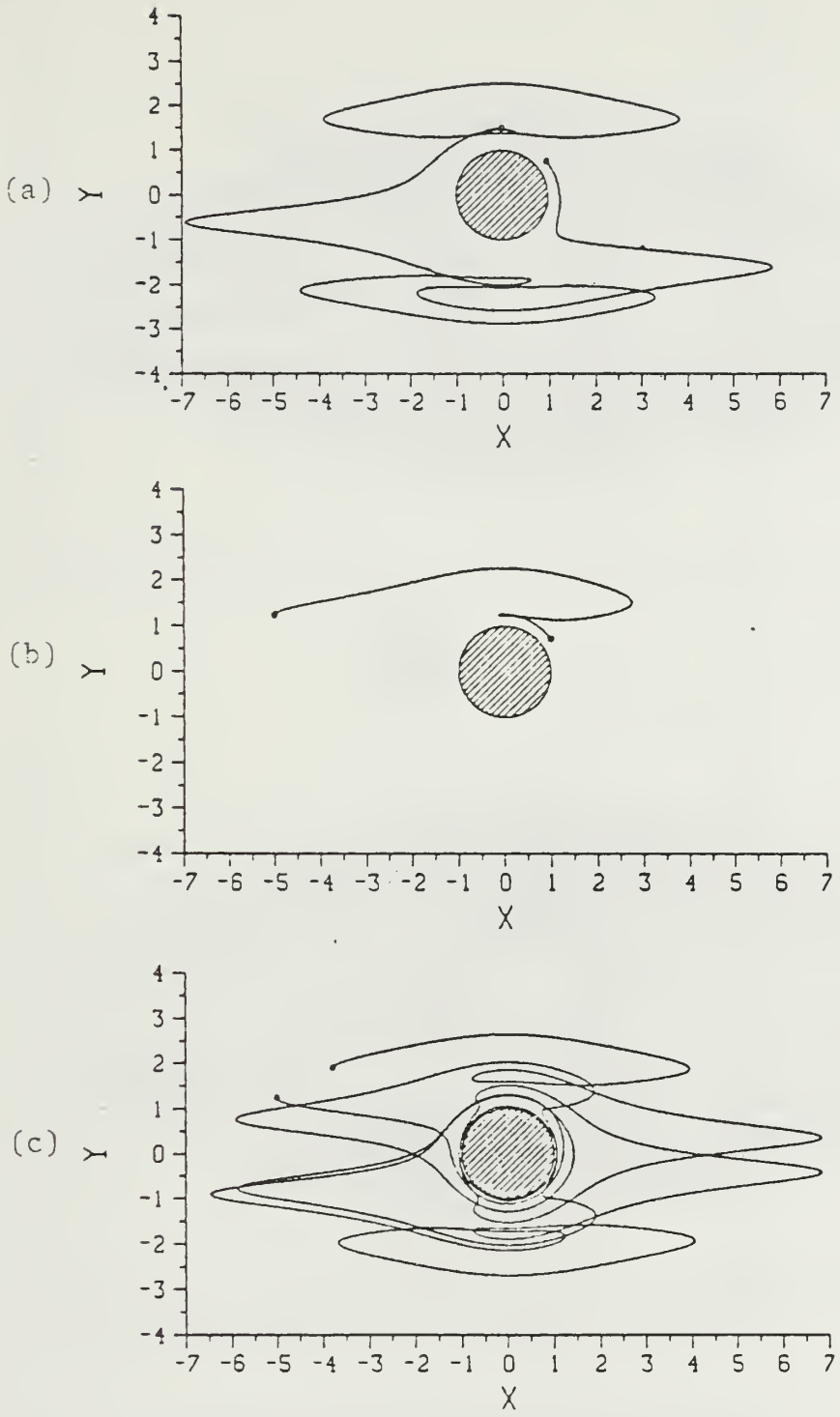

Figure E.7 Vortex Path Z(1) = (0, 1.5083)

Ti = 0.0

(a) Cycles 1-5, (b) Cycle 6, (c) Cycles 7-15

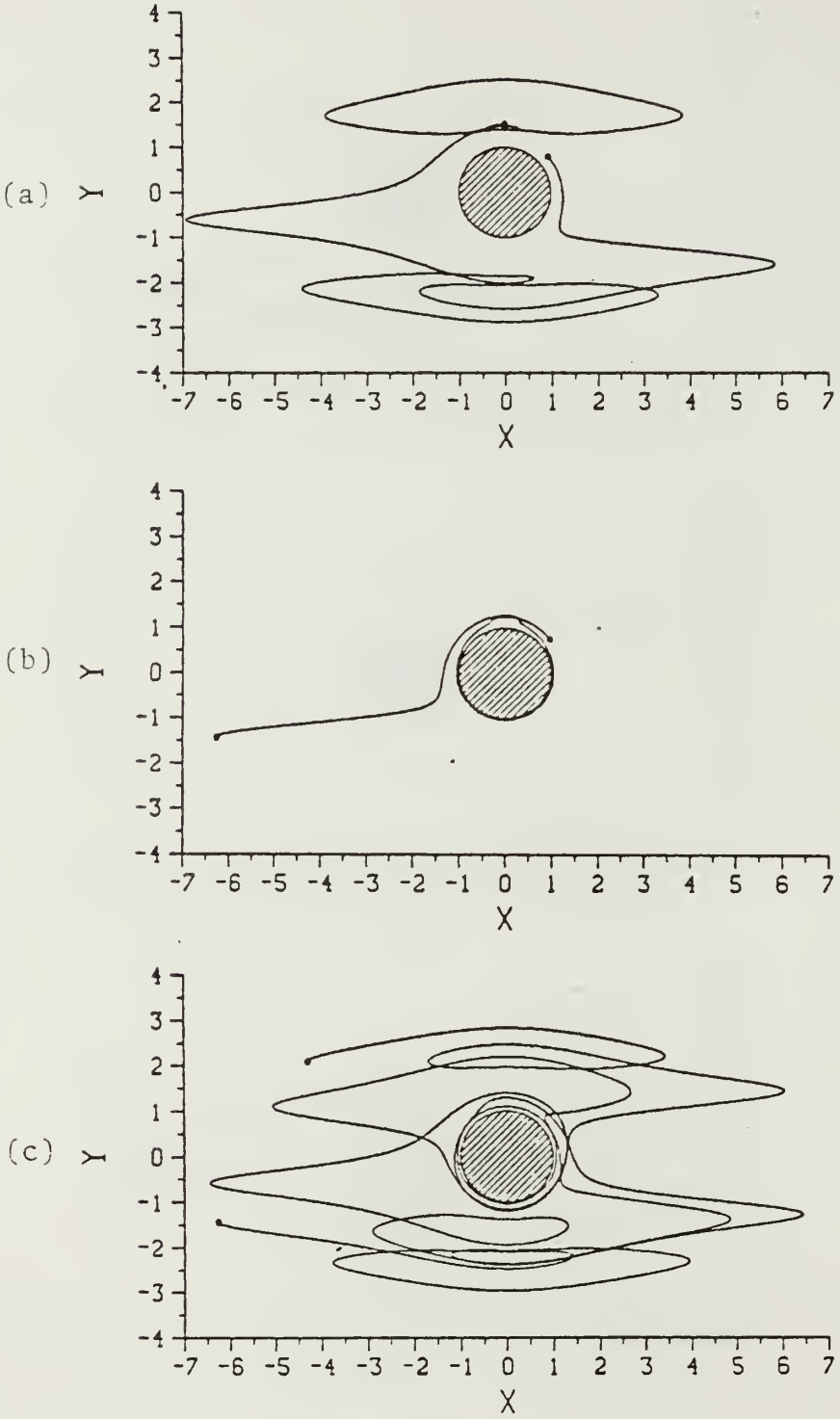

Figure E.8 Vortex Path Z(1) = (0, 1.5084)

Ti = 0.0

(a) Cycles 1-5, (b) Cycle 6, (c) Cycles 7-15

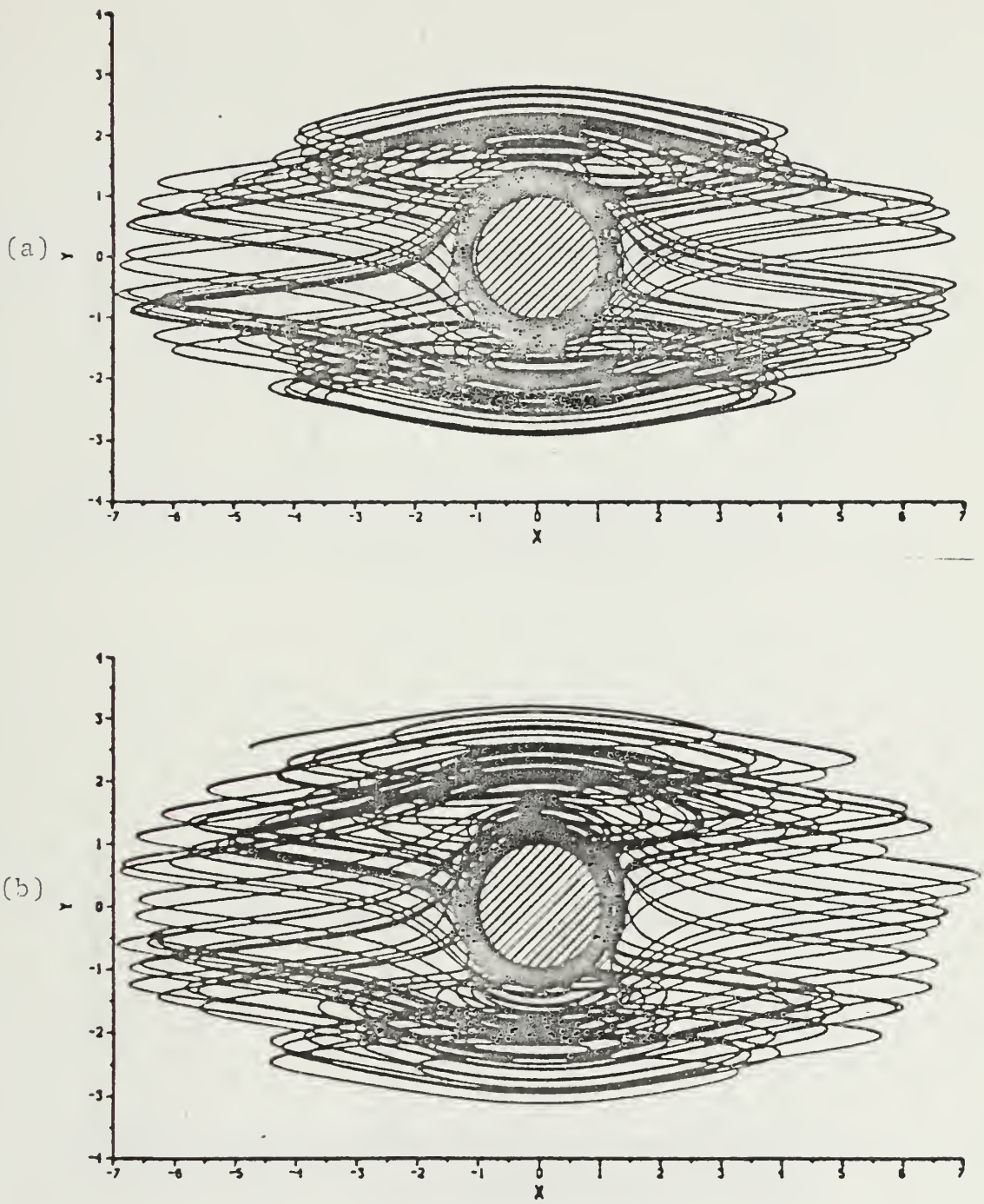

Figure E.9 Vortex Paths for 100 Cycles

Ti = 0.0

(a) Z(1) = (0, 1.5083), (b) Z(1) = (0, 1.5084)

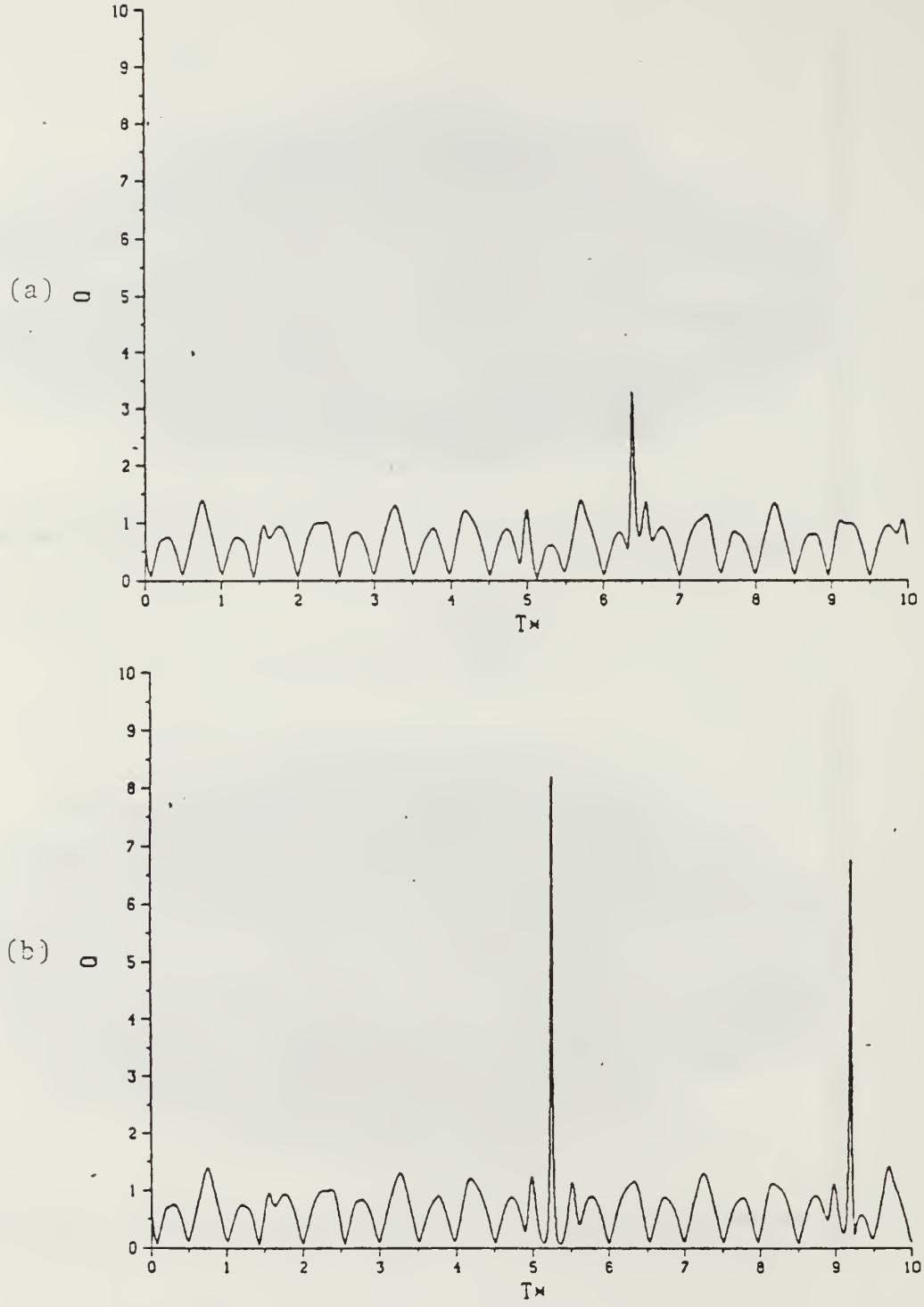

Figure E.10 Velocity Magnitudes for 10 Cycles

Ti = 0.0

(a) Z(1) = (0, 1.5083), (b) Z(1) = (0, 1.5084)

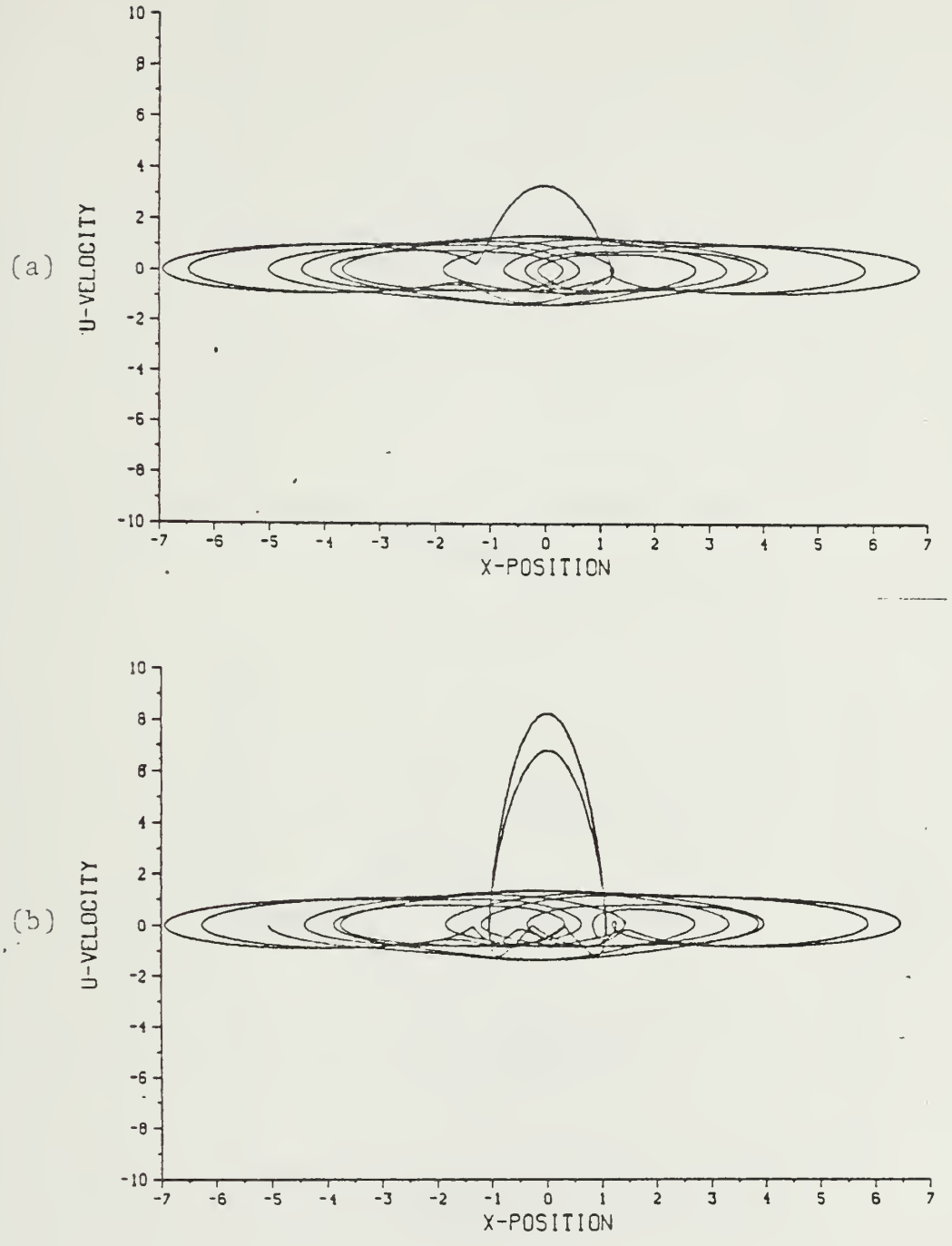

Figure E.11 u-Velocity vs x-Position for 10 Cycles

Ti = 0.0

(a) Z(1) = (0, 1.5083), (b) Z(1) = (0, 1.5084)

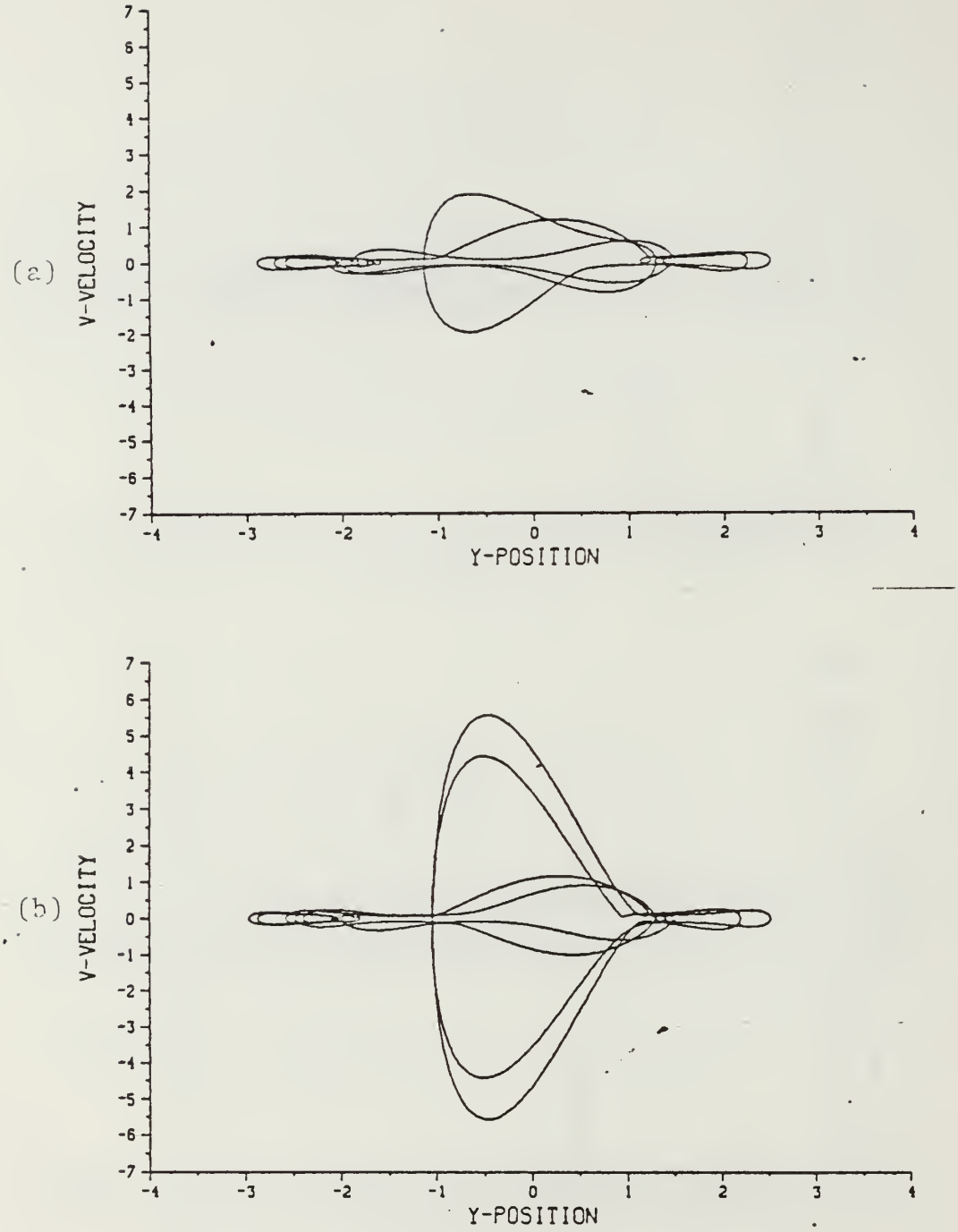

Figure E.12 v-Velocity vs y-Position for 10 Cycles

Ti = 0.0

(a) $Z(1) = (0, 1.5083)$, (b) $Z(1) = (0, 1.5084)$

(a)

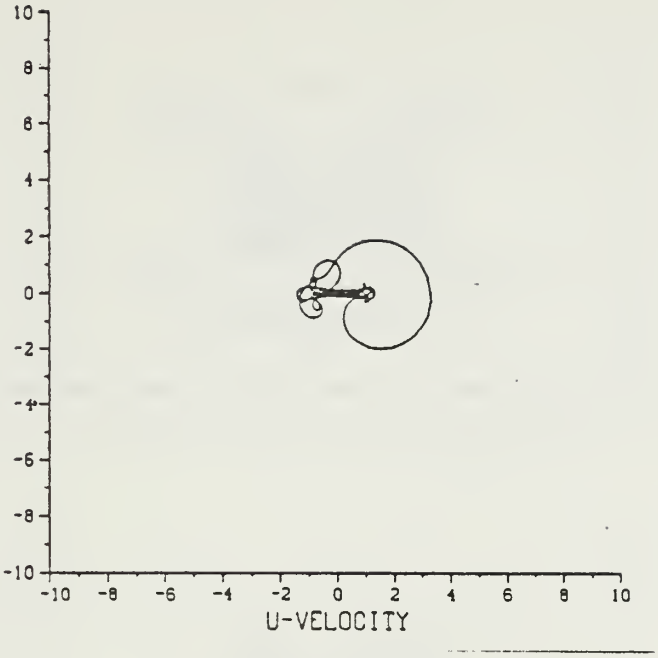

(b)

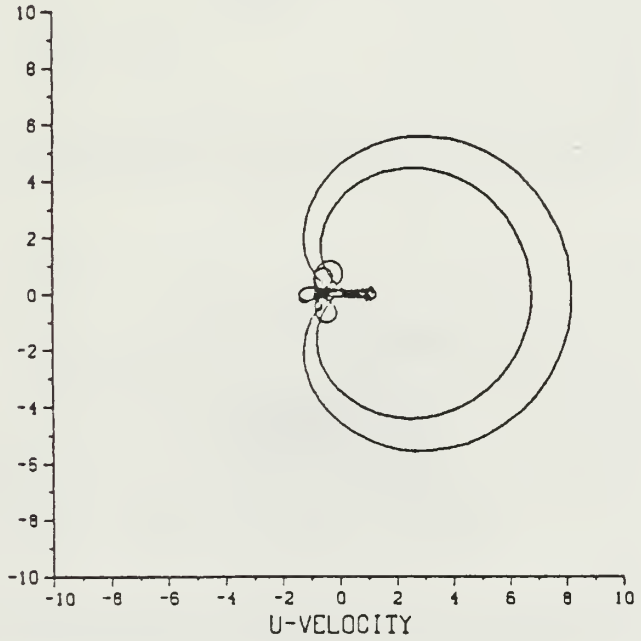

Figure E.13 u-Velocity vs v-Velocity for 10 Cycles

Ti = 0.0

(a) Z(1) = (0, 1.5083), (b) Z(1) = (0, 1.5084)

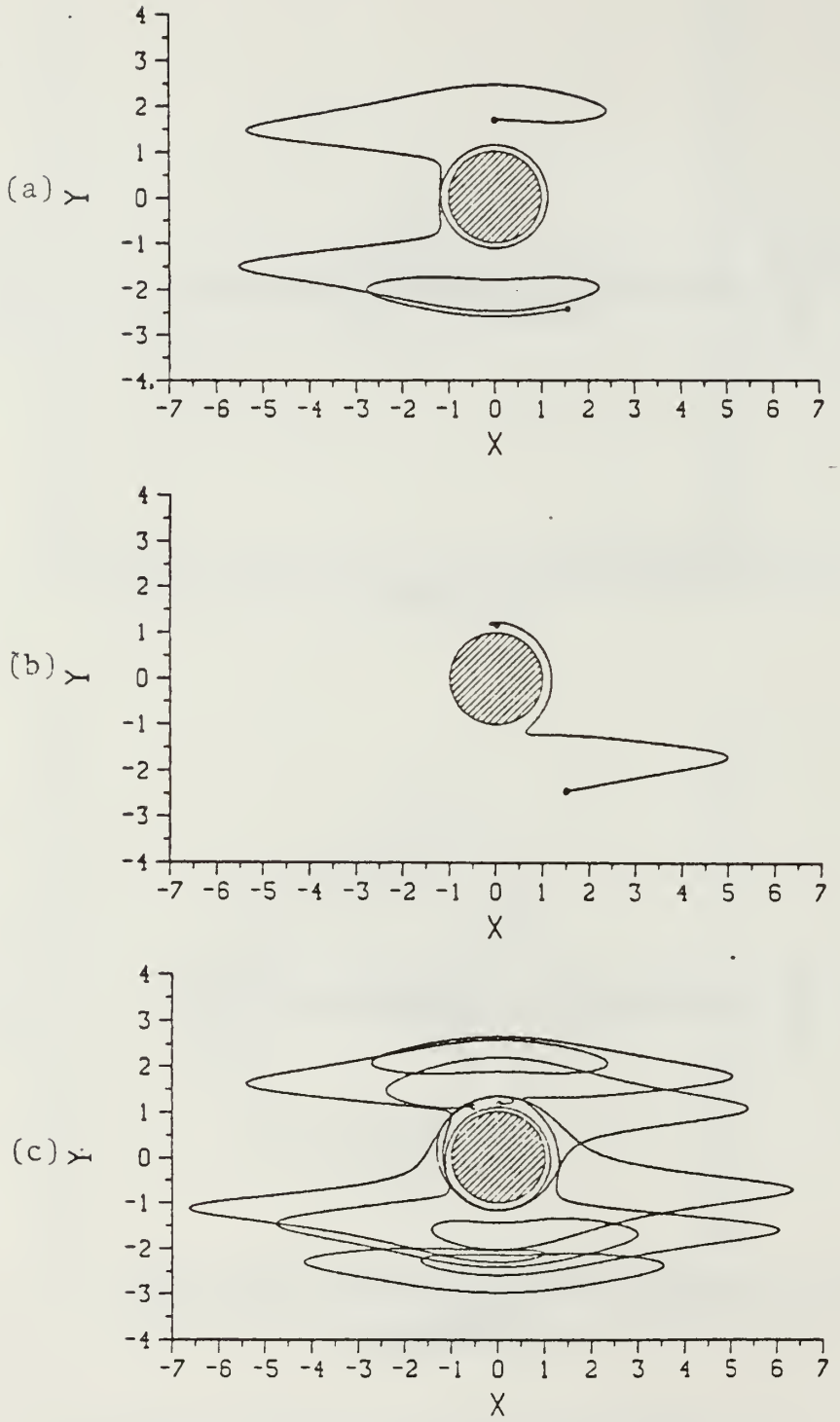

Figure E.14 Vortex Path Z(1) = (0, 1.6885)

Ti = 0.25

(a) Cycles 1-3, (b) Cycle 4, (c) Cycles 5-15

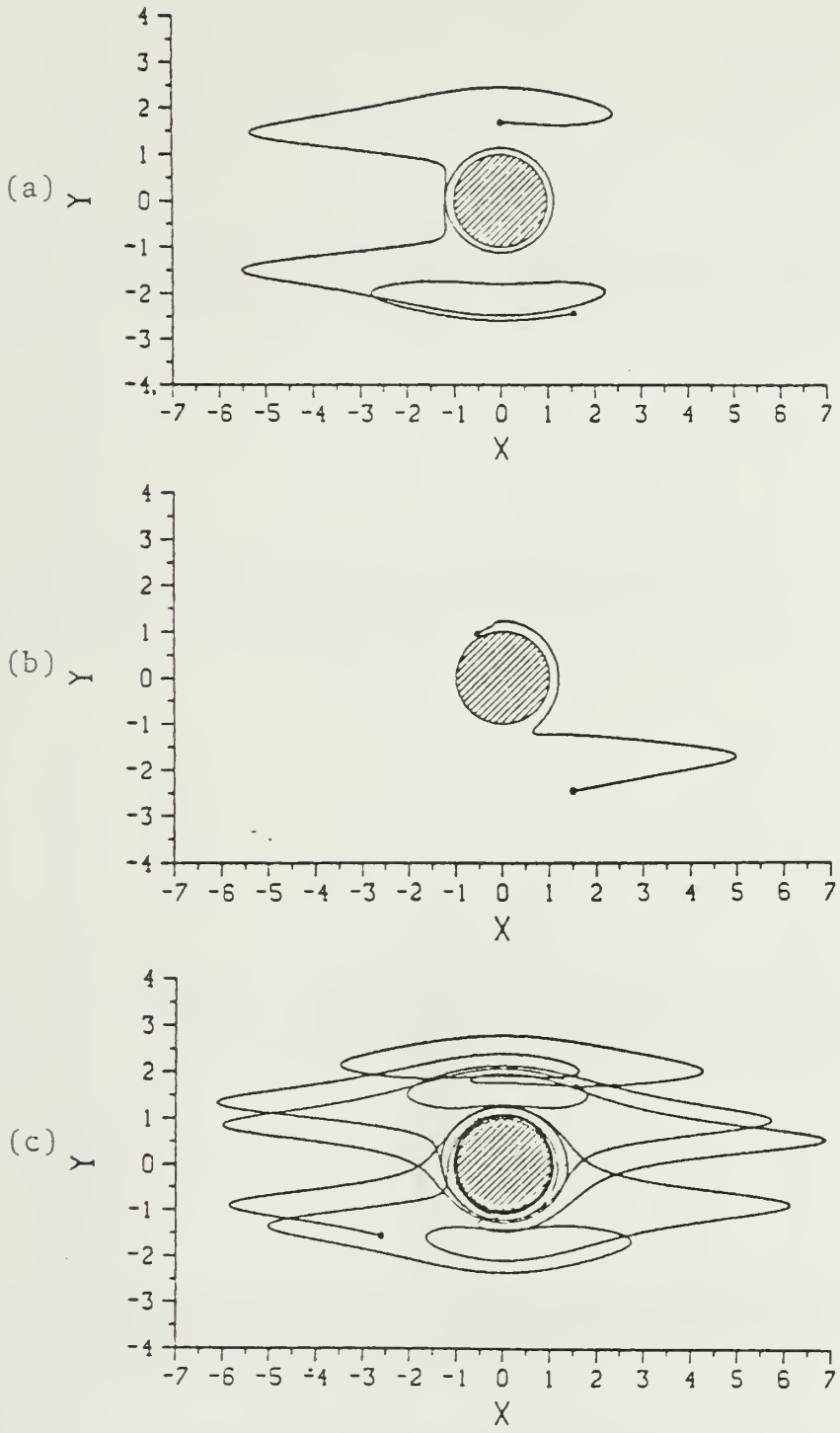

Figure E.15 Vortex Path Z(1) = (0, 1.6886)

Ti = 0.25

(a) Cycles 1-3, (b) Cycle 4, (c) Cycles 5-15

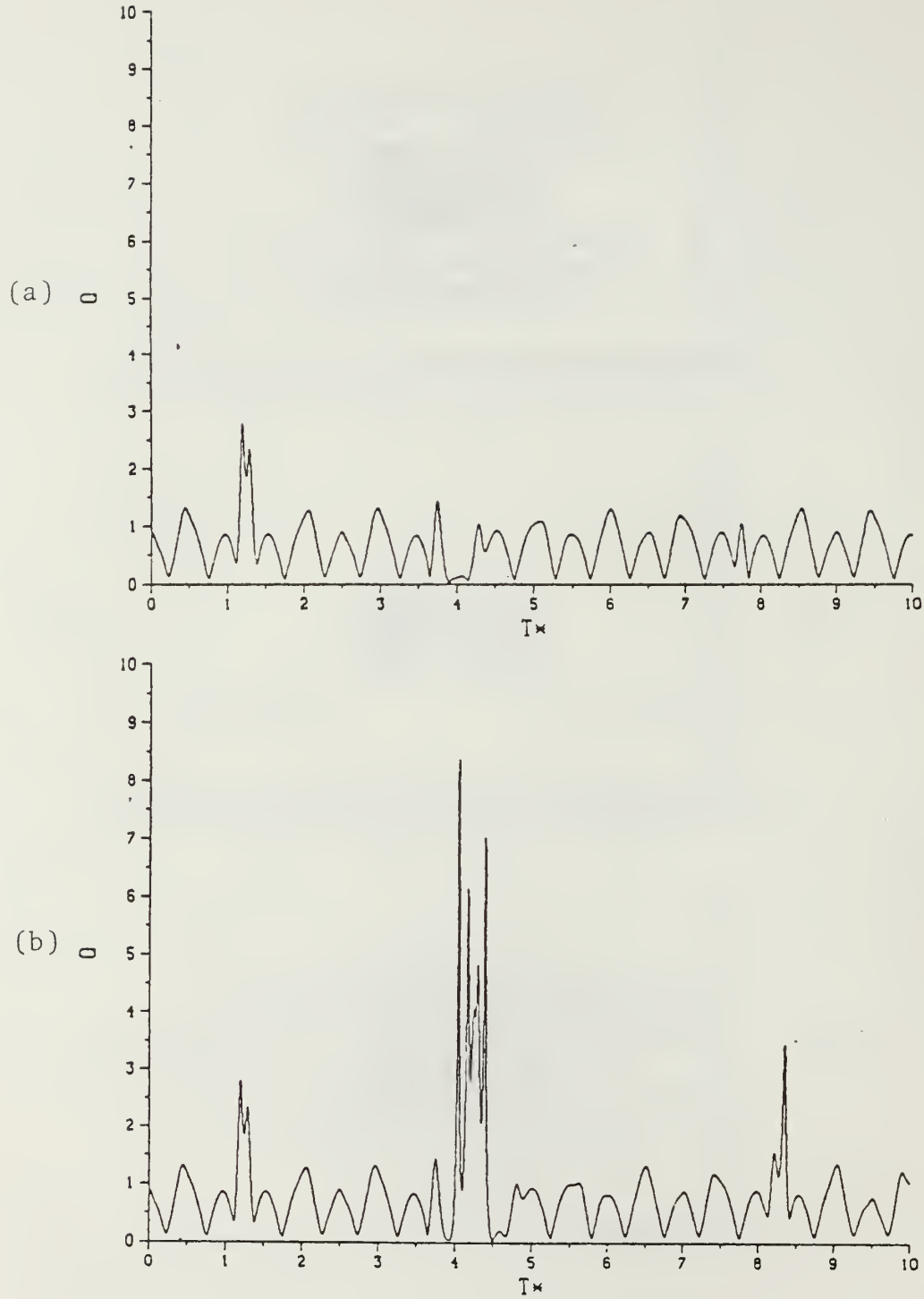

Figure E.16 Velocity Magnitudes for 10 Cycles

Ti = 0.25

(a) Z(1) = (0, 1.6885), (b) Z(1) = (0, 1.6886)

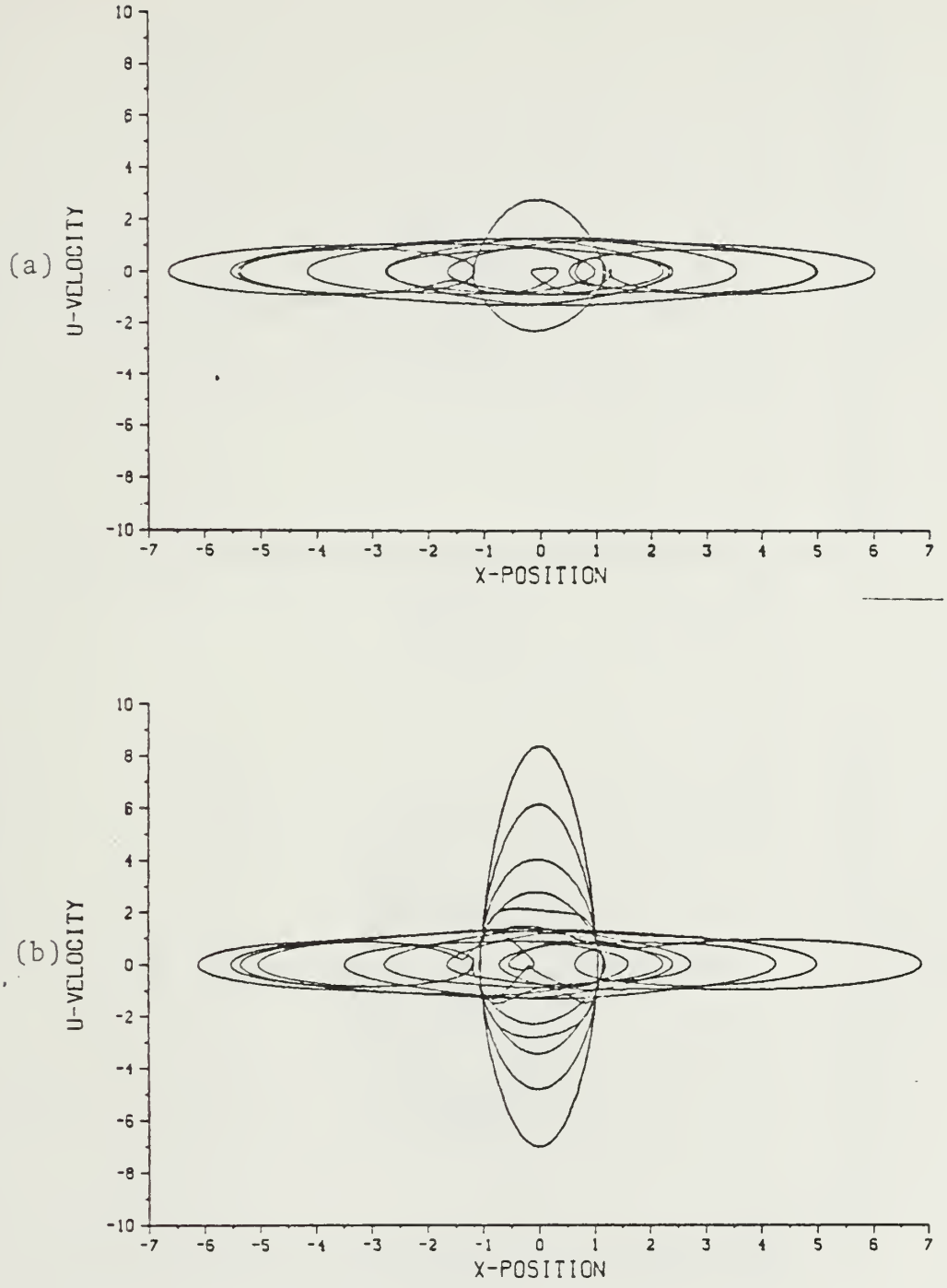

Figure E.17 u-Velocity vs x-Position for 10 Cycles

Ti = 0.25

(a) Z(1) = (0, 1.6885), (b) Z(1) = (0, 1.6886)

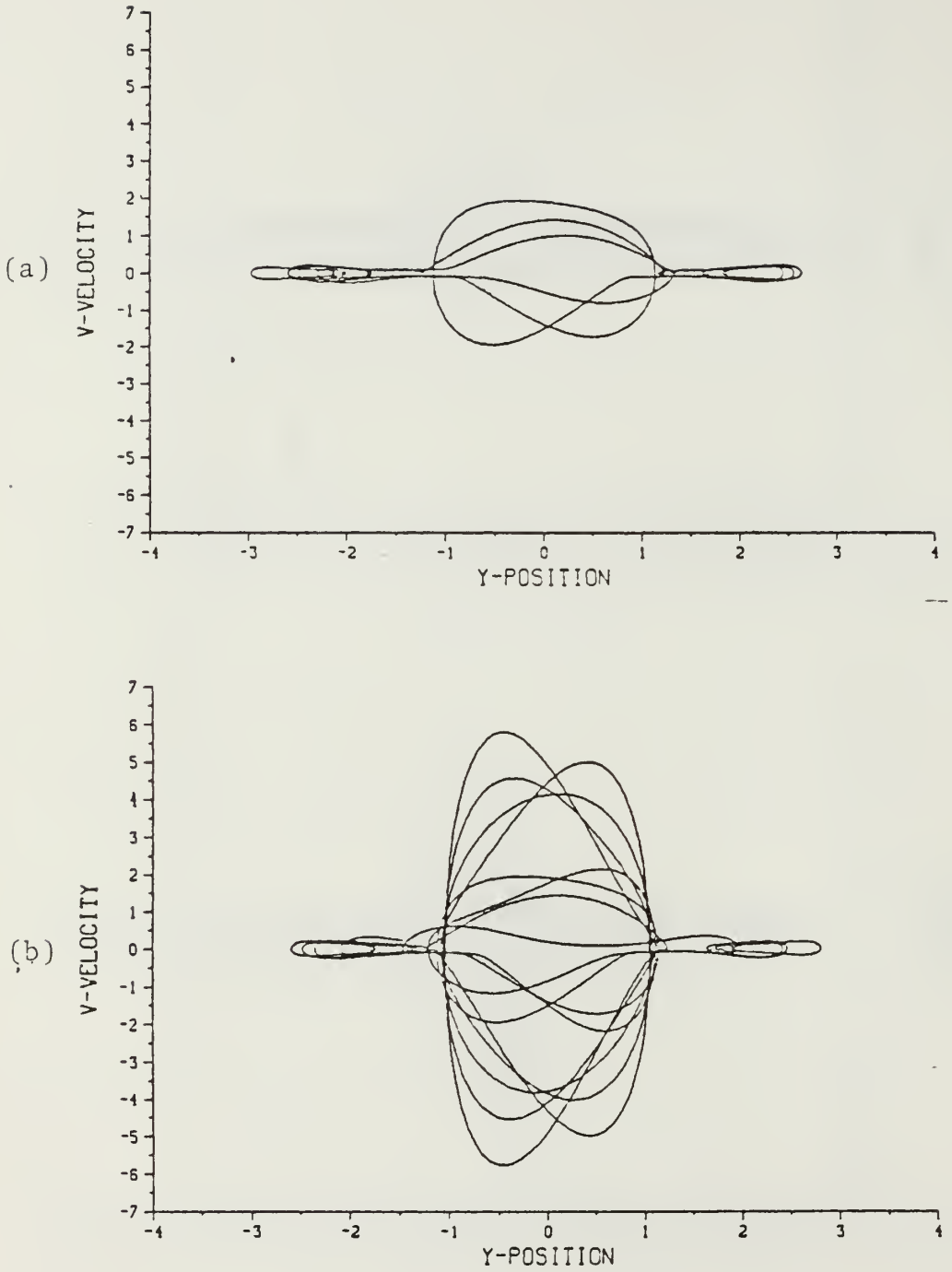

Figure E.18 v-Velocity vs y-Position for 10 Cycles

Ti = 0.25

(a) Z(1) = (0,1.6885), (b) Z(1) = (0, 1.6886)

(a)

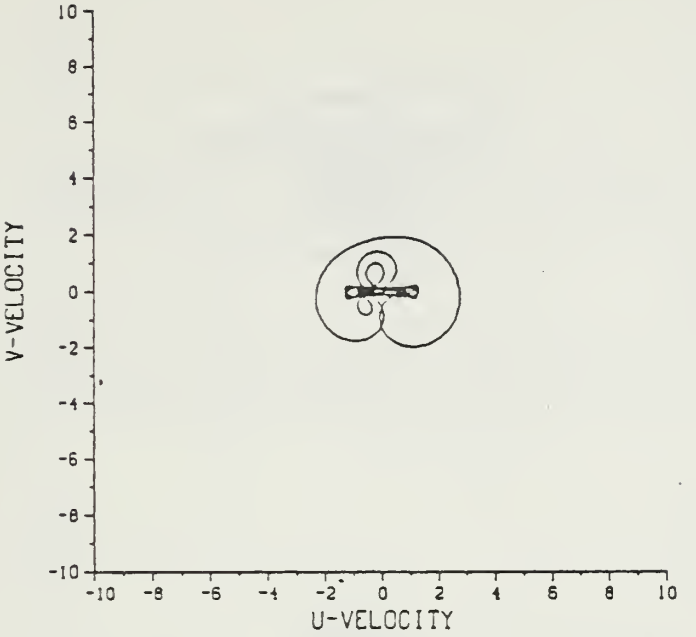

(b)

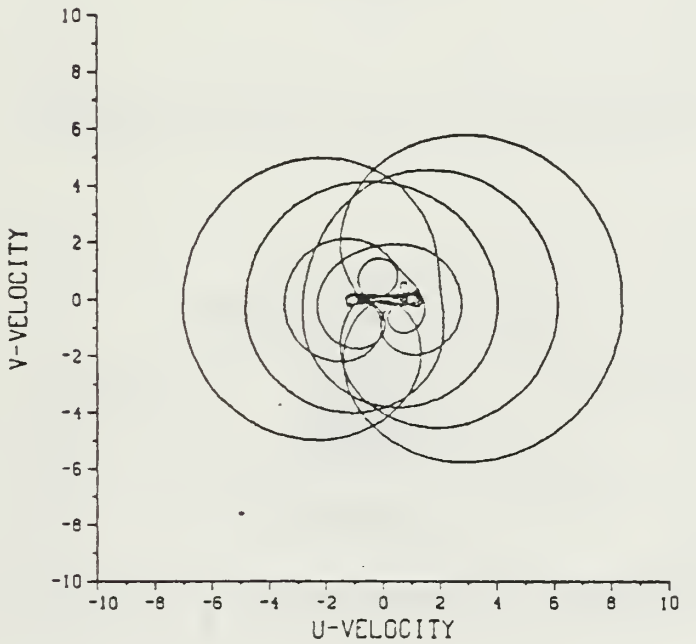

Figure E.19 u-Velocity vs v-Velocity for 10 Cycles

Ti = 0.25

(a) Z(1) = (0, 1.6885), (b) Z(1) = (0, 1.6886)

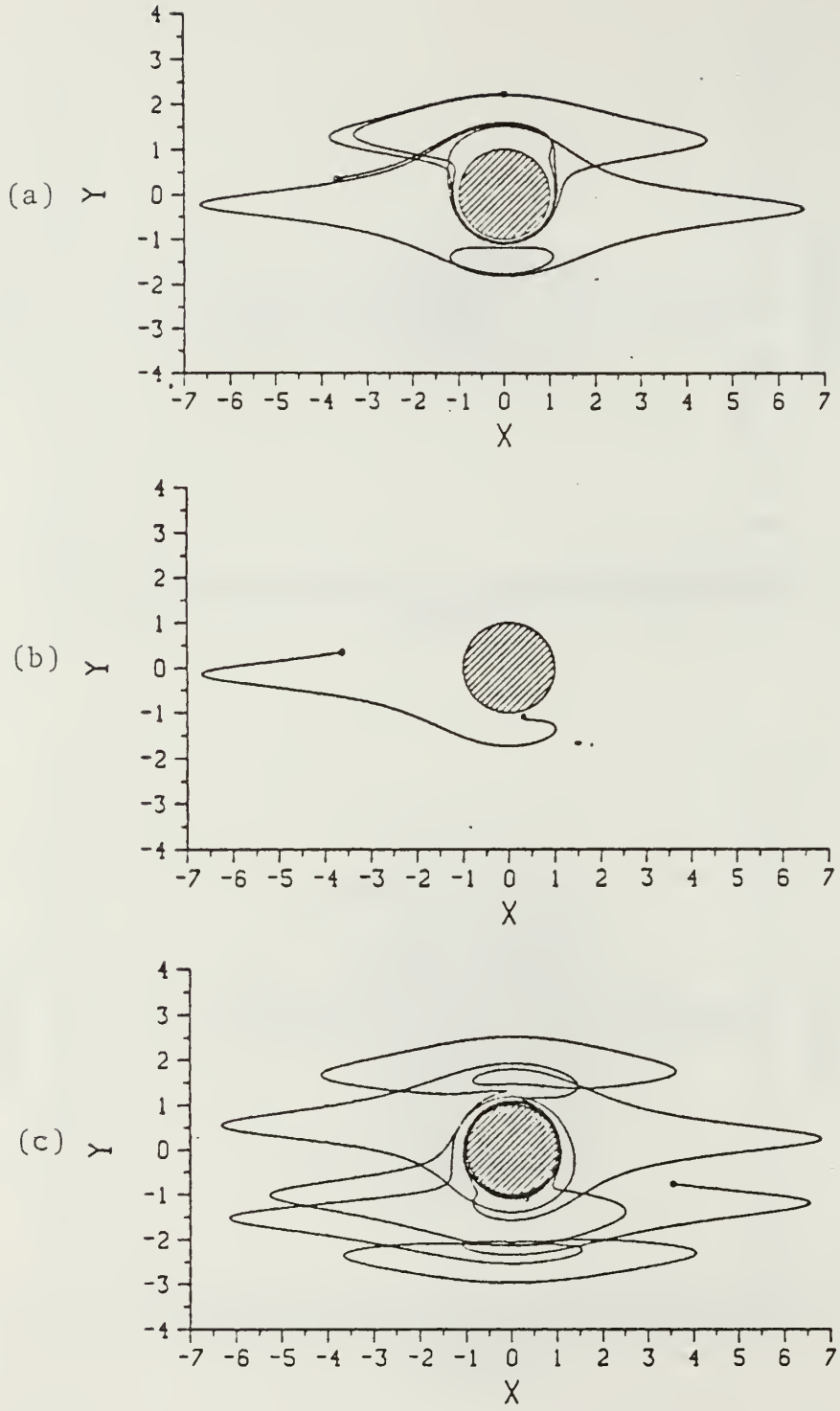

Figure E.20 Vortex Path Z(1) = (0, 2.2192)

Ti = 0.75

(a) Cycles 1-5, (b) Cycle 6, (c) Cycles 7-15

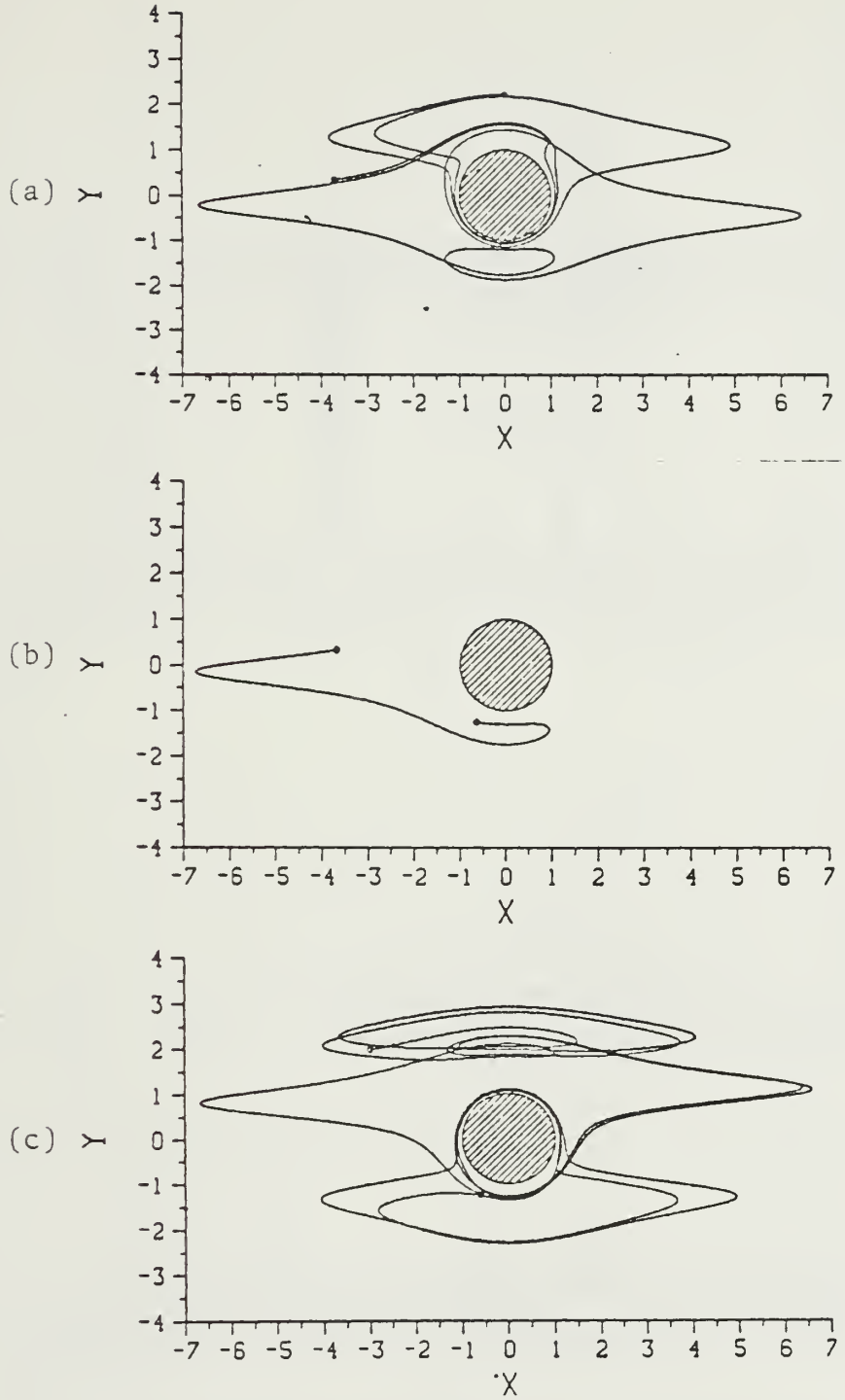

Figure E.21 Vortex Path Z(1) = (0, 2.2193)

Ti = 0.75

(a) Cycles 1-5, (b) Cycle 6, (c) Cycles 7-15

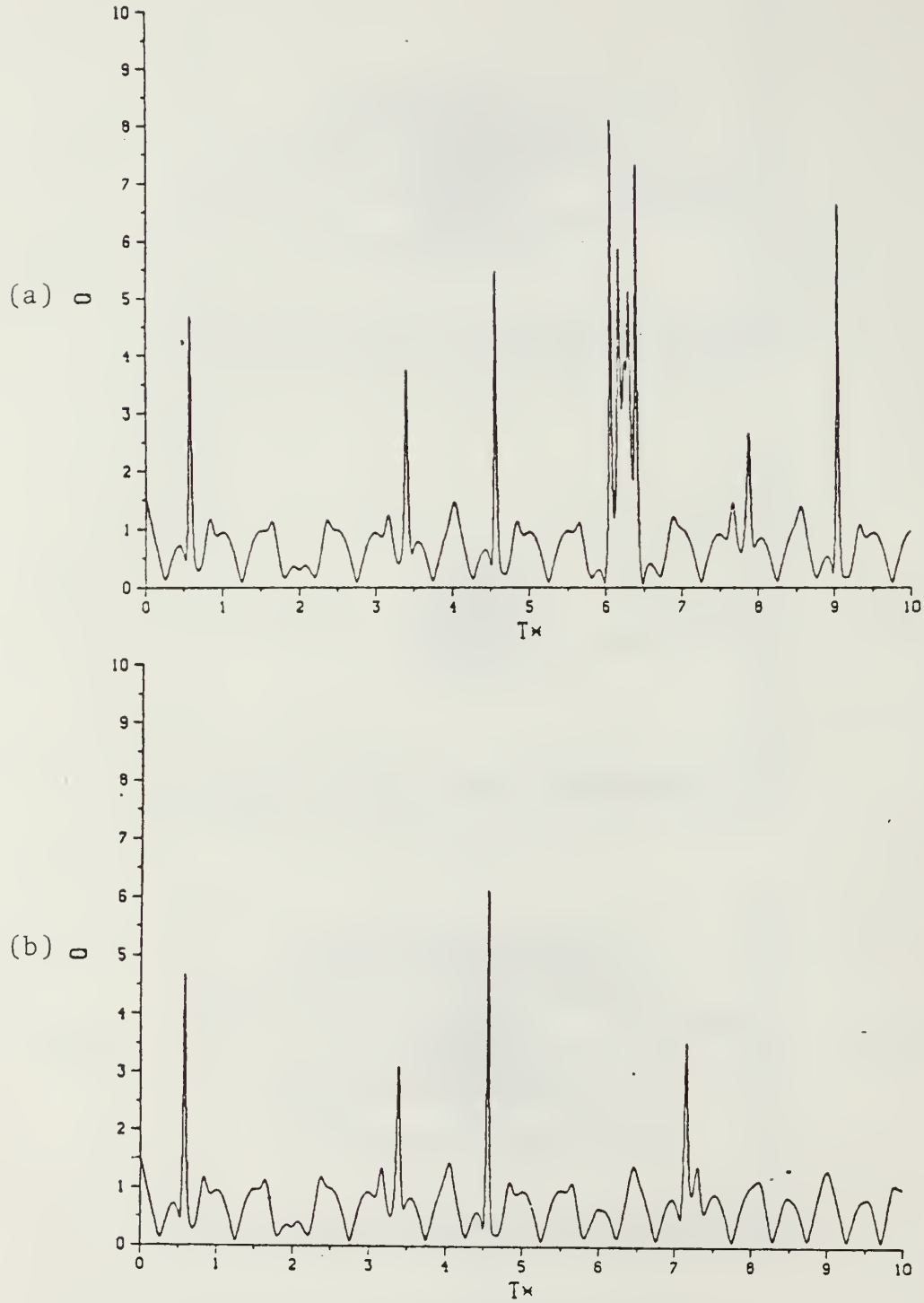

Figure E.22 Velocity Magnitude for 10 Cycles

Ti = 0.75

(a) Z(1) = (0, 2.2192), (b) Z(1) = (0, 2.2193)

(a)

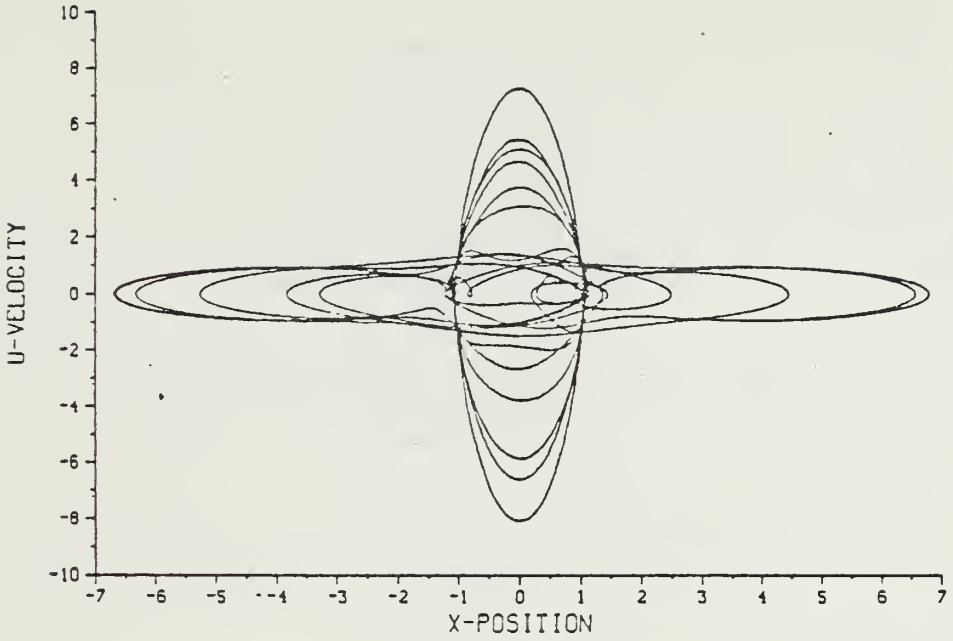

(b)

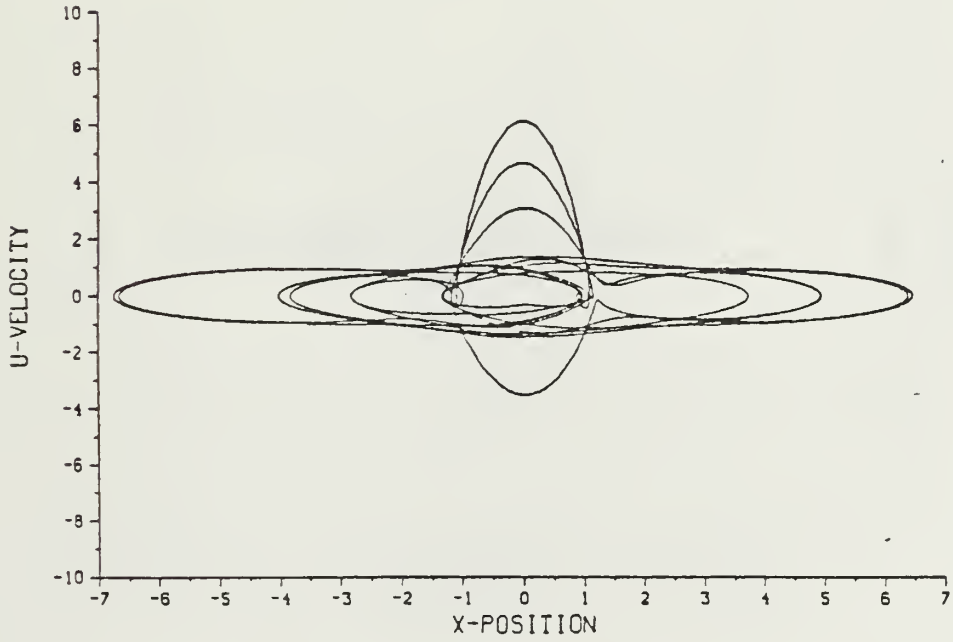

Figure E.23 u-Velocity vs x-Position for 10 Cycles

Ti = 0.75

(a) Z(1) = (0, 2.2192), (b) Z(1) = (0, 2.2193)

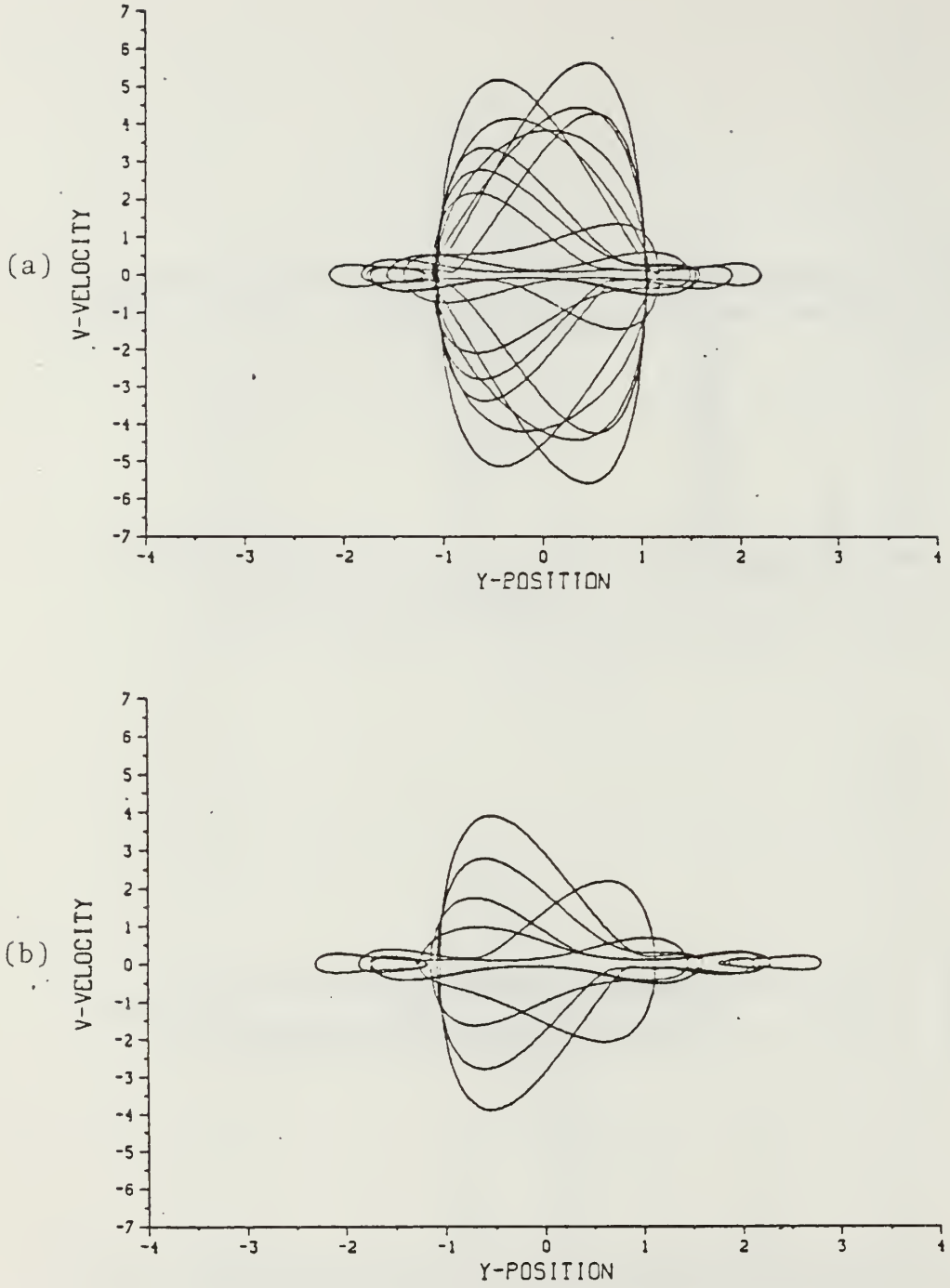

Figure E.24 v-Velocity vs y-Position for 10 Cycles

Ti = 0.75

(a) Z(1) = (0, 2.2192), (b) Z(1) = (0, 2.2193)

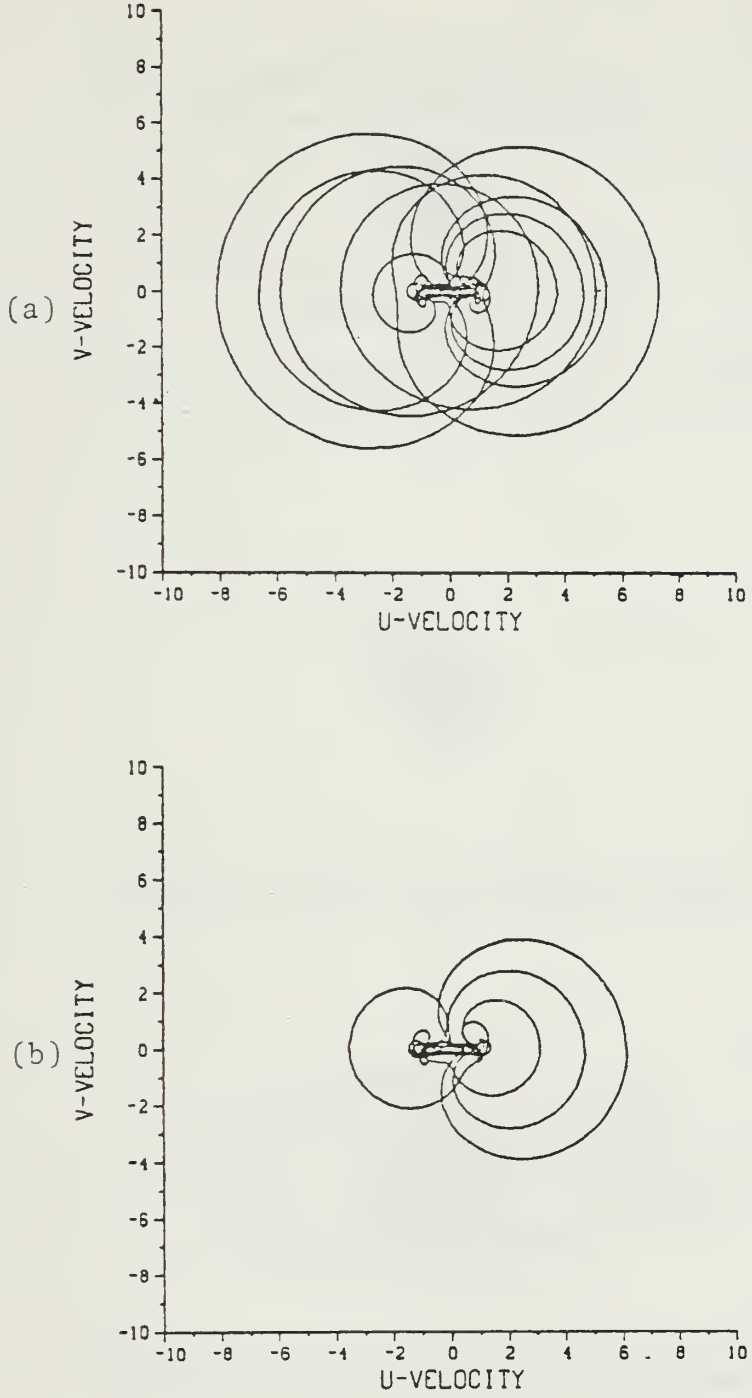

Figure E.25 u-Velocity vs v-Velocity for 10 Cycles

Ti = 0.25

(a) Z(1) = (0, 2.2192), (b) Z(1) = (0, 2.2193)

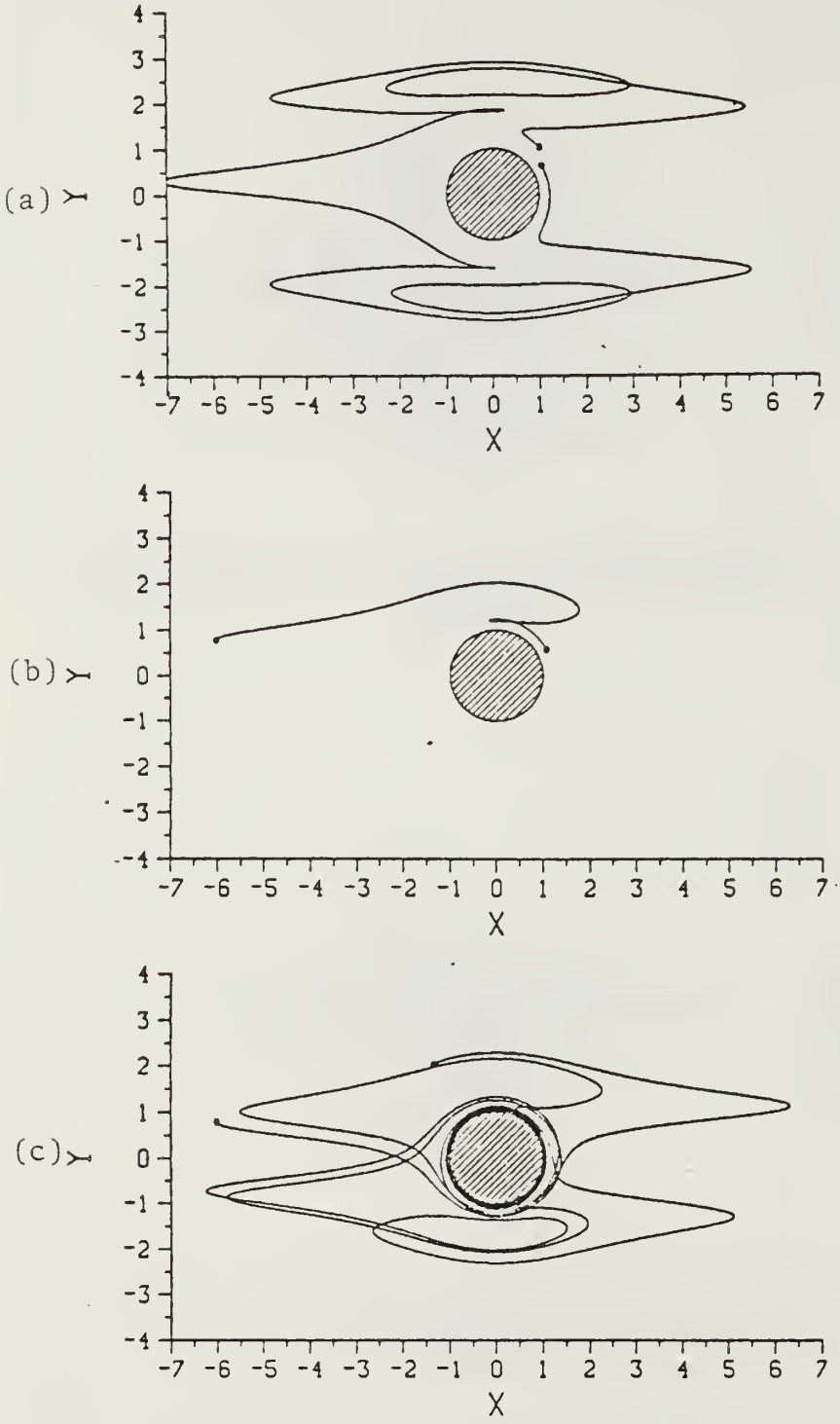

Figure E.26 Vortex Path Z(1) = (1.0, 1.0272)

Ti = 0.0

(a) Cycles 1-6, (b) Cycle 7, (c) Cycles 8-15

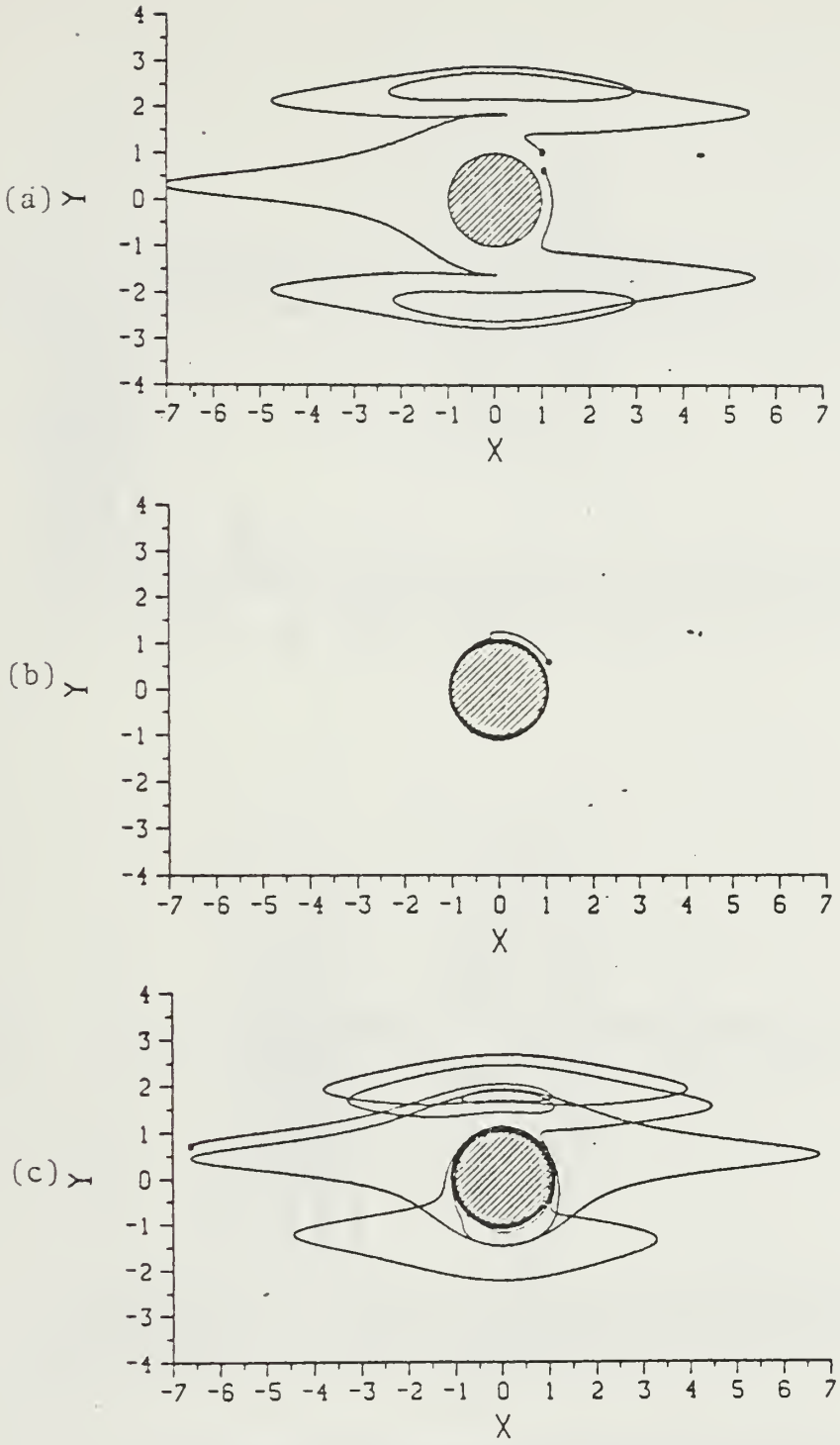

Figure E.27 Vortex Path Z(1) = (1.0, 1.0273)

Ti = 0.0

(a) Cycles 1-6, (b) Cycle 7, (c) Cycles 8-15

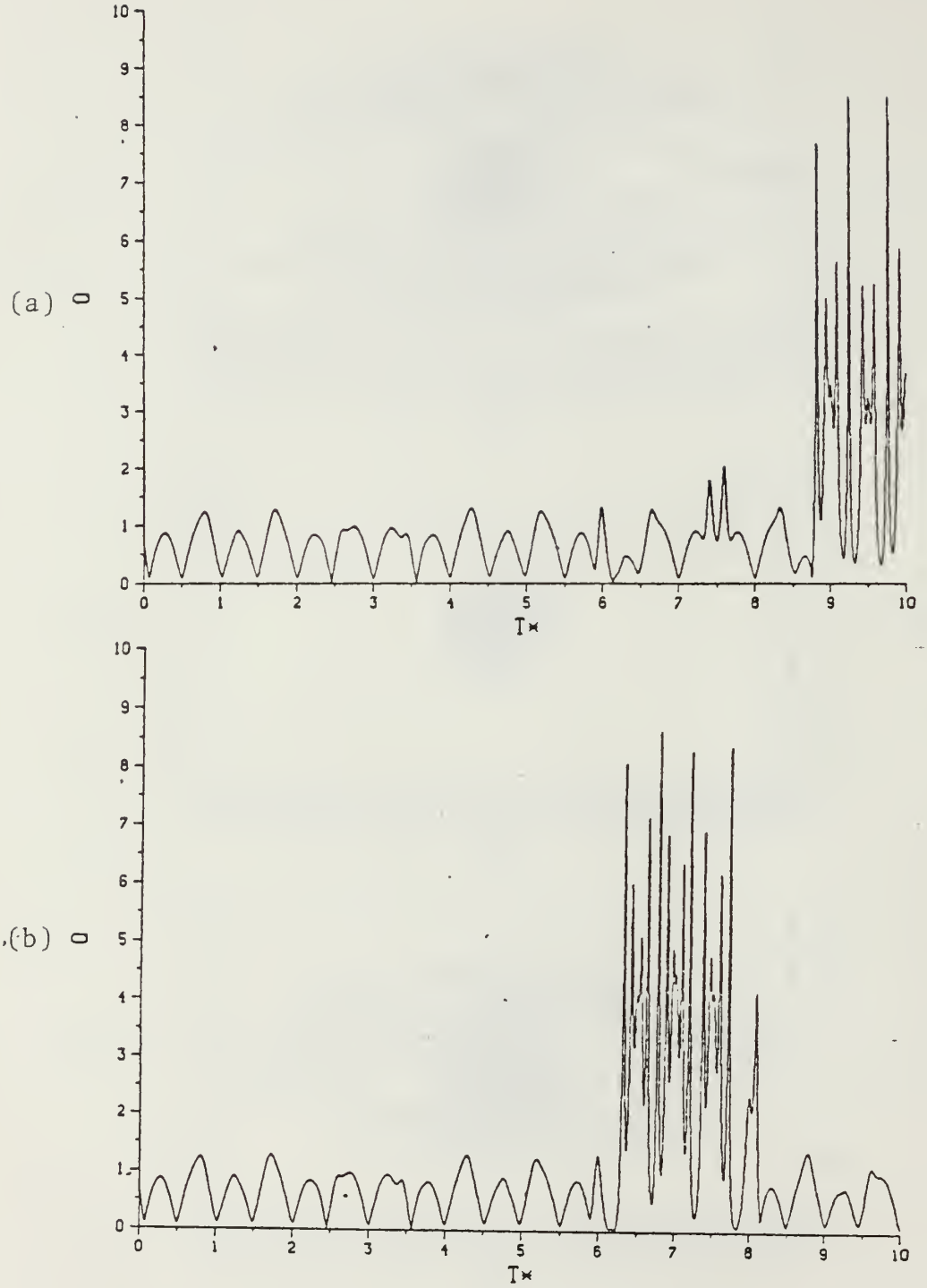

Figure E.28 Velocity Magnitudes for 10 Cycles

Ti = 0.0

(a) Z(1) = (1.0, 1.0272), (b) Z(1) = (1.0, 1.0273)

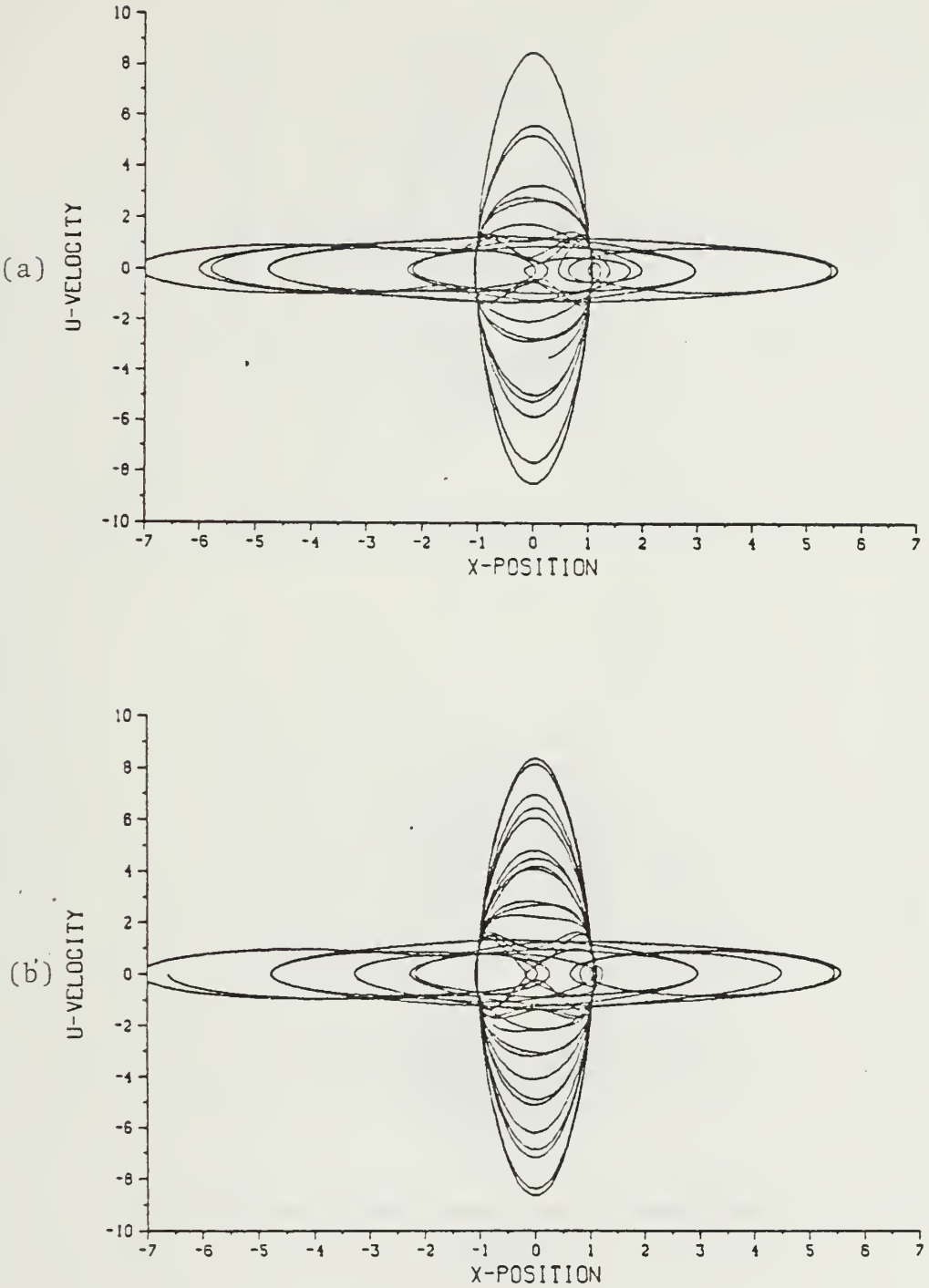

Figure E.29 u-Velocity vs x-Position for 10 Cycles

Ti = 0.0

(a) Z(1) = (1.0, 1.0272), (b) Z(1) = (1.0, 1.0273)

(a)

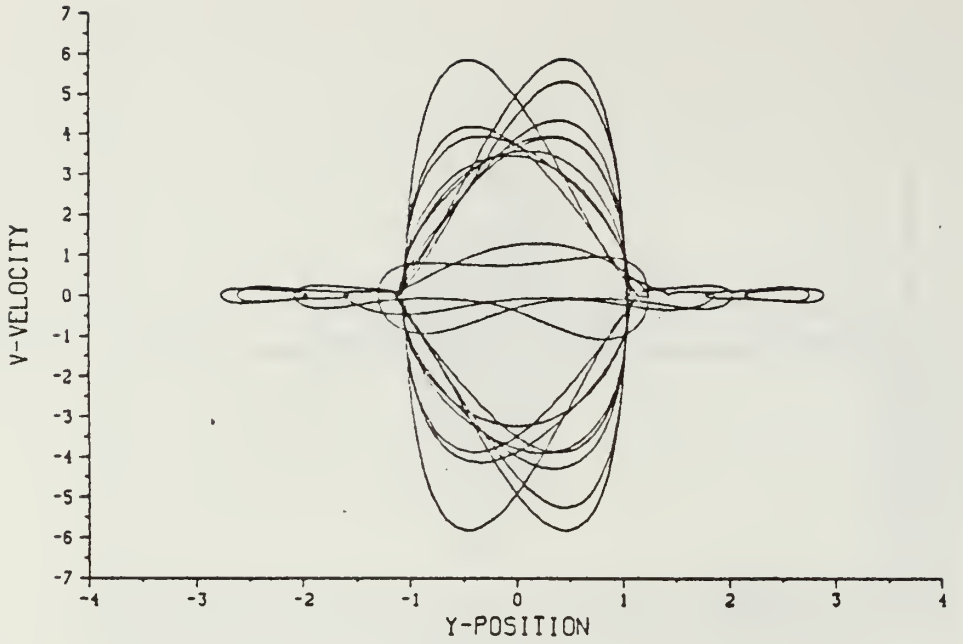

(b)

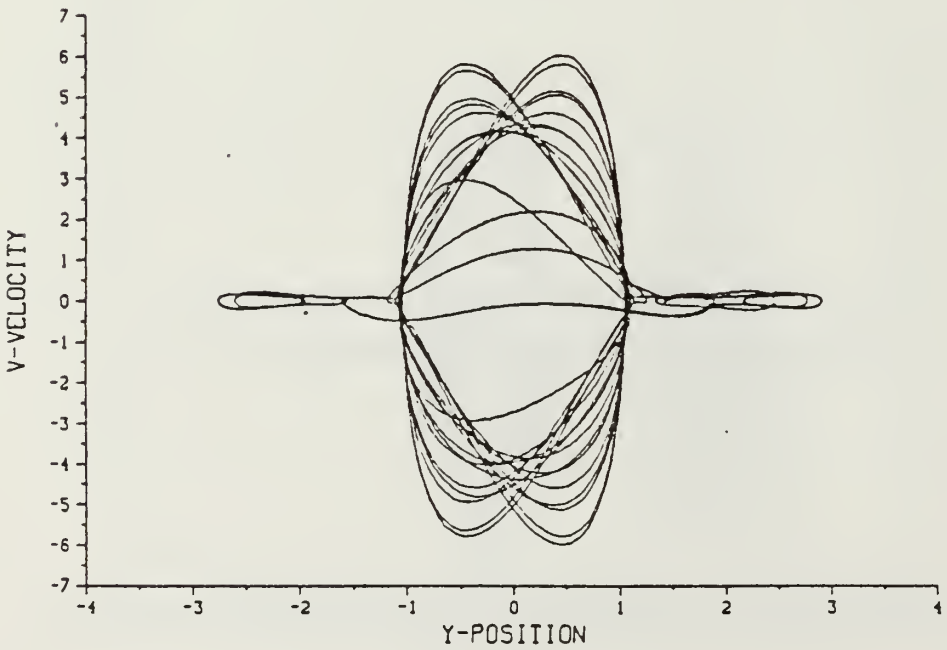

Figure E.30 v-Velocity vs y-Position for 10 Cycles

Ti = 0.0

(a) Z(1) = (1.0, 1.0272), (b) Z(1) = (1.0, 1.0273)

(a)

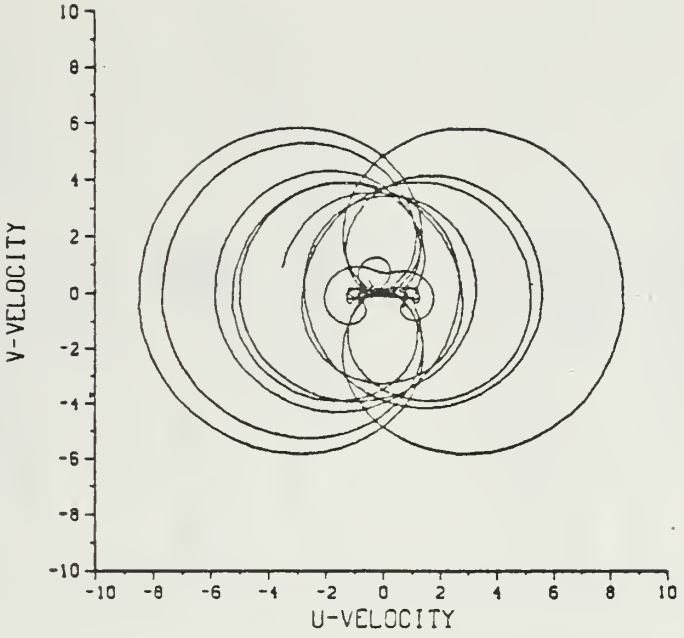

(b)

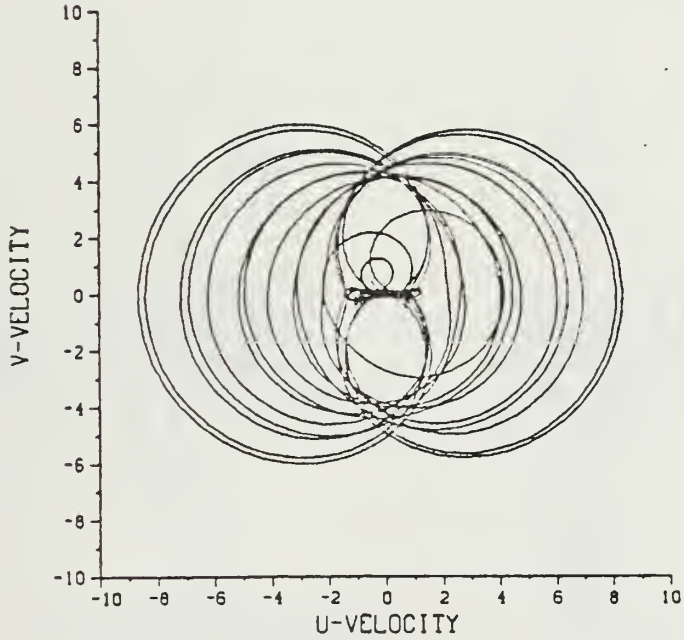

Figure E.31 u-Velocity vs v-Velocity for 10 Cycles

Ti = 0.0

(a) Z(1) = (1.0, 1.0272), (b) Z(1) = (1.0, 1.0273)

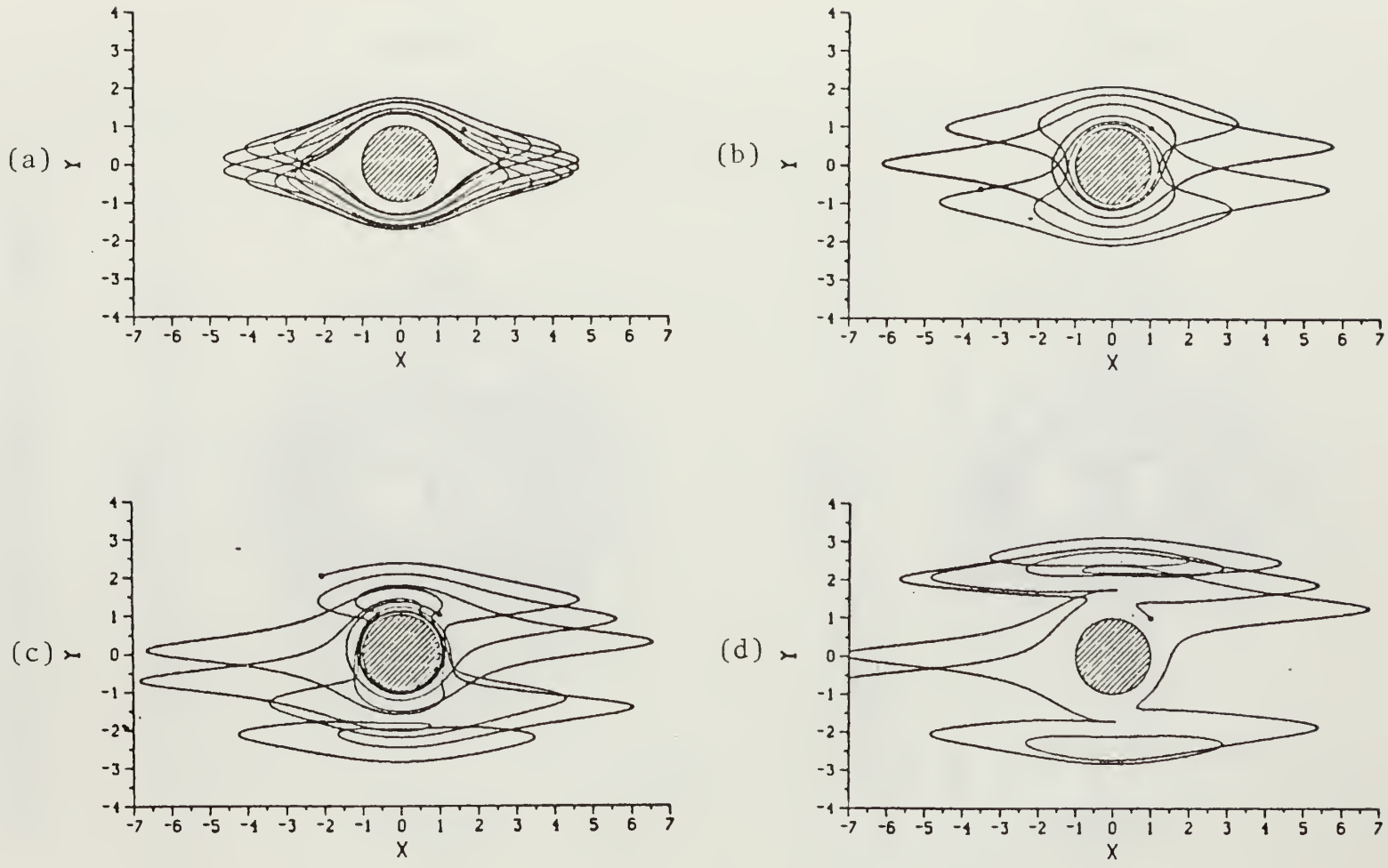

Figure E.32 Investigation of Phase Shift and Vortex Path Z(1) = (1,1)

(a) Ti = 0.75, (b) Ti = 0.85, (c) Ti = 0.88, (d) Ti = 1.00

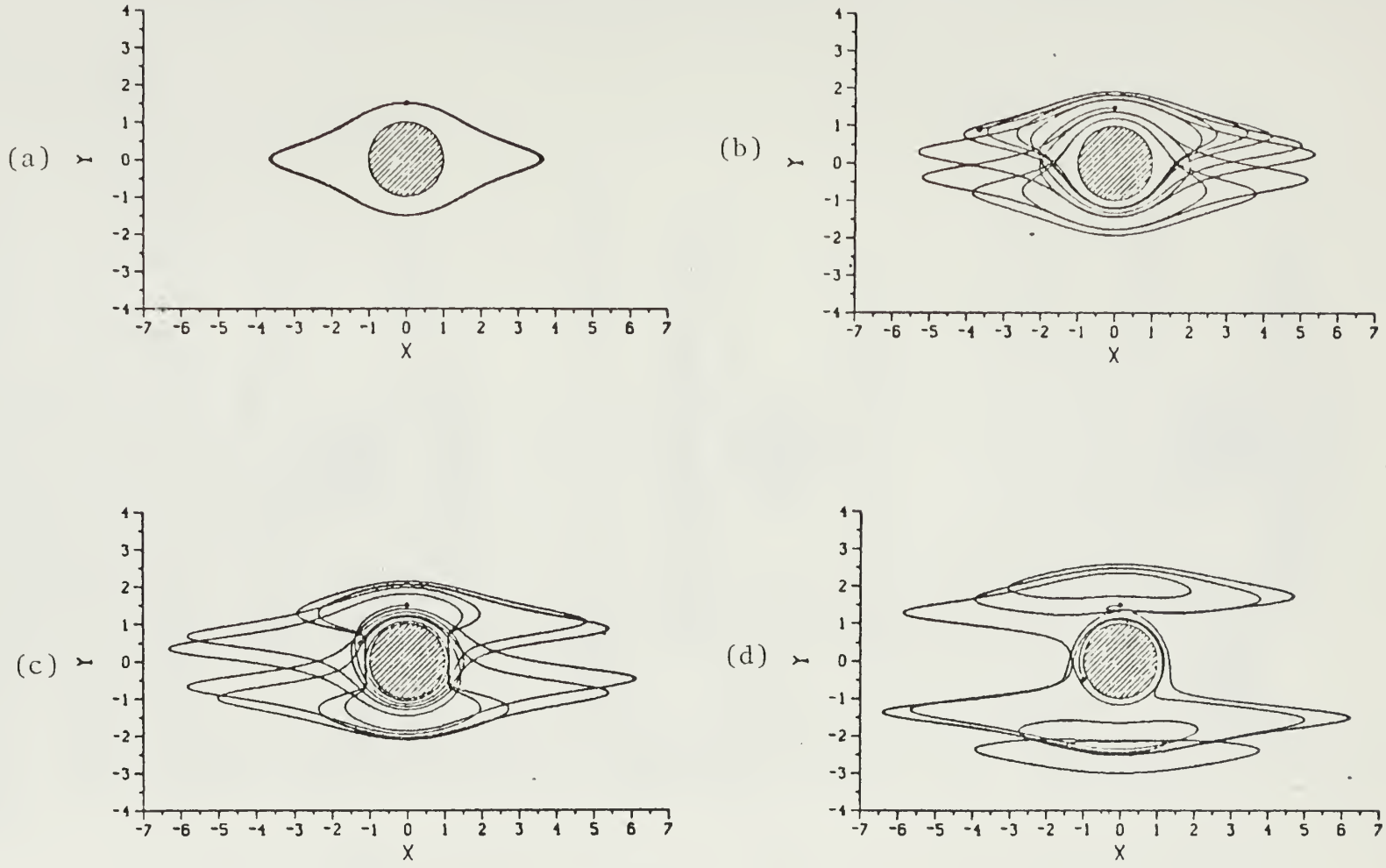

Figure E.33 Investigation of Phase Shift and Vortex Path Z(1) = (0,1.50)

(a) Ti = 0.75, (b) Ti = 0.85, (c) Ti = 0.92, (d) Ti = 1.00

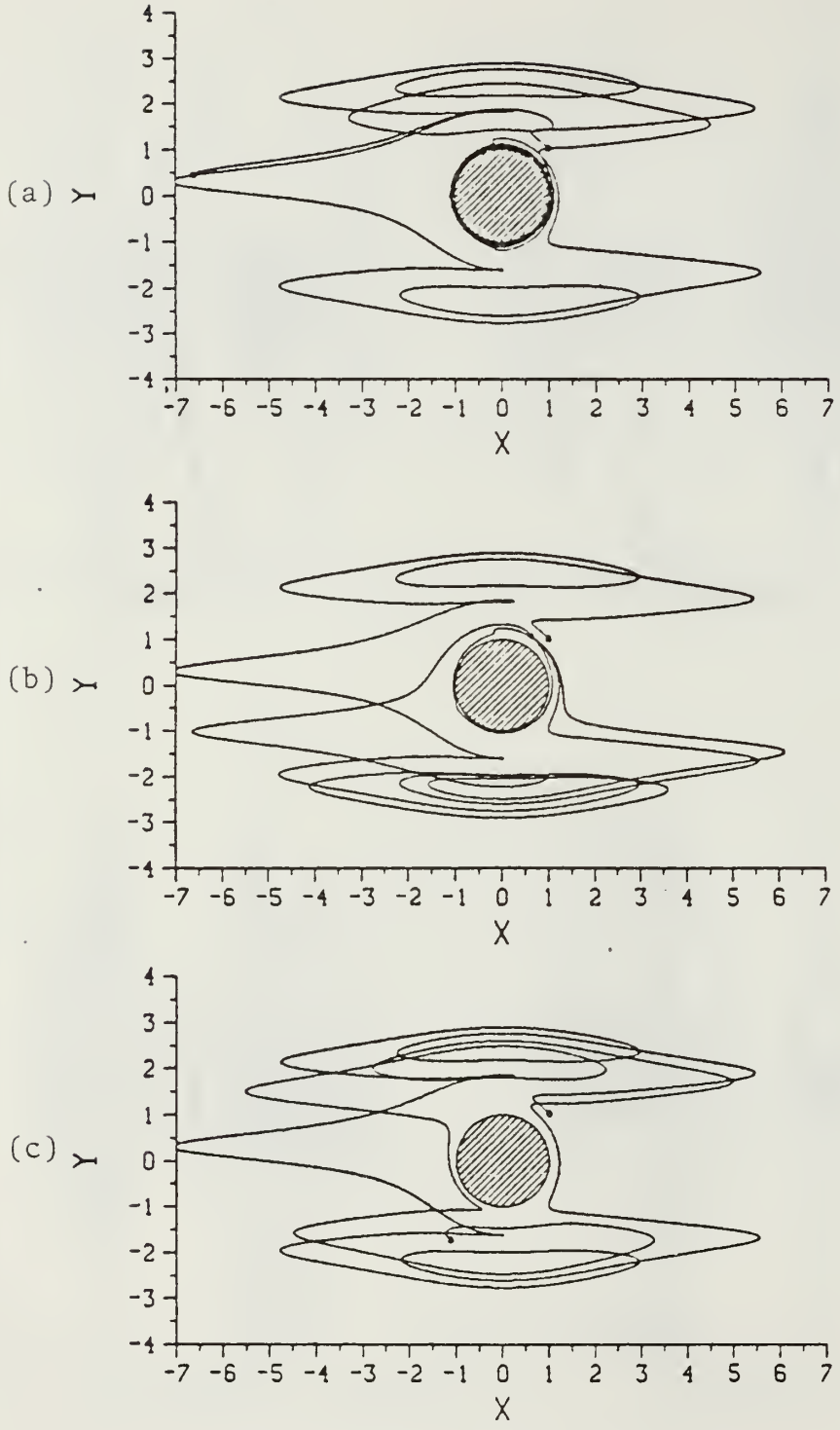

Figure E.34 Comparison of Vortex Models

Z(1) = (0.1.0273), Ti = 0.0

(a) Ideal, (b) Rankine, (c) Gaussian Time Dependent

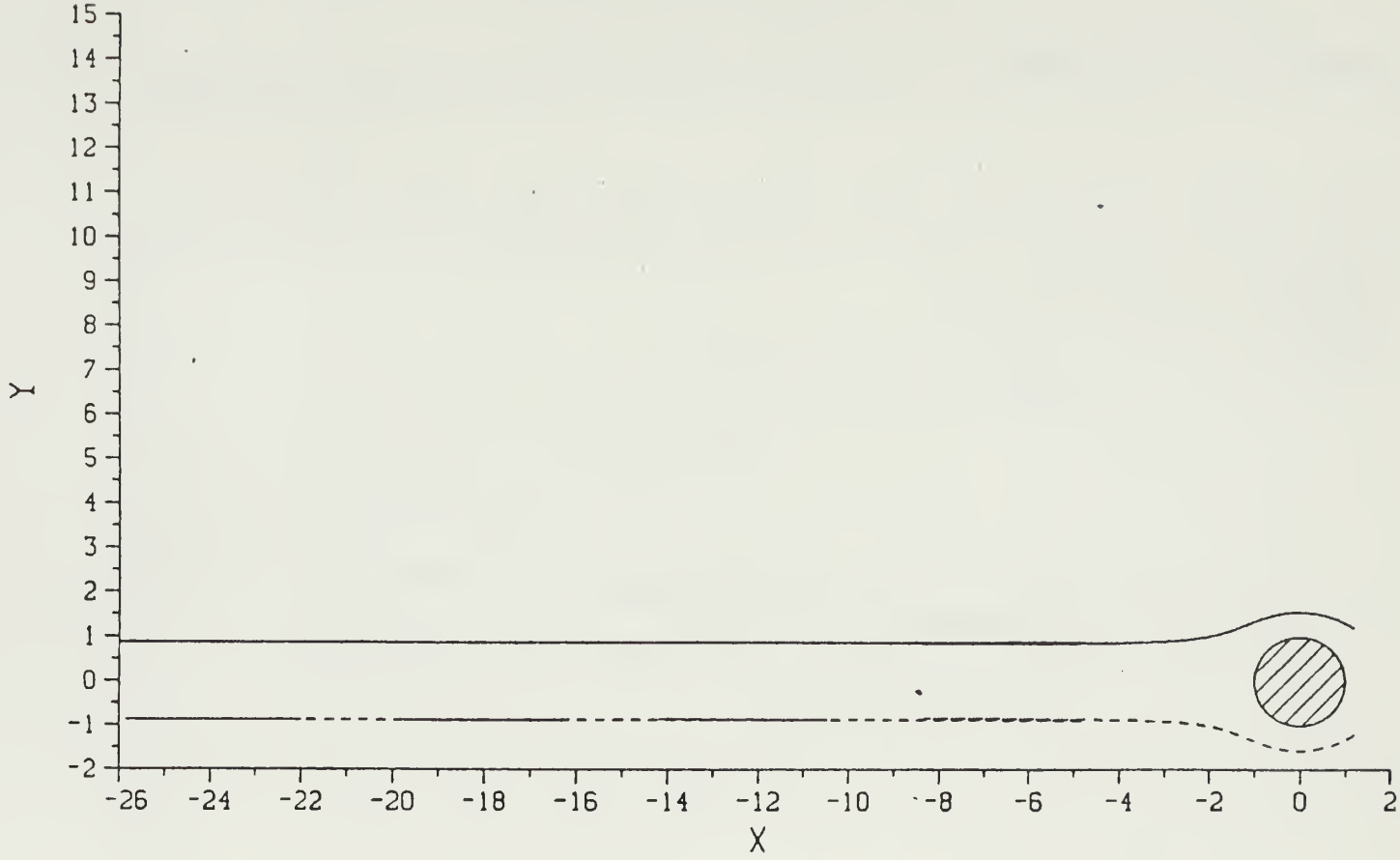

Figure E.35 Symmetric Two Vortex Model $Z_A = (1.2, 1.2), Z_B = (1.2, -1.2)$

$K_A = K_B = 0.5$

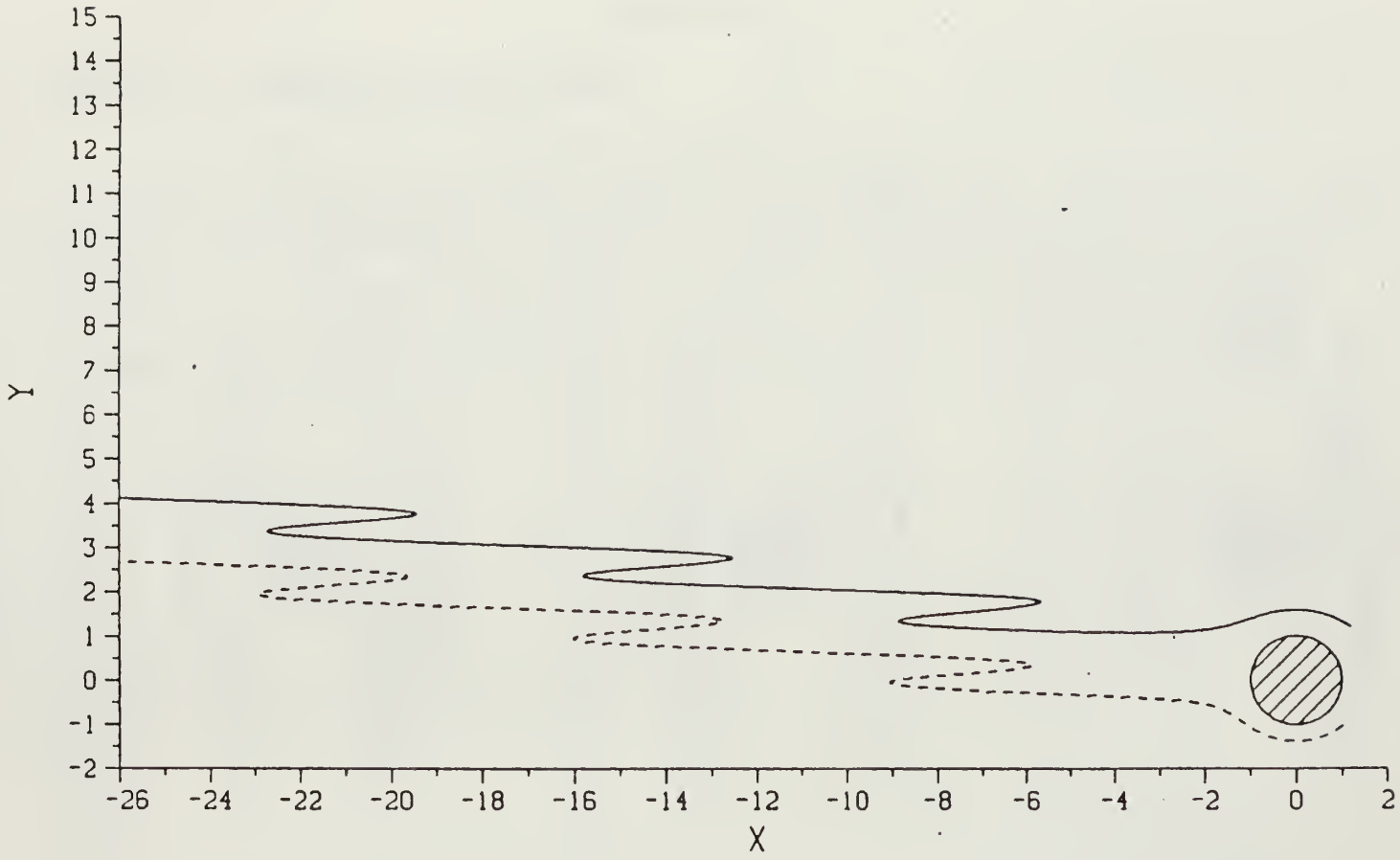

Figure E.36 Two Vortex Model - Asymmetric Locations $Z_A = (1.2, 1.2)$, $K_A = K_B = 0.5$

$\varepsilon_r = 0.85$

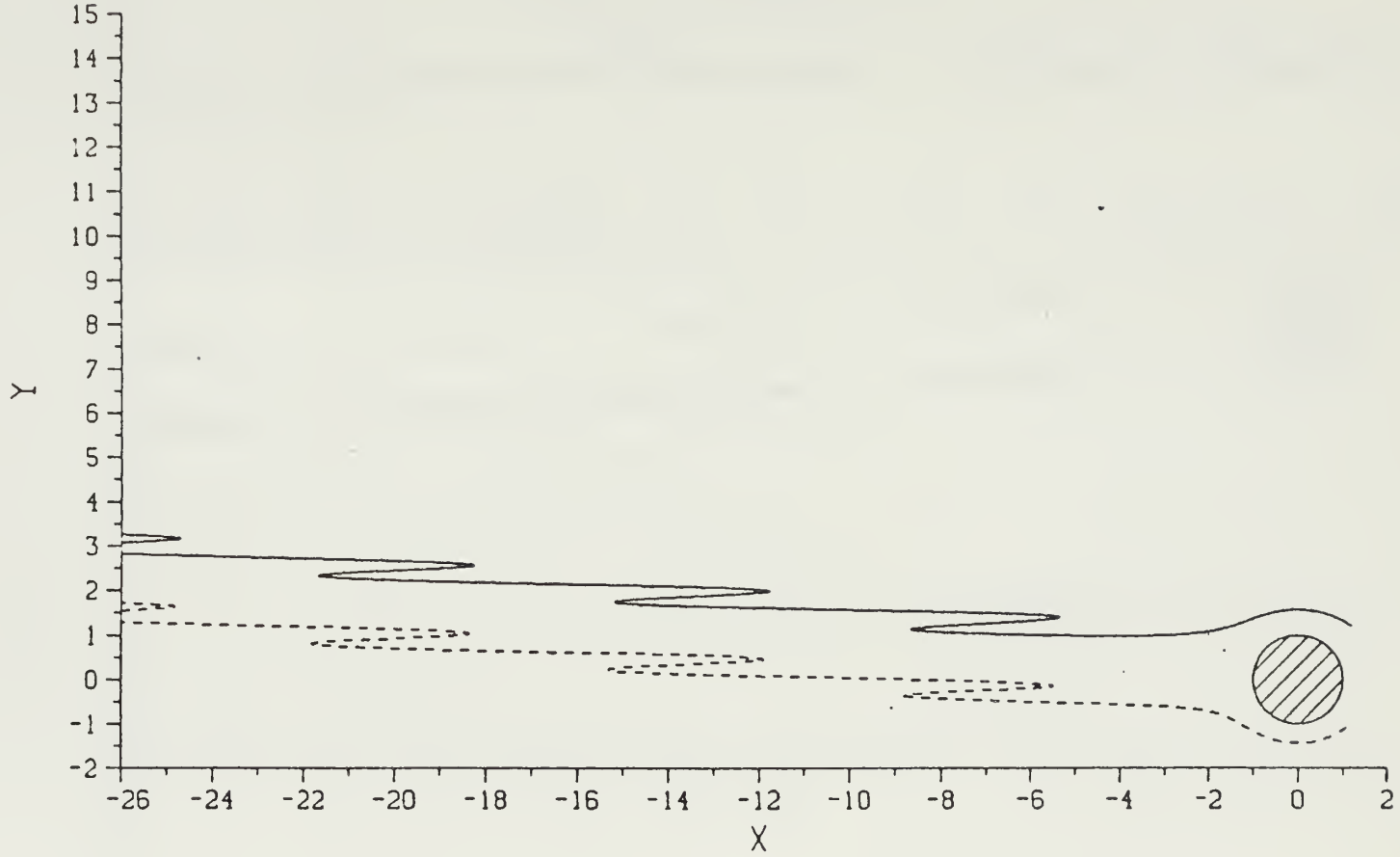

Figure E.37 Two Vortex Model - Asymmetric Locations $Z_A = (1.2, 1.2)$, $K_A = K_B = 0.5$

$\varepsilon_r = 0.90$

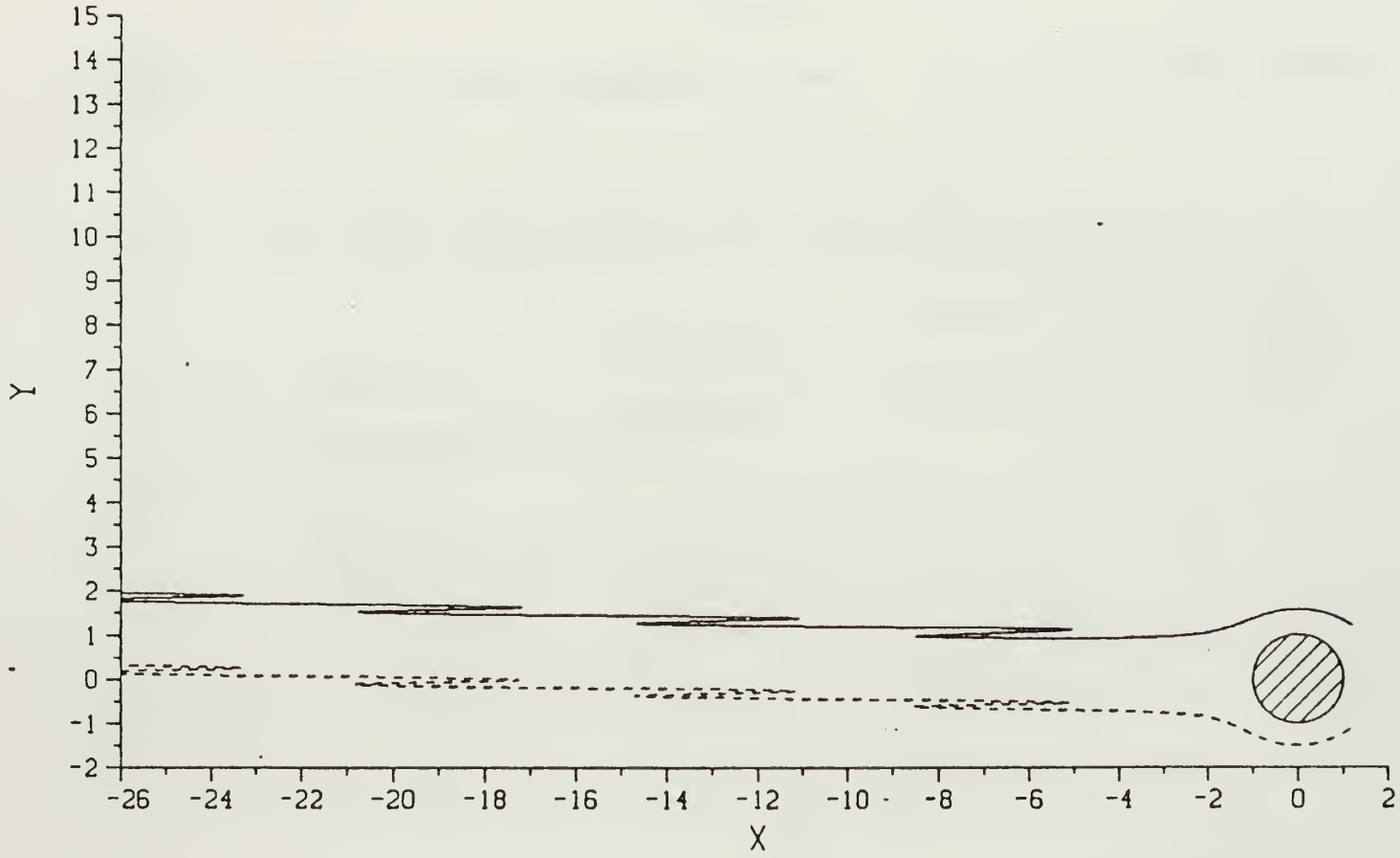

Figure E.38 Two Vortex Model - Asymmetric Locations $Z_A = (1.2, 1.2)$, $K_A = K_B = 0.5$

$\varepsilon_r = 0.95$

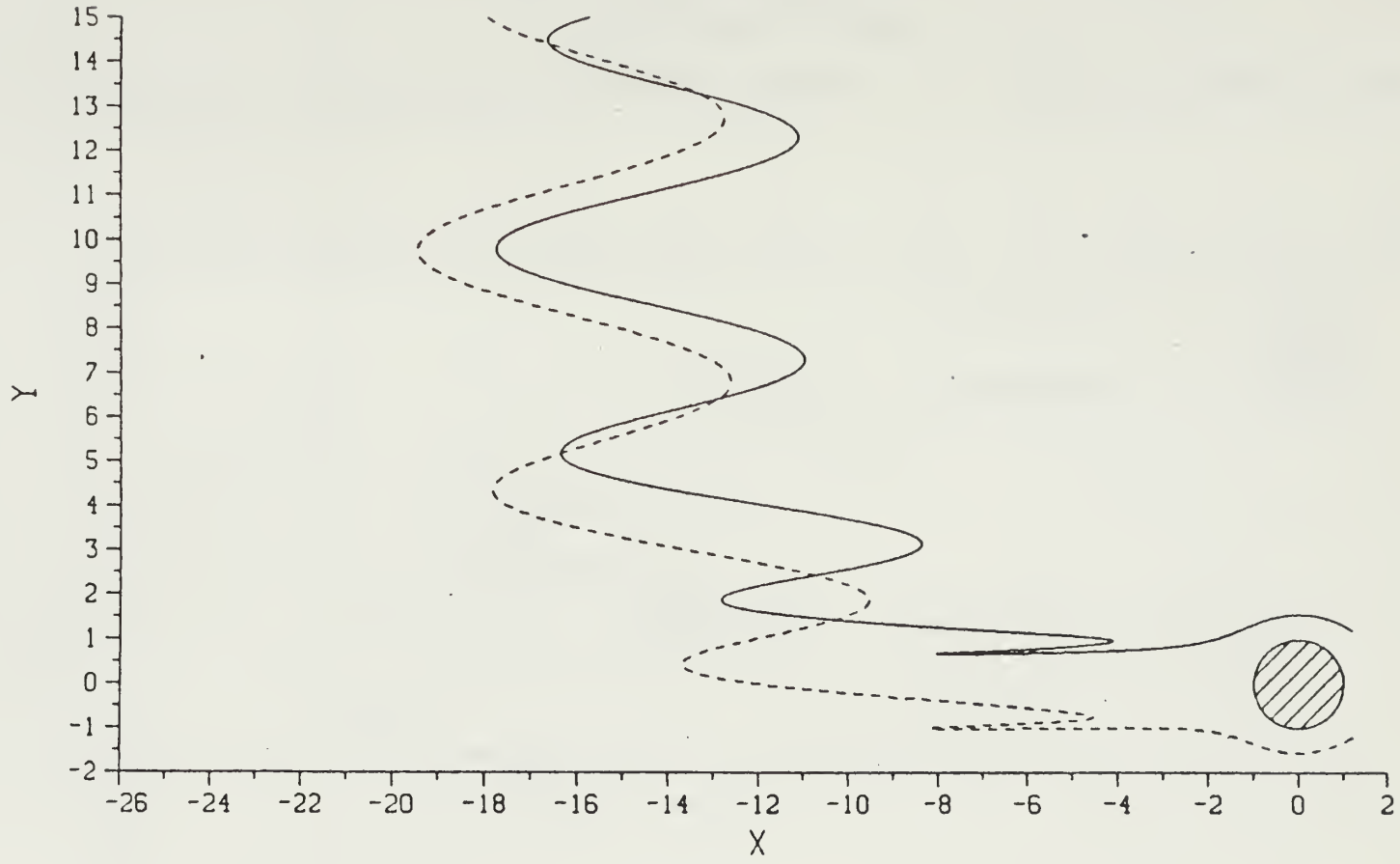

Figure E.39 Two Vortex Model - Asymmetric Strengths $Z_A = (1.2, 1.2), Z_B = (1.2, -1.2)$

$K_A = 0.50, \varepsilon_K = 0.85$

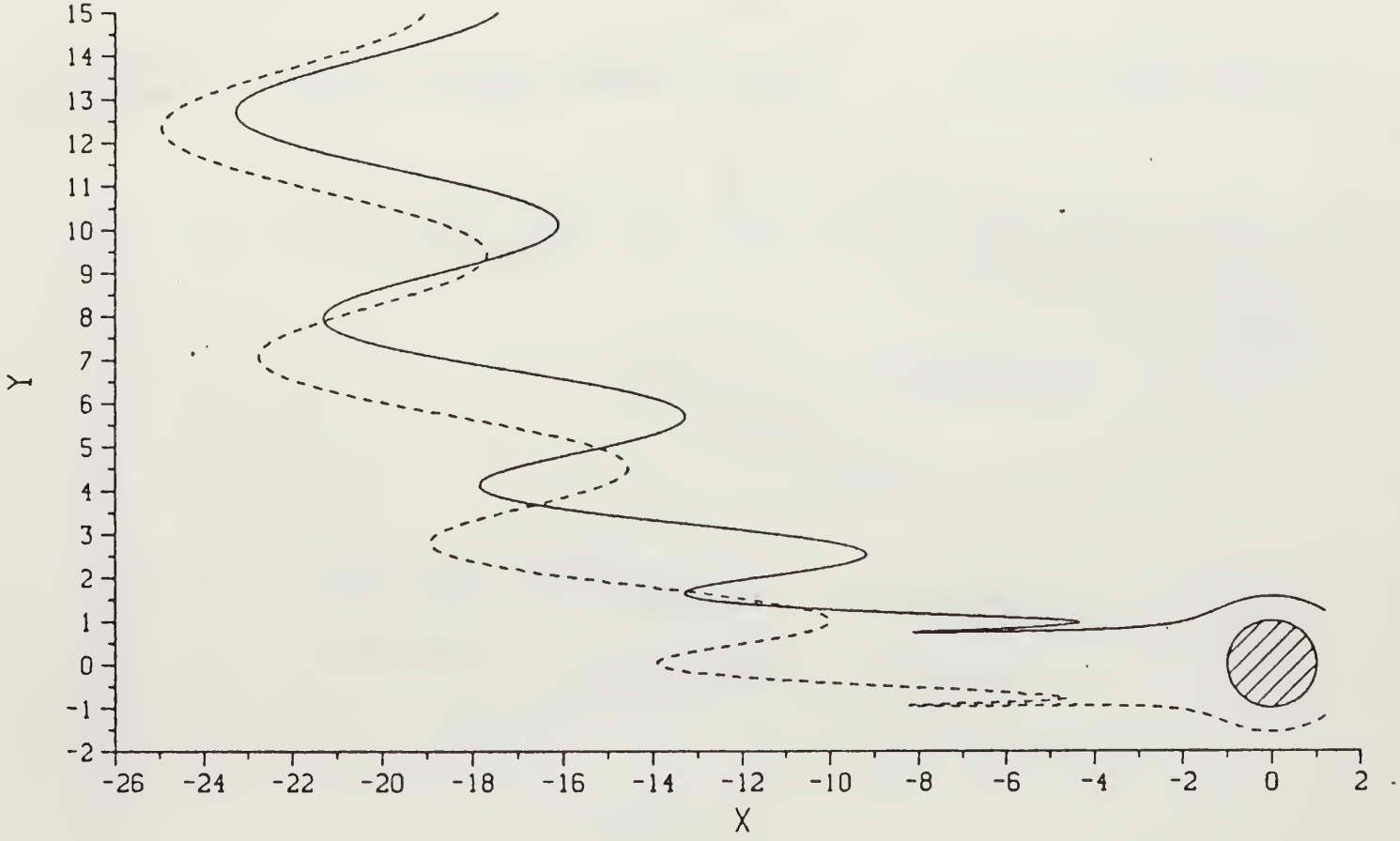

Figure E.40 Two Vortex Model - Asymmetric Strengths $Z_A = (1.2, 1.2), Z_B = (1.2, -1.2)$

$K_A = 0.50, \varepsilon_K = 0.90$

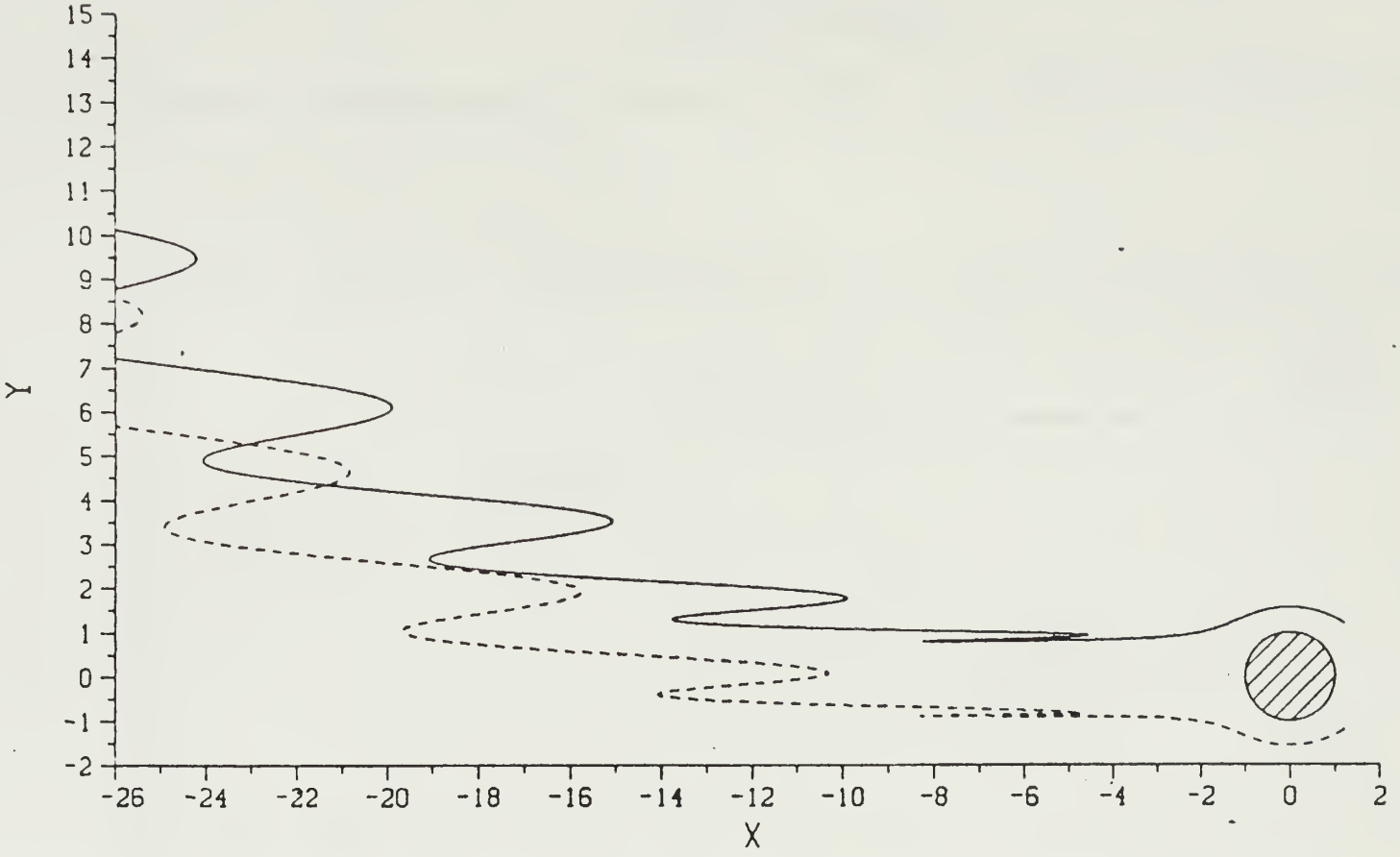

Figure E.41 Two Vortex Model - Asymmetric Strengths $Z_A = (1.2, 1.2), Z_B = (1.2, -1.2)$

$K_A = 0.50, \varepsilon_K = 0.95$

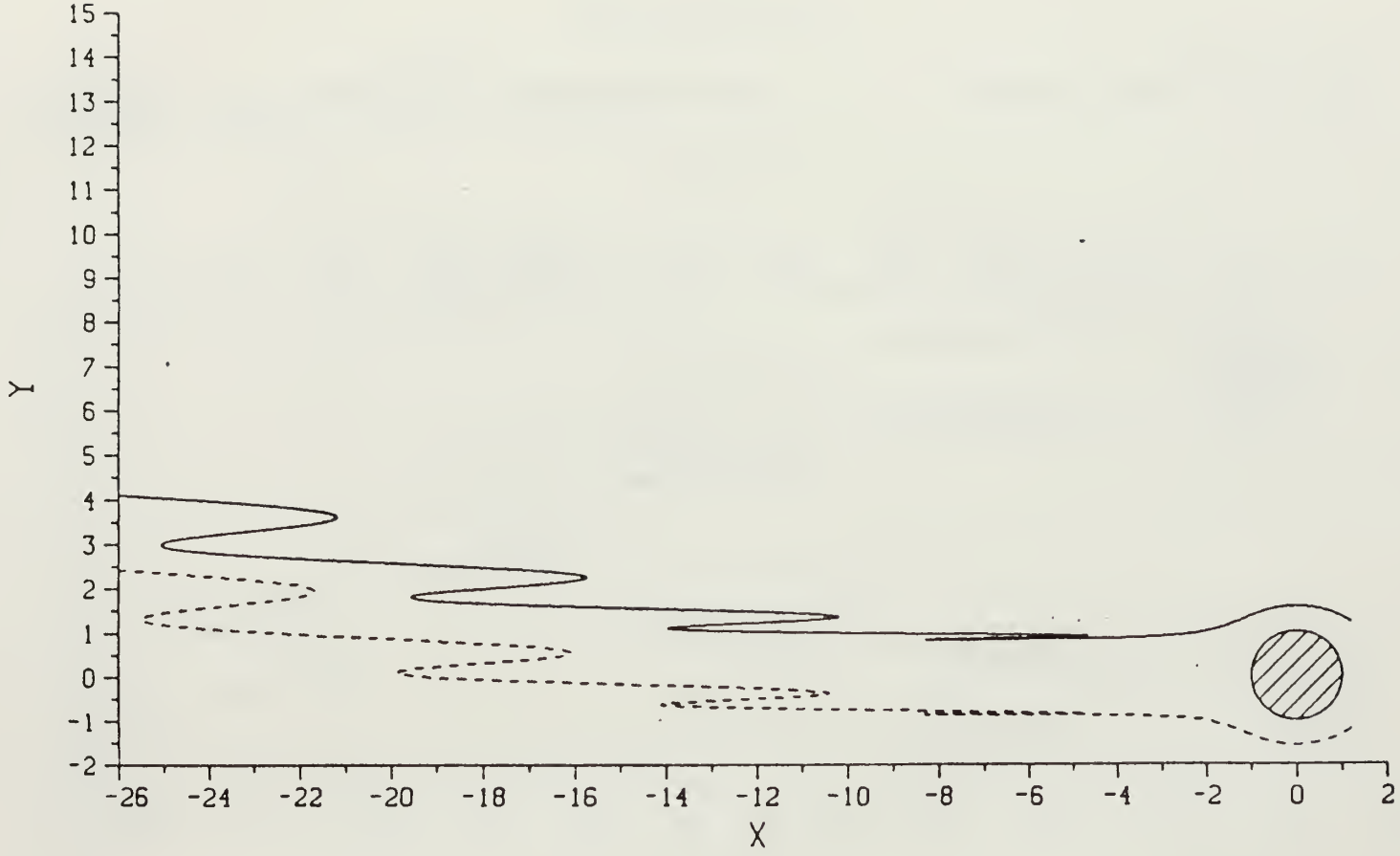

Figure E.42 Two Vortex Model - Asymmetric Strengths $Z_A = (1.2, 1.2), Z_B = (1.2, -1.2)$

$K_A = 0.50, \varepsilon_K = 0.975$

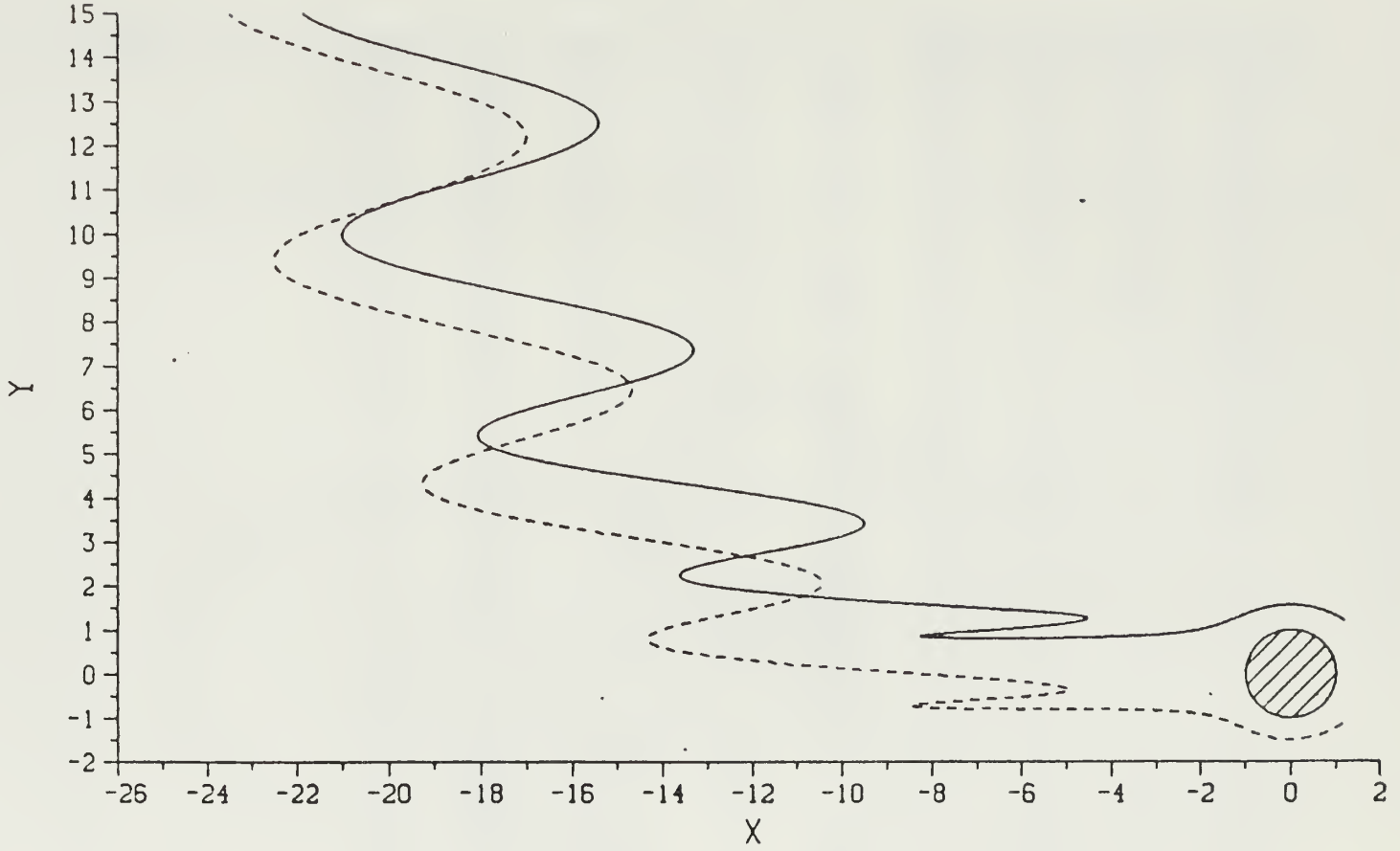

Figure E.43 Two Vortex Model - Asymmetric Strengths & Locations $Z_A = (1.2, 1.2)$, $K_A = 0.50$

$\varepsilon_r = 0.90$, $\varepsilon_K = 0.95$

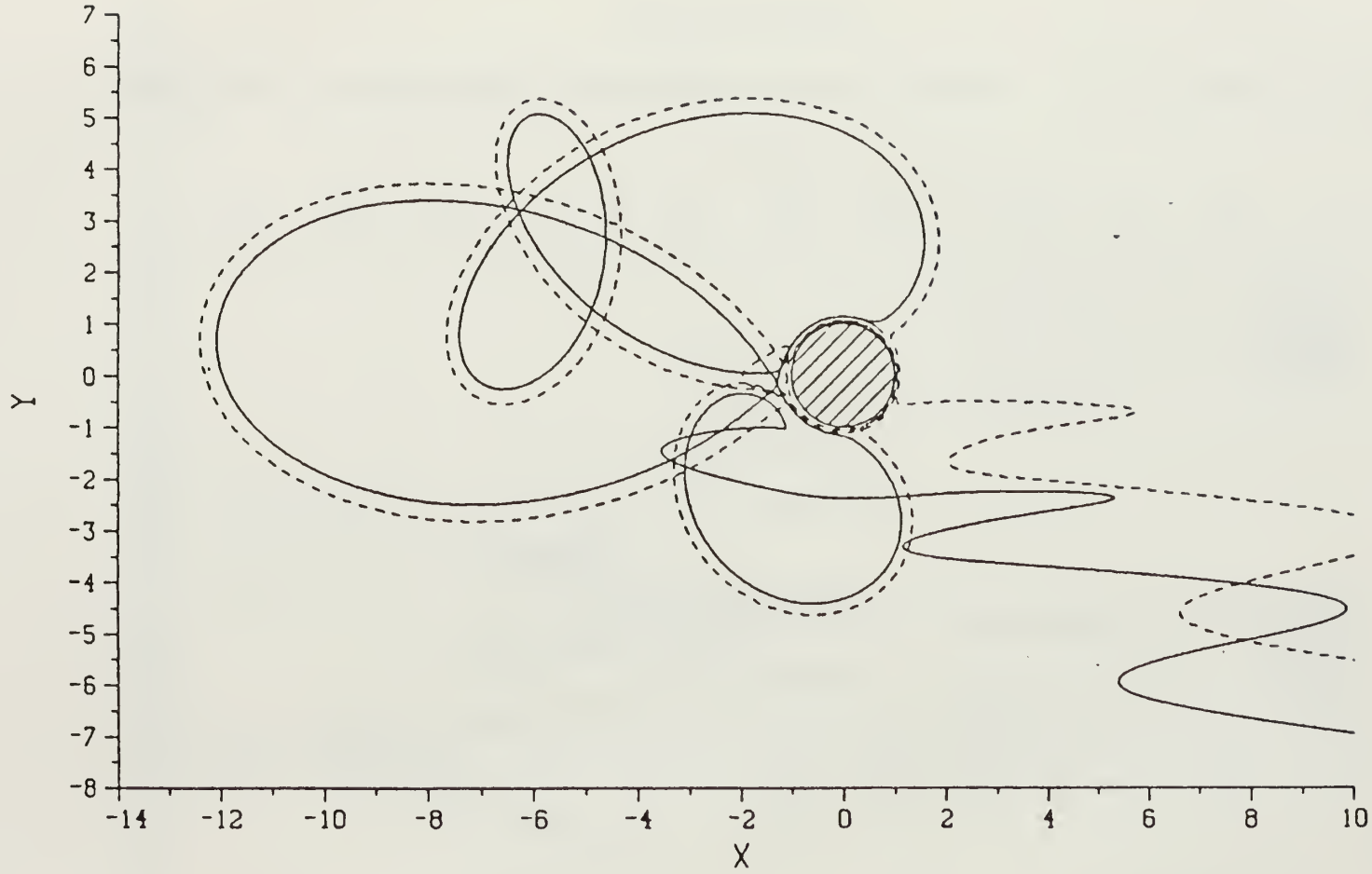

Figure E.44 Two Vortex Model - Cylinder Influenced $Z_A = (0.8, 0.8), Z_B = (0.8, -0.8)$

$K_A = 0.50, \varepsilon_K = 0.9$

LIST OF REFERENCES

1. Holmes, P.J., "Averaging and Chaotic Motions in Forced Oscillations," *Journal of Applied Mathematics, Society of Industrial and Applied Mathematics*, vol. 38, no. 1, pp. 543-545, Feb 1980.

2. Aref, H., "Stirring by Chaotic Advection," *Journal of Fluid Mechanics*, vol. 143, pp. 1-21, 1984.

3. Hardin, J.C. and Mason, J.P., "Periodic Motion of Two and Four Vortices in a Cylindrical Pipe," *Physics of Fluids*, vol. 27, no. 7, pp. 1583-1584, July 1984.

4. Dowell, E.H. and Pezeshki, C., "On the Understanding of Chaos in Duffings Equation Including a Comparison With Experiment," *Journal of Applied Mechanics*, vol. 53, pp 5-9, March 1986.

5. Sarpkaya, T., "Vortex Shedding and Resistance in Harmonic Flow About Smooth and Rough Cylinders at High Reynold's Numbers," Naval Postgraduate School Report No. NPS-59SL76021, 1976.

6. Keulegan, G.H. and Carpenter, L.H., "Forces on Cylinders and Plates in an Oscillating Fluid," Research Paper No. 2857, *Journal of Research of the National Bureau of Standards*, vol. 60, no. 5, May 1958.

7. Gerlach, C.R., "An Engineering Approach to Tube Flow-Induced Vibrations," *Proceedings of the Conference on Flow Induced Vibrations in Reactor System Components*, pp. 205-224, 1970.

8. Graham, C., "A Survey of Correlation Length Measurements of the Vortex Shedding Process Behind a Circular Cylinder," Report 76028-1, Contract No. 3963(25), Engineering Products Laboratory, MIT, October 1966.

9. O'Keefe, J.L., *Time-Dependant Flow About Bilge Keels and Smooth and Rough Circular Cylinders*, M.S.-M.E. Thesis, Naval Postgraduate School, Monterey, California, March 1986.

INITIAL DISTRIBUTION LIST

		No. Copies
1.	Defense Technical Information Center Cameron Station Alexandria, Virginia 22304-6145	2
2.	Library, Code 0142 Naval Postgraduate School Monterey, California 93943-5002	2
3.	Department Chairman, Code 69 Department of Mechanical Engineering Naval Postgraduate School Monterey, California 93943-5000	1
4.	Prof. T. Sarpkaya, Code 69SL Department of Mechanical Engineering Naval Postgraduate School Monterey, California 93943-5000	10
5.	Lt. William T. McCoy, USN 5400 General Diaz St. New Orleans, Louisiana 70124	2

221063

Thesis
M18245 McCoy
c.1 Stability of the vortex motion in oscillating flow.